Universidade de Lisboa

Faculdade de Farmácia

Impact of superoxide dismutase mimics in non-small cell lung cancer cells *in vitro*

Rita Barbosa Pacheco Soares

Dissertation supervised by Professor Doutor Nuno Oliveira and
co-supervised by Professor Doutor Paula Guedes de Pinho

Master in Biopharmaceutical Sciences

2022

Universidade de Lisboa

Faculdade de Farmácia

Impact of superoxide dismutase mimics in non-small cell lung cancer cells *in vitro*

Rita Barbosa Pacheco Soares

Dissertation supervised by Professor Doutor Nuno Oliveira and
co-supervised by Professor Doutor Paula Guedes de Pinho

Master in Biopharmaceutical Sciences

2022

Abstract

Lung cancer (LC) continues to be the leading cause of cancer-related deaths for both genders combined, being non-small cell lung cancer (NSCLC) the most common subtype. NSCLC is commonly diagnosed in advanced stages and thus has a low survival rate. For these cases, one of the current standard treatments is cisplatin-based chemotherapy. Despite being widely used, cisplatin has several adverse effects associated, being resistance to the treatment also a major limitation to its clinical success. Oxidative stress is present in several pathologies, including cancer. Malignant cells have often been demonstrated to possess higher reactive oxygen species (ROS) levels than healthy cells. In addition, the main antioxidant enzymes responsible for the detoxification of hydrogen peroxide are usually present in lower levels or inactivated in malignant cells when compared to healthy cells. These findings encouraged the usefulness of superoxide dismutase mimics (SODm) in the context of cancer therapy. SODm are synthetic compounds with the ability to mimic the properties of native SOD enzymes, by dismutating the superoxide anion, being also considered modulators in different redox pathways. Among the different classes of SODm, the manganese(III) porphyrins (MnPs), particularly MnTnHex and MnBuOE are very promising compounds, with several applications. In this context, the aim of the innovative work herein developed was to assess the effects of these two MnPs alone and combined with cisplatin in two NSCLC cell lines (A549 and H1975). Several endpoints were performed, including cell viability, migration, cell cycle distribution, invasion, and the analysis of the exometabolome. Also, both cell lines were initially characterized in terms of innate expression levels of catalase, glutathione peroxidase 1 (GPX1), and peroxiredoxins 1 (PRDX1) and 2 (PRDX2). Both cell lines displayed low expression levels in particular for catalase, but also GPX1 and PRDX2. PRDX1 was the enzyme with the higher mRNA expression levels. Both compounds displayed cytotoxic features in these cell lines, with MnTnHex showing very low IC_{50} values ranging from 0.7 and 2.1 μM, while MnBuOE only decreased the viability of these cells to approximately 50% for concentrations above 100 μM. When combined with cisplatin, MnTnHex was able to enhance the cytotoxicity of cisplatin in A549 and H1975 cells. In turn, MnBuOE did not potentiate the effect of cisplatin in A549 cells, although significantly enhanced the cytotoxicity of cisplatin in H1975 cells. This cell line was more sensitive to both MnPs, either alone or combined with cisplatin. Regarding collective cell migration, MnBuOE caused a higher impairment, reducing cell migration up to more than 40%, whereas MnTnHex led to a reduction of collective migration up to 30%. Moreover, MnTnHex *per se* or combined with cisplatin altered the cell cycle distribution, inducing cell cycle arrest. Metabolomics revealed an increase in the levels of a few carbonyl compounds associated with oxidative stress in cells treated with MnTnHex alone or combined with cisplatin. MnBuOE was able to reduce chemotactic migration and invasion either *per se* or upon co-treatment with cisplatin. Overall, these results suggest that these MnPs are considered promising drug candidates for NSCLC, which might be valuable in combination with cisplatin, allowing lower doses of this drug towards an improved efficacy.

Keywords: non-small cell lung cancer; SOD mimic; MnTnHex; MnBuOE; metabolomics; cisplatin; antioxidant enzymes; cytotoxicity.

Resumo

O cancro do pulmão continua a ser a principal causa de mortes relacionadas com cancro em ambos os sexos, sendo o cancro do pulmão de células não pequenas (NSCLC) o subtipo mais comum. Este subtipo de cancro é normalmente diagnosticado nos estádios mais avançados tendo, consequentemente, uma baixa taxa de sobrevida. Neste tipo de cancro o tratamento mais comum consiste na quimioterapia baseada em fármacos de cisplatina. No entanto, apesar do seu uso generalizado, a cisplatina possui diversos efeitos adversos (AE), entre os quais, a nefrotoxicidade. Para além disso, a resistência que as células malignas tendem a desenvolver a este tipo de fármaco é uma das suas principais limitações no seu sucesso clínico. O stress oxidativo está presente em diversas patologias, incluindo no cancro. As células cancerosas muitas vezes possuem níveis mais elevados de espécies reativas de oxigénio (ROS) do que as células saudáveis. Além disso, as células malignas possuem, de um modo geral, níveis mais baixos de enzimas responsáveis por destoxificar as ROS quando comparadas com células saudáveis, sendo que, em alguns casos estes sistemas podem mesmo encontrar-se inativados.

Estas evidências incentivaram o uso de compostos miméticos das superóxido dismutases (SODm), no contexto da terapia do cancro. Estes são compostos sintéticos capazes de mimetizar as propriedades da SOD nativa, dismutando o radical anião superóxido em peróxido de hidrogénio (H_2O_2) e oxigénio. Esta sua capacidade leva a que esteja envolvido em diversas vias de sinalização, afetando a proliferação, diferenciação e morte celular. O modo de ação dos SODm determina um aumento adicional de H_2O_2 intracelular que, consequentemente, poderá ser incrementado até valores superiores ao limite a partir da qual a toxicidade se torna evidente, induzindo assim uma redução da proliferação celular e um aumento da eficácia da quimio/radioterapia. Além disso, estes compostos são capazes de proteger as células saudáveis dos AE da quimio/radioterapia. Existem diversas classes de SODm, sendo as porfirinas de manganês(III) (MnPs) as mais estudadas. Nos últimos anos, as MnPs MnTnHex e MnBuOE, consideradas muito promissoras, têm sido particularmente estudadas devido à sua eficácia, biodisponibilidade e farmacocinética.

O composto MnTnHex já foi estudado em diversos tipos de cancro, entre eles, cancro renal, cancro da mama e glioblastoma, onde foi demonstrado que é capaz de reduzir a viabilidade e migração das células cancerosas. Para além disso, o MnTnHex também já demonstrou ter um efeito protetor em células saudáveis, não mostrando também, de acordo com trabalhos anteriores do nosso grupo, citotoxicidade em linhas celulares não-malignas (células V79 e Vero).

MnBuOE é um composto derivado do MnTnHex, sendo considerada como a mais recente e bem sucedida MnP. Semelhante ao MnTnHex, o MnBuOE consegue ultrapassar a barreira hematoencefálica, tendo sido, até à data, bastante utilizado em diversos estudos relacionados com o cérebro. Estes estudos demonstraram que o MnBuOE é capaz de melhorar a memória e manter o comprimento dendrítico de ratinhos expostos a quimioterapia. No cancro da cabeça e pescoço, o MnBuOE foi capaz de aumentar a janela terapêutica da radioterapia. Atualmente, este composto encontra-se em diversos ensaios clínicos em fase I e II, devido ao seu papel como radioprotetor, estando a ser testado em metástases no cérebro, cancro da cabeça e pescoço e cancro anal.

Neste contexto, o principal objetivo deste projeto inovador foi aferir o efeito destas duas MnPs, tanto isoladamente como combinadas com cisplatina em duas linhas celulares de NSCLC (A549 e H1975). Foram realizados diversos ensaios celulares, entre os quais, ensaios de viabilidade, migração, distribuição do ciclo celular, invasão e análise do exometaboloma. Estas duas linhas celulares foram também caracterizadas

relativamente aos seus níveis basais de catalase, glutationa peroxidase 1 (GPX1) e peroxirredoxinas 1 (PRDX1) e 2 (PRDX2).

Em primeiro lugar, ambas as linhas celulares demonstraram níveis baixos de expressão, particularmente da catalase, mas também da GPX1 e PRDX2. A PRDX1 revelou ter a maior expressão de RNAm, sendo duas vezes mais elevada nas células A549 do que nas células H1975. Contudo, esta diferença não foi significativa. O perfil citotóxico de ambas MnPs foi determinado através do ensaio de cristal violeta (CV) e MTS. As células foram expostas durante 72 h a MnTnHex (0,5-25 μM). O MnTnHex demonstrou ser bastante citotóxico para as células, possuindo valores de IC_{50} muito baixos, variando entre 0,7 e 2,1 μM. O perfil citotóxico do MnBuOE também foi determinado através do CV e MTS (0,5-200 μM). Este composto demonstrou ser bastante menos citotóxico que o MnTnHex, diminuindo a viabilidade celular destas células para cerca 50% apenas para concentrações superiores 100 μM. É também importante referir que as células H1975 mostraram ser mais sensíveis a ambos os compostos que as células A549.

Para determinar se estes compostos poderiam potenciar o efeito da quimioterapia baseada em fármacos de platina, procedeu-se ao co-tratamento das MnPs com cisplatina durante 72 h, seguido da avaliação da citotoxicidade através do ensaio do CV. No caso do MnTnHex utilizou-se duas concentrações, *i.e*. 0,5 e 1 μM, representativas de níveis diferentes de citotoxicidade. Estas concentrações foram iguais para ambas as linhas celulares. Para a cisplatina utilizou-se a concentração de 1 μM, em ambas as linhas, e 2 e 5 μM nas células A549 e H1975, respetivamente. O MnTnHex potenciou o efeito da cisplatina em todas as condições testadas, observando-se um maior efeito nas células H1975. Relativamente ao MnBuOE, foram testadas também duas concentrações (10 e 20 μM), sendo que as concentrações de cisplatina foram as mesmas. Neste caso, o MnBuOE potenciou significativamente o efeito da cisplatina nas células H1975. Contudo, nas células A549, observou-se apenas uma redução marginal da viabilidade sem significado estatístico.

De modo a analisar o efeito destas MnPs, isoladamente ou combinadas com cisplatina, em endpoints associados à metastização, foram realizados ensaios de migração coletiva. Primeiramente, escolheram-se concentrações não citotóxicas, tanto das MnPs como da cisplatina, usando o ensaio do MTS. Foram selecionadas as concentrações de 5 μM de MnTnHex e 0,5 μM de cisplatina para as células A549 e as concentrações de 0,5 μM e 1 μM de MnTnHex e cisplatina para as células H1975, respetivamente. No caso do MnBuOE selecionou-se as concentrações de 5 e 10 μM para as células A549 e a concentração de 5 μM para as células H1975. Após a seleção das concentrações não-citotóxicas procedeu-se à realização do ensaio de migração coletiva (32 h). Neste ensaio, o MnBuOE (per se ou combinado com a cisplatina) demonstrou possuir uma maior redução da migração coletiva em comparação com o MnTnHex.

Adicionalmente foi também avaliado o impacto do MnTnHex sozinho ou combinado com cisplatina a nível da distribuição do ciclo celular. Utilizando as mesmas concentrações que nos ensaios combinatórios, observou-se um aumento da percentagem da população sub-G1 de ambas as células quando expostas ao MnTnHex (1 μM). Este aumento foi acentuado quando o MnTnHex foi combinado com a cisplatina. É de realçar que nas células A549 houve ainda um aumento da fase G2/M acompanhado por uma redução na fase G0/G1 quando o MnTnHex e a cisplatina foram adicionados simultaneamente.

Ao analisar o exometaboloma das células cancerosas expostas ao MnTnHex sozinho ou combinado com cisplatina, detetou-se um aumento dos níveis de alguns

compostos carbonílicos voláteis (VCCs), especificamente isobutanal, benzaldeido e 3-metilpentanal, os quais estão associados a stress oxidativo. Apesar destes VCCs só terem sido detetados, com significado estatístico, nas células H1975 quando expostas à concentração mais elevada de MnTnHex (per se ou combinado com cisplatina), foi possível observar um aumento dos níveis de isobutanal e benzaldeido nas células A549, ainda que sem significado estatístico.

Por fim, analisou-se o efeito do MnBuOE na migração individual e na invasão realizando-se ensaios de quimiotaxia transwell e quimioinvasão transwell, respetivamente, utilizando as mesmas concentrações que nos ensaios da migração coletiva. O MnBuOE isoladamente reduziu significativamente a migração individual em ambas as células. No entanto, quando esta MnP foi combinada com a cisplatina levou a uma redução da migração individual das células A549 em mais de 50%, observando-se um valor semelhante nas células H1975. Na invasão, a combinação mais eficiente nas células H1975 foi observada no tratamento com MnBuOE per se, pois induziu uma redução na invasão de 34% ($p<0,001$). Contudo, quando combinado com cisplatina foi também possível observar uma redução de 18% ($p<0,05$).

Em conclusão, os resultados obtidos no âmbito deste trabalho sugerem que ambas as MnPs são compostos promissores para serem considerados no tratamento do NSCLC, tanto em monoterapia como em combinação com a cisplatina, uma vez que poderão permitir o uso de doses mais baixas deste fármaco citotóxico, de modo a aumentar a sua eficácia e reduzir os AE associados. No entanto, é ainda necessário realizar estudos adicionais para melhor compreender, a nível molecular, o modo de ação destes compostos.

Palavras chave: cancro do pulmão de células não pequenas; SOD miméticos; MnTnHex; MnBuOE; metaboloma; cisplatina; enzimas antioxidantes; citotoxicidade.

Acknowledgments / Agradecimentos

Gostaria de começar por agradecer à Professora Doutora Cecília Rodrigues por toda a sua disponibilidade e orientação ao longo destes dois anos de mestrado. Por me ter aconselhado sobre possíveis orientadores e por estar sempre disponível para nos ajudar com qualquer dúvida que tenhamos, seja a que horas for.

Gostaria também de prestar o meu enorme agradecimento ao Professor Doutor Nuno Oliveira por me ter orientado e ter aceitado desde início como sua aluna. Muito obrigada por todos os ensinamentos, paciência e tempo que investiu em mim ao longo deste ano. Agradeço também a sua prontidão em garantir que não me faltava nada nas minhas viagens ao Porto. Muito obrigada à Professora Doutora Paula Guedes de Pinho por ter sido extremamente amável desde início e me ter recebido sempre tão bem, mesmo que a minha estadia no Porto tenha sido curta. A nossa aventura para a estação de Campanhã ficará na memória. A ti Filipa, um grande obrigado por teres sido a minha mentora no Norte e me teres ajudado com tudo o que era necessário no metaboloma. Obrigada por toda a boa disposição.

Agradeço também ao grupo CBIOS da Universidade Lusófona pela preciosa ajuda e colaboração nas técnicas realizadas durante este trabalho. Um agradecimento especial ao Professor Nuno Saraiva por toda ajuda e disponibilidade durante todos os problemas que fomos encontrando com o ciclo celular. Agradeço também à Professora Ana Sofia Fernandes pelos seus *inputs* ao longo deste projeto e ao Professor João Costa por me ter ajudado na estatística.

Um especial e enorme obrigada a todos os meus colegas do grupo *Advanced Cell Models for Predictive Toxicology & Cell-based Therapies*. Primeiramente, um enorme obrigada à Professora Doutora Joana Miranda por me ter rapidamente integrado no seu laboratório e por me estar sempre a incentivar a ser cada vez mais prática e autónoma. Obrigada Sérgio por me ensinares todos os truques quando algum ensaio não corria bem e por estares sempre lá quando era necessário. Um grande obrigada a ti Rita. Sem ti nada disto teria sido possível. Obrigado por me teres iniciado no mundo das culturas celulares, pelas várias vezes que me tiveste de passar células porque o covid gostava demasiado de mim e eu tinha que ficar em casa em isolamento e um grande obrigada por me ajudares sempre a planear todas as ideias que o Professor Nuno queria fazer. Obrigada Joaninha, Ana e Catarina por todo o vosso apoio e boa disposição no laboratório e por toda a companhia que me fizeram na ilha durante os meus inúmeros ensaios de cristal violeta.

Às minhas "meninas da faculdade": Catarina, Mariana e Raquel. Obrigada por me ouvirem e desesperarem comigo. Obrigada pelos vários jantares e convívios que tivemos que, milagrosamente, aconteciam sempre na altura certa. Obrigada por me animarem, mesmo quando as coisas andavam mais negras, por nunca me deixarem desistir e, especialmente, por serem as pessoas a quem eu podia contar as coisas porque, melhor que ninguém, sabiam o que eu estava a passar.

Catarina "drama queen" Roque eu nem sei por onde começar. Conhecemo-nos no fim da licenciatura, mas fomos juntas para o mestrado e, mesmo sem sabermos, fomos parar ao mesmo laboratório. Infelizmente não conseguimos conviver muito devido aos inúmeros percalços que tiveste durante a tese, mas ficas a saber que te admiro imenso por toda a

tua resiliência que tiveste durante este ano. Obrigado por estares sempre cá para mim amiga, mesmo quando tudo na tua tese corria mal.

Obrigada ´fada por toda a companhia que me fizeste durante o mês de agosto, naquela cave, dias a fio, eu a escrever a tese e tu a trabalhar. Genuinamente, acho que se não fosses tu eu tinha desesperado dez vezes mais do que aquilo que desesperei.

Obrigado amiga e amigo!! Por todas as fofocas, idas ao jonhnys, baco e afins que me ajudaram a desanuviar de todos os stresses da tese (e não só). Obrigada por, mesmo não percebendo nada do que dizia, perguntarem sempre como é que eu andava e como andava a tese.

Por fim, um gigante obrigada a ti amor. Foste sem dúvida a pessoa que mais levou com o meu mau-humor, o meu stress infinito, a minha ansiedade e as minhas preocupações. A pessoa que teve um fim de semana inteiro comigo a verificar referencias para uma coisa que nem sabia o que era. Obrigado por teres ido ter comigo todos os dias durante o verão, mesmo sabendo que eu não te podia dar atenção. Obrigada por me ensinares a acalmar e a respirar fundo no meio do caos que foi este ano. No fundo, um grande e gigante obrigado!

Publications

The work developed in this thesis was presented in the following publications:

Poster Presentation

1. Soares R., Manguinhas R., Costa J. G., Fernandes A. S., Saraiva N., Gil N., Rosell R., Camões S.P., Batinic-Haberle I., Spasojevic I., Castro M., Miranda J. P., Guedes de Pinho P., and Oliveira N. G., Effect of the SOD Mimic MnTnHex-2-PyP^{5+} *per se* and in combination with platin-based chemotherapy in non-small cell lung cancer cells *in vitro*, 13th Post-Graduate iMed.ULisboa Students Meeting & 6th i3DU Students Meeting, 2022, Lisbon, Portugal

2. Soares R., Manguinhas R., Costa J. G., Fernandes A. S., Saraiva N., Gil N., Rosell R., Camões S.P., Batinic-Haberle I., Spasojevic I., Castro M., Miranda J. P., Guedes de Pinho P., and Oliveira N. G., Cytotoxic effects of the SOD mimic MnTnHex-2-PyP^{5+} and its combination with cisplatin in non-small cell lung cancer cells, 16th International Congress of Toxicology, 2022, Maastricht, the Netherlands

Oral Communications

1. Soares R., Manguinhas R., Costa J. G., Fernandes A. S., Saraiva N., Gil N., Rosell R., Camões S.P., Batinic-Haberle I., Castro M., Miranda J. P., Guedes de Pinho P., and Oliveira N. G., Impact of the SOD mimic MnTnHex-2-PyP^{5+} and its combination with cisplatin in non-small cell lung cancer cells *in vitro*, 52° Reunião da Sociedade Portuguesa de Farmacologia, 40° Reunião de Farmacologia Clínica e 21° Reunião de Toxicologia, 2022, Porto, Portugal

Publications

1. Soares, R.B.; Manguinhas, R.; Costa, J.G.; Saraiva, N.; Gil, N.; Rosell, R.; Camões, S.P.; Batinic-Haberle, I.; Spasojevic, I.; Castro, M.; Miranda, J.P.; Amaro, F.; Pinto, J.; Fernandes A.S.; Guedes de Pinho, P.; Oliveira, N.G. MnTnHex-2-PyP^{5+} Displays Anticancer Properties and Enhances Cisplatin Effects in Non-Small Cell Lung Cancer Cells. *Antioxidants* 2022, 11, https://doi.org/10.3390/antiox11112198

Grants

1. EU-ROS COST Action CA20121 grant to attend the 16th International Congress of Toxicology, 2022, Maastricht, the Netherlands

Table of Contents

Index of Figures and Tables

List of Abbreviations

$^1O_2$	Singlet oxygen
4-HNE	4-Hydroxynonenal
8-OHG	8-hydroguanine
ABC	Adenosine triphosphate biding cassette
AJCC	American joint commission on cancer
BBB	Blood brain barrier
BRAF	B-raf proto-oncogene
Cat	Catalase
CT	Computed tomography
CTR	Copper transport protein
CV	Crystal violet
DNA	Deoxyribonucleic acid
ECM	Extracellular matrix
EDTA	Ethylenediamine tetraacetic acid
EGFR	Epidermal growth factor receptor
FA	Fanconi anemia
FBS	Fetal bovine serum
FC	Fold-change
FDA	Food and drugs administration
GPx	Glutathione peroxidase
GR	Glutathione reductase
GSH	Reduced glutathione
GSSG	Oxidized glutathione
HMGB1	High mobility group box 1
HSA	Human serum albumin
IC_{50}	Half-maximal inhibitory concentration
KRAS	Kirsten rate sarcoma viral oncogene homolog
LC	Lung cancer
MDA	Malondialdehyde

MeOH	Methanol
MMP	Mitochondrial membrane potential
MnPs	Mn(III) porphyrins
MnSOD	Manganese superoxide dismutase
MOA	Mode of action
MS	Mass spectrometer
MTS	[3-(4,5-dimethylthiazol-2-yl)-5-(3-carboxymethoxyphenyl)-2-(4-sulphophenyl)-2H-Tetrazolium]
NADPH	Nicotinamide adenine dinucleotide phosphate
NHE	Normal hydrogen electrode
Nrf2	Nuclear factor erythroid 2–related factor 2
NSCLC	Non-small cell lung cancer
$O_2^{\bullet-}$	Anion superoxide
$OH^{\bullet}$	Hydroxyl radical
$ONOO^-$	Peroxynitrite
OS	Overall survival
PBS	Phosphate buffered saline
PCA	Principal component analysis
PD-1	Programmed cell death-1
PD-L1	Programmed cell death-ligand 1
PET	Positron emission tomography
PET	Polyethylene terephthalate
PFBHA	O-(2,3,4,5,6-pentafluorobenzyl) hydroxylamine
PI	Propidium iodide
PK	Pharmacokinetic
PLS-DA	Partial least squares discriminant analysis
Prdx	Peroxiredoxins
QC	Quality control
qRT-PCR	Quantitative real-time polymerase chain reaction
RI	Retention index
$RO^{\bullet}$	Alkoxyl radical

$ROO^{\bullet}$	Peroxyl radical
ROS	Reactive oxygen species
RSD	Relative standard deviations
SABR	Stereotactic ablative body radiotherapy
SCLC	Small cell lung cancer
SODm	Superoxide disumtase mimics
TKI	Tyrosine kinase inhibithor
TR	Thioredoxin reductase
Trx	Thioredoxin
VCC	Volatile carbonyl compound
WHO	World health organization
XDH	Xanthine dehydrogenase
XO	Xanthine oxidase

Chapter 1

General Introduction

1.1 Lung cancer

1.1.1. Epidemiology

Globally, lung cancer (LC) continues to be the leading cause of cancer-related deaths for both sexes combined (**Figure 1**). Worldwide, in men, LC is the leading cause of cancer related deaths and it is also the most incident cancer (14.3%). In women LC is the third most incident cancer and the second in mortality, after breast cancer (Sung et al., 2021). Despite affecting more men than women, LC incidence decreased by almost 3% annually in men, between 2009 and 2018, and only 1% in women (Siegel et al., 2022). Similarly to other diseases, age is also a factor in the appearance of cancer. LC is quite rare in the first 50 years of life, then it begins to slowly increase over time, reaching its peak between the age of 65 and 84 years old (Duma et al., 2019; Nasim et al., 2019). Incidence and mortality rates of LC also vary depending on the geographic location. In both sexes, the highest incidence rates are in Micronesia, Eastern and Western Asia, and Eastern and Southern Europe. Turkish men possess the highest country-specific incidence rate (Mao et al., 2016; Sung et al., 2021). The incident rate in women is higher in Northern America, Northern and Western Europe and Australia/New Zealand (Sung et al., 2021). These epidemiologic trends are usually associated with cigarette smoking habits (Mao et al., 2016; Siegel et al., 2022). Siegel *et al*. estimated that in 2022 81% of LC cases would be due to direct cigarette smoking (Siegel et al., 2022). Finally, ethnicity is also one of the criteria that affects incidence and mortality rates. At the beginning of the last decade, black Americans had the highest incidence and mortality rates, while Hispanics had the lowest rates (Mao et al., 2016).

Currently, the 5-year relative survival rate is 22% for all the LC stages combined (Siegel et al., 2022), with Japan, Israel and the Republic of Korea having the higher survival rates (Sung et al., 2021). The high mortality rate and the low 5-year survival rate are mostly associated with more than half of LC cases being diagnosed in advanced stages (Rodriguez-Canales et al., 2016). The World Health Organization (WHO) estimates that LC deaths will continue to increase, especially in Asia, due to an increase in global tobacco use (Duma et al., 2019). By 2050 the number of diagnosed cancer patients is supposed to double, with LC being at the top of the chart (Nooreldeen & Bach, 2021).

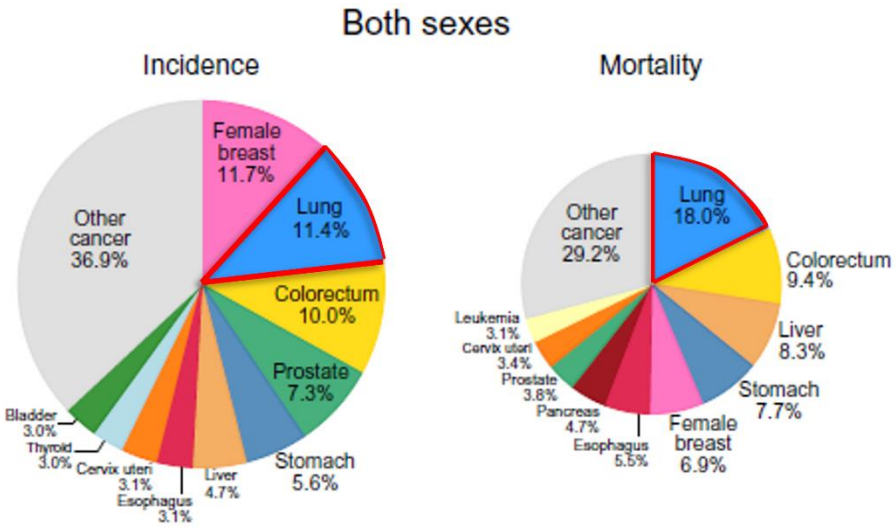

Figure 1. Incidence and mortality rates for the top 10 most common cancers in 2020 for both sexes combined. Adapted from Sung et al., 2021.

1.1.2. Classification

LC can be histologically divided into two main groups: non-small cell lung cancer (NSCLC), which represents up to 85% of all LC cases, and small cell lung cancer (SCLC) (Schabath & Cote, 2019). Given that NSCLC is highly resistant to standard therapeutic treatments, it has a 5-year survival rate of approximately 15% (Luo et al., 2016). Adenocarcinoma, squamous cell carcinoma and large cell carcinoma are the three main types of NSCLC, as classified by WHO (Travis et al., 2015), being the last two more associated with cigarette smoking (Herbst et al., 2018).

Firstly, adenocarcinomas, the most common type, accounts for approximately 40% of all NSCLC cases (Duma et al., 2019). Generally, adenocarcinomas originate in the periphery of the lung, more precisely, in the alveolar cells of the smaller airway epithelium (Duma et al., 2019; Rodriguez-Canales et al., 2016). Although this type of tumor can be found in smokers or former smokers, it is more common in never-smokers (Herbst et al., 2018). Also, adenocarcinomas are more common in women than in men (Barta et al., 2019). This type of NSCLC usually activates mutations in driver genes, like kirsten rat sarcoma virus homolog (KRAS), B-rad proto-oncogene (BRAF) and the epidermal growth factor receptor (EGFR) (Nooreldeen & Bach, 2021). Early stages of LC can be classified as adenocarcinomas *in situ* and may be invasive or minimally invasive adenocarcinomas (Travis et al., 2015).

Squamous cell carcinomas represent 25% to 30% of LC and arise in the main or lobar bronchus (Rodriguez-Canales et al., 2016; Schabath & Cote, 2019)**.** To properly identify this specific type of NSCLC immunohistochemical markers such as CK5, CK6 and p40 are commonly used (Duma et al., 2019). Lastly, large cell carcinoma is accountable for 10% to 15% of all LC (Schabath & Cote, 2019). The histological identification of this type of cancer is the most difficult, since it does not show histological evidence of squamous cell, glandular, or, small-cell differentiation (Rodriguez-Canales et al., 2016). However, recent immunophenotyping techniques are emerging, allowing a

better classification (Duma et al., 2019). Despite these three main types of NSCLC there are other less common histological types, such as adenosquamous carcinoma (1–2%), large cell neuroendocrine carcinoma (3%) and carcinoid tumor (1-2%) (Barta et al., 2019; Schabath & Cote, 2019).

Although SCLC only accounts for approximately 15% of all LC it is still an aggressive type of tumor. It can be typically found in the basal bronchial epithelium and originates from neuroendocrine cells (Nooreldeen & Bach, 2021). SCLC cells can be pure or combined with NSCLC cells, and usually, these cells form a perihilar mass that may already have early or extensive lymph node metastases (Barta et al., 2019; Nooreldeen & Bach, 2021). The standard treatment for SCLC consists of a combination of chemotherapy and chest radiotherapy (Nooreldeen & Bach, 2021).

The foundation for staging LC tumors is the tumor, nodal involvement, and distant metastasis system (TNM). At the begging of the last decade American Joint Commission on Cancer (AJCC) updated the classification of the lung cancer stage. The staging of each tumor and the correspondent treatment are determined by this system, in which the size of the primary tumor and its characteristics (T) are analyzed, as well as the spread of lymph nodes involved (N) and the presence of metastases (M) (Hoy et al., 2019; Nooreldeen & Bach, 2021).

Despite the classic binary division of LC tumors, most cases are now classified and characterized with the help of tumor biomarkers and genetic alterations, *e.g.*, gene expression and driver mutations.

1.1.3. Diagnosis

Early diagnosis has a vast impact on the survival rate. Patients diagnosed with early stages of NSCLC have a 5-year survival rate higher than 50%, whereas patients diagnosed with NSCLC in advanced stages, *e.g.*, stage IV where metastases have already developed, have a survival rate of only 5% (Luo et al., 2016). Unfortunately, it is very common for NSCLC to only be detected in advanced stages. In early-stage LC the main symptoms are cough (seen in 75% of patients), fatigue, nausea and vomiting, dyspnea, and chest pain (Duma et al., 2019; Hoy et al., 2019). At the time of the diagnosis, if LC is already metastasized, the most common symptoms are bone pain, neurological deficits, headaches, seizures, and weight loss for no apparent reason (Collins et al., 2007).

Currently, there are seven different techniques to identify the presence of cancerous lung cells: Chest X-rays, computed tomography scans (CT), magnetic resonance imaging (MRI), positron emission tomography (PET), cytology sputum and breath analysis (Thakur et al., 2020). Axial CT imaging is the gold standard for diagnosis and staging since it is able to detect cancer cells within the submillimeter range and it provides 3D images of tumors and their anatomic structures (Hoy et al., 2019; Luo et al., 2016). Despite all these techniques, the diagnosis of LC still falls short. Therefore, it is necessary to adapt the diagnostic tools to obtain a more personalized diagnosis. Screening of specific genes has been a crucial diagnostic tool for personalized treatment. The most frequent genes responsible for the development of NSCLC are *KRAS* (25%), *EGFR* (10%), *ALK* (7%), *MET, LKB1, BRAF, PIK3CA, RET* and *ROS1* (Romaszko &

Doboszynska, 2018). These last genes are less frequent to suffer mutations in comparison with the first three genes (Rodriguez-Canales et al., 2016).

The *EGFR* gene is often mutated in 40-80% of NSCLC cases. This mutation is usually heterozygous, with the mutant allele showing an amplification of this gene (Rodriguez-Canales et al., 2016). It is involved in intracellular signaling pathways that regulates cell proliferation and survival. However, when mutated, there is an hyperactivation of downstream prosurvival signaling pathways (Landmesser et al., 2020). EGFR mutations are more common in adenocarcinomas, more specifically in female never-smokers (Rodriguez-Canales et al., 2016). Interestingly, this mutation is often found in primary lung cancer but not in metastases (Romaszko & Doboszynska, 2018). Initially, EGFR mutations are highly responsive to EGFR tyrosine kinase inhibitors (EGFR TKIs), *e.g.,* gefitinib and erlotinib. Nonetheless, the majority of patients develop a resistance to these inhibitors (Rodriguez-Canales et al., 2016; Wagener-Ryczek et al., 2020).

As stated, *KARS* is the most common gene mutated in NSCLC. It is involved in the RAS/MAPK signaling pathway and it regulates cell division (Rodriguez-Canales et al., 2016). KRAS mutations have been detected in more than 25% of patients with adenocarcinomas (Ogawa et al., 2019). However, they are quite rare in squamous cell carcinoma (Romaszko & Doboszynska, 2018). Currently, there are new small molecule KRAS inhibitors in clinical trials (reviewed in Xie et al., 2021).

Interestingly, metabolomics has been a recent and useful tool for the prediction of cancer development and characterizing the stage of NSCLC. Metabolomics is defined as the extensive analysis of hundred or thousand small molecules (metabolites) present in a sample of biofluid, tissue, or cell system, combining analytical chemistry, bioinformatics, statistics, and biochemistry (Bouhifd et al., 2015; Clish, 2015; Kennedy et al., 2018). Metabolomics studies have shown that it is possible to differentiate between healthy and lung cancer patients through the analysis of different fluids such as plasma or serum. Aspartic acid, taurine, and pyruvic acid were upregulated in cancer patients, while in healthy control patients the same was not detected (Kumar et al., 2017). Singh *et al.* analyzed the serum of LC patients and healthy controls and determine that circulatory metabolites such as histidine, alanine, valine, and glycine were discriminatory between LC patients and healthy controls (Singh et al., 2022). Despite the potential of metabolomics as a diagnostic tool, it still needs to be validated, since several factors might influence the results obtained, including the time of sampling, methods of analysis ,and the daily changes that metabolites suffer throughout the day (Nooreldeen & Bach, 2021).

1.1.4. Treatment

In the last 20 years, the treatment for NSCLC substantially progressed, especially due to the application of immunotherapy, either alone or combined with more conventional treatments. Nowadays, the treatment of NSCLC is more personalized, since it depends on the stage of the disease at the time of the diagnosis, and possible driver mutations that the patient may have.

The standard treatment for early-stage NSCLC (I-IIIA) is surgery, more specifically lobectomy (Duma et al., 2019). However, there is the possibility that the tumor is inoperable, even though it is still in its early stages, due to the tumor's characteristics or fitness for surgery (Broderick, 2020). In these cases, stereotactic ablative body radiotherapy (SABR) or chemoradiotherapy are the best options (Brown et al., 2019; Nasim et al., 2019). When tumors are only treated with surgery there is a high probability that the tumors will recur, since the 5-year survival rate for stage IA and IIIA are 83% and 36%, respectively (Herbst et al., 2018). Therefore, neoadjuvant (systemic therapy administered before surgery) and adjuvant therapy (systemic therapy administered after surgery) have been applied to increase the overall survival (OS) of patients (Broderick, 2020). Neoadjuvant chemotherapy is able to treat micrometastases and downstaging the tumor so that it can possibly be surgically removed. Adjuvant chemotherapy is advisable for patients with stage II and IIIA and it consists of cisplatin-based combinations capable of eliminating distant metastases (Duma et al., 2019). Neoadjuvant therapy appears to be the best option compared to adjuvant therapy since it has a higher probability of patients completing the chemotherapy treatment and it eliminates micrometastases earlier (Miller & Hanna, 2021). Nonetheless, when adjuvant chemotherapy is used several factors are involved, such as age, chemotherapy regimens, and adequate performance status (Nagasaka & Gadgeel, 2018). Despite the advantages that neoadjuvant therapy has, this treatment may increase treatment toxicity and prevent the accuracy of pathologic staging (Uprety et al., 2020). There has been a growing interest in incorporating molecular targeted agents, immunotherapy, and neoadjuvant immunotherapy as part of the possible treatments for early-stage NSCLC (Duma et al., 2019; Uprety et al., 2020).

Locally advanced NSCLC comprises a complex group of patients. Most patients in this group have stage III NSCLC but depending on the nodal involvement of the tumor there are different treatment options. If the patient has a partial nodal involvement (N1) the tumor can still be surgically removed, followed by chemotherapy and/or radiotherapy. However, if the patient has the highest nodal involvement (N3) surgery is no longer a viable option (Nasim et al., 2019). In these cases, the standard treatment is chemotherapy and thoracic radiation (Herbst et al., 2018). Nevertheless, the prognosis is still poor, since the 5-year survival rate is only 15% (Duma et al., 2019). Recently, the standard of care has changed for these patients. The PACIFIC trial proved that immunotherapy after chemoradiation would be the optimal treatment for stage III patients with inoperable tumors (Antonia et al., 2018). Gefitinib and Erlotinib were the first TKIs tested against EGFR and they set the passe for the development of other effective target therapies in gene alterations like *ALK* rearrangements, *ROS1* fusions and *BRAF* mutations (Herbst et al., 2018).

As abovementioned, most NSCLCs are diagnosed in advanced stages (stage IV). In these cases, the standard treatment is chemotherapy, *i.e.* platinum doublet with carboplatin or cisplatin combined with gemcitabine, vinorelbine, or taxanes (paclitaxel or docetaxel) (Duma et al., 2019). Even though chemotherapy is still a standard treatment, immunotherapy has been an important tool in this specific stage, so the two type of

treatments have been combined (chemoimmunotherapy). By combining platinum doublet and pembrolizumab, an anti-PD-1 drug, the treatment efficacy and the OS improved, when compared to chemotherapy alone (Wang et al., 2021). Programmed death ligand-1 (PDL1) levels have been used to direct treatments with some immunotherapies (Nasim et al., 2019). There are several studies that demonstrated the impact that immune checkpoint inhibitors have on the survival of patients with metastatic disease (Brown et al., 2019; Miller & Hanna, 2021; Uprety et al., 2020). Besides PDL1, other approved targetable mutations are: EGFR exon 19 deletion and exon 21 L858R mutations; fusions in ALK, ROS-1, RET, and NTRK; MET exon 14 splice mutations; and BRAF V600E mutations (Miller & Hanna, 2021). The immune checkpoint inhibitors combined with platinum doublet increased OS at 1 year by 20% (Uprety et al., 2020). Despite chemoimmunotherapy being currently the best chance for treating stage IV NSCLC, there are still several challenges remaining, such as a better understanding of mechanisms of resistance to prevent its appearance and better predictors of response to immunotherapy (Herbst et al., 2018).

1.2 Cisplatin

1.2.1. An overview

Cis-diamminedichloroplatinum (II), commonly known as cisplatin, is an inorganic complex with a platinum atom in the +2 oxidation state in the center with four ligands in *cis* configuration: two chlorides (Cl) ion ligands and two relative inert ammonia (NH_3). This complex has a square planar geometry (Qi et al., 2019; Safirstein et al., 1984). Its biological activity was only discovered accidentally in 1965 by the biophysicist Barnett Rosenberg (Abu-Surrah & Kettunen, 2006), and in 1971 the first patients were treated with cisplatin (Kelland, 2007). It became the first FDA-approved platinum drug for cancer treatment in 1978 (Dasari & Tchounwou, 2014). Nowadays, it is used as an effective therapy in several types of cancer, including bladder (Jiang et al., 2021); breast (Meng et al., 2021); cervical (Kitagawa et al., 2015); head and neck (Patil et al., 2019); lung (Liang et al., 2017); ovarian (Armstrong et al., 2006) and prostate (Buonerba et al., 2011) cancers, among others. In stage II-III of NSCLC cisplatin is used in adjuvant chemotherapy (Dasari & Tchounwou, 2014).

For cisplatin to target the DNA, it must first undergo some structural changes in the blood. In the bloodstream the concentration of chloride is approximately 100 mM, so once cisplatin enter the blood (*i.v.* administration) it maintains its uncharged and neutral structure. A large part of cisplatin reacts with proteins in the blood, such as transferring, cysteine, and especially human serum albumin (HSA), leading to the deactivation of most of the applied cisplatin (Ghosh, 2019; Makovec, 2019). The small percentage of cisplatin that reaches the cell is transported inside the cell by passive and facilitated diffusion using copper transport proteins, most likely using the copper transport proteins CTR1 and CTR2 (Makovec, 2019). Once inside the cell, the much lower concentration of chloride ions (*i.e.* 4-22 mM) leads to the hydrolysis of cisplatin and originates cationic monoaquo

and/or diaquo complexes, which makes them more capable of interacting with several biomolecules, since the platinum atom of these water-soluble compounds allows them to interact with the biomolecules by nucleophile coordination or charge-charge interactions (Qi et al., 2019). In the cytoplasm, cisplatin accumulates mainly in the acidic organelles, *e.g.*, lysosomes and nucleus (Legin et al., 2014). When in the nucleus, most of the cisplatin binds to the nucleolus, leaving only 1-10% of intracellular cisplatin to react with its main target, DNA (Raudenska et al., 2019) (**Figure 2**).

The cytotoxic effect of cisplatin is due to its binding to DNA. It interacts with the N7-sites of purine bases (guanine) and forms intrastrand adducts and, in small amounts, monofunctional and interstrand cross-links (Crona et al., 2017; Qi et al., 2019). Of all the adducts formed, 1,2-cross-linking of cisplatin is the most common structural change in the DNA (Qi et al., 2019). These significant changes are recognized by high mobility group box 1 (HMGB1) forming a DNA-Pt-HMGB1 complex and preventing it from being repaired, which consequently results in cell cycle arrest and apoptosis (Siddik, 2003). Besides nuclear DNA, cisplatin also targets other biomolecules in different organelles, which contributes to its lethal effect. One of these organelles is the mitochondria. Since the mitochondrial DNA (mtDNA) does not have the classical repairing systems, cisplatin can enter the mitochondria and form high amounts of adducts, creating a higher level of DNA adducts in the mitochondria than in the nucleus (Raudenska et al., 2019). Besides DNA damage, cisplatin can also increase reactive oxygen species (ROS) production, which depends on the cisplatin concentration and time of exposure (Dasari & Tchounwou, 2014). This will lead to oxidative stress, one of the most important mechanisms to enhance cisplatin toxicity (Dasari & Tchounwou, 2014). The oxidative stress in the mitochondria will result in the inhibition of calcium uptake and reduction of mitochondrial membrane potential (MMP), which causes a mitochondrial rupture and ultimately apoptosis (Ghosh, 2019).

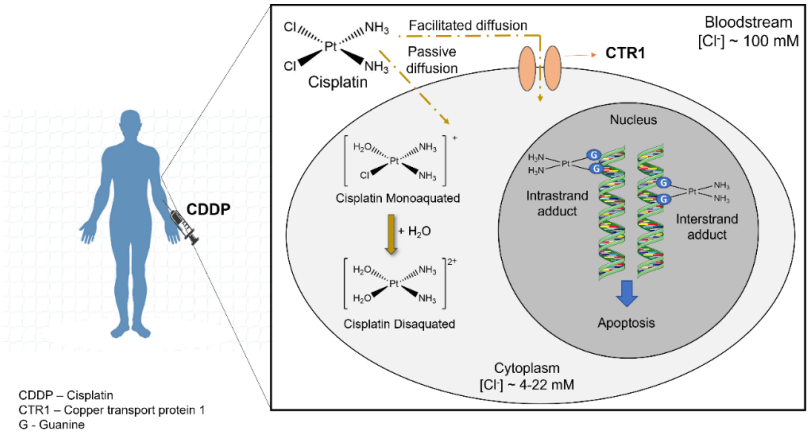

Figure 2. Cisplatin mode of action and the most common DNA adducts generated upon its exposure. Cisplatin enters the cells by passive and/or facilitated diffusion and is activated by changing the chloride ions for water molecules, originating two different complexes. These complexes can bind to the DNA and form intra- or inter-strand cross-links that, if not repaired, will lead to apoptosis. Adapted from Browning et al., 2017.

1.2.2. Resistance to cisplatin and common adverse effects

Although cisplatin is highly used to treat several types of cancer, its off-target toxicity and the resistance that cancer cells tend to acquire over time are major problems associated with this chemotherapeutic drug. The factors that lead to the development of cisplatin resistance have been extensively investigated and three main cellular mechanisms were considered responsible: enhanced DNA repair, increase drug efflux and decreased drug influx, and increased drug inactivation (Berkel & Cacan, 2021). The enhanced DNA repair can be due to an upregulation of DNA response and DNA damage tolerance (Kryczka et al., 2021). Translesion synthesis polymerases, a specialized set of low fidelity DNA polymerases, are able to synthesize DNA across the lesion and by the homologous recombination (HR) pathway repair the damaged DNA template (Haynes et al., 2015). Besides this repair pathway, there are several others that can be activated depending on the type and location of the DNA damage. Chen *et al.* analyzed how DNA repair pathways may affect the sensitivity of NSCLC cells. They suggest that Fanconi anemia (FA) and HR pathways may be responsible for the acquired resistance of cells, since the silencing of FA- and HR-associated genes in A549/DR, a cell line cisplatin-resistant derived from A549 cells, and Calu-1, a moderate innate resistant cell line, significantly potentiated their sensitivity to cisplatin (Chen et al., 2016). Cells with overexpression of NER factors, particularly the ERCC1, have demonstrated very low sensitivity to cisplatin (Chen et al., 2016; Ghosh, 2019; Rosell et al., 2007). The altered accumulation of cisplatin can be due to either an inhibition of drug uptake and/or an increase in drug efflux. The precise mechanism of this alteration continues to be unknown. Nonetheless, there are several hypotheses that are being studied. The overexpression of ATP-biding cassette (ABC) transporters is a prime example. ABC proteins are responsible for the efflux of several small molecules from the cytosol by using energy from ATP hydrolysis and are expressed in various tissues, *e.g.*, liver, kidney and intestine (Liu & Liu, 2019). So, if these proteins are overexpressed, they can reduce the intracellular accumulation of cisplatin (Kryczka et al., 2021). In LC, the ABCA1, ABCC2 and ABCC6 are responsible for the direct effluxion of cisplatin from the cell (Kryczka et al., 2021). CTR1 is the main transporter responsible for cisplatin influx. However, the continuous presence of cisplatin leads to degradation in concentration of CTR1 and, consequently, to the development of cisplatin resistance (Ghosh, 2019). Besides these factors, there are other possibilities for the development of cisplatin resistance. Mutations in the genes involved in several signaling pathways can also lead to drug resistance. The decreased expression of BAD, Bid, caspases 4 and 6 were correlated with cell lines resistant to cisplatin (Cetintas et al., 2012). Wang *et al.* found that hypoxia-induced exosomes transmitted cisplatin resistance to previous sensitive NSCLC cells by using PKM2 (Wang et al., 2021). MiRNAs have also been demonstrated to play a crucial role in the development of cisplatin resistance and/or restoring its sensitivity in both ovarian and lung cancer (Kryczka et al., 2021; Moghbeli, 2021).

Regarding off-target toxicity, nephrotoxicity appears to be the major dose-limiting factor of cisplatin. It can be presented in several ways, being the most serious and common acute kidney injury, which affects 15-35% of patients (Desilets et al., 2020).

Hypomagnesemia, hypokalemia, chronic renal failure and proximal tubular dysfunction are other ways in which nephrotoxicity can be presented (Qi et al., 2019; Zhang et al., 2021). The main approaches to ameliorate these side effects are hydration and diuretics. They help improve the excretion of cisplatin and reduce the incidence of nephrotoxicity (Duffy et al., 2018). Nephrotoxicity can be caused by an accumulation of cisplatin in the renal proximal tubule and the intracellular transformation of cisplatin into toxic metabolites, since almost all cisplatin is expelled by the urine (Duffy et al., 2018; Zhang et al., 2021). Other factors like direct tubular epithelial cell toxicity and vasoconstriction in the renal microvasculature also contribute to renal toxicity (Desilets et al., 2020).

Vomiting and nausea are the most common side effects of cisplatin, affecting more than 90% of patients (Qi et al., 2019). Anti-emetics can be used to prevent patients from suffering dehydration due to vomiting (Qi et al., 2019). These side effects may cause the most impairment in patients' quality of life since they persist up to seven days post-administration. Vomiting and nausea are more common in patients under 50 years, females and with a history of depression and anxiety (Desilets et al., 2020). Ototoxicity, other common side effect, can be presented as a bilateral sensorineural hearing loss, tinnitus and vertigo and is usually more common in children (Desilets et al., 2020; Ghosh, 2019). Hepatotoxicity, cardiotoxicity and neurotoxicity are also documented adverse effects caused by cisplatin (Dasari & Tchounwou, 2014; Qi et al., 2019).

1.3 Oxidative stress and the antioxidant status in lung cancer cells

1.3.1. ROS and oxidative stress

ROS are a very important group of reactive species in biology and medicine. Some ROS are radicals, *i.e.*, species with one or more unpaired electrons while others, like hydrogen peroxide (H_2O_2) are non-radicals. The most relevant ROS are superoxide anion ($O_2^{\bullet-}$), H_2O_2, hydroxyl radical ($^{\bullet}OH$), singlet oxygen ($^1O_2$), alkoxyl radicals ($RO^{\bullet}$) and peroxyl radicals ($ROO^{\bullet}$) (Li et al., 2016; Pisoschi & Pop, 2015; Sosa et al., 2013). ROS can be originated from endogenous and exogenous sources. In the case of endogenous sources, the main responsible for the production of ROS is the mitochondrial respiratory chain (Poprac et al., 2017). In aerobic metabolism, cells uptake oxygen to produce ATP in the mitochondria, and, as a consequence, there is also the production of ROS, especially in complexes I and III (Gupta et al., 2014). Xanthine dehydrogenase (XDH)/ xanthine oxidase (XO) is also a crucial enzymatic source of ROS (Li et al, 2016). In the presence of inflammatory conditions XDH is transformed into XO through the oxidation of cysteine residues. XO uses oxygen as an electron acceptor, which produces high amounts of $O_2^{\bullet-}$ and H_2O_2 (Lugrin et al., 2014). Besides these two main endogenous sources, cytochrome P450 (Lugrin et al., 2014), peroxisomes (Klaunig & Wang, 2018), NADPH oxidase (Gorrini et al., 2013) and dysfunctional endothelial NOS (eNOS) (Poprac et al., 2017) also contribute to the intracellular production of ROS. Exogenous sources, such as exposure to UV light and X-rays (Gupta et al., 2014), pharmaceuticals, industrial chemicals, therapeutic and environmental agents (Klaunig & Wang, 2018) also interact

with cells to generate ROS. Cigarettes are known for inducing DNA damage that cause lung cancer (Jelic et al., 2021).

There must be a sensitive balance of ROS production so that it does not become toxic for our cells (**Figure 3**). At low and moderate concentrations, ROS are beneficial and essential, since they can regulate cytokine, growth factors (Gupta et al., 2014), participate in signal transduction, enzyme activation, gene expression (Sosa et al., 2013), sperm and oocyte maturation, uterine function, immune response (Costa et al., 2021) and is involved in cell proliferation and apoptosis (Pisoschi & Pop, 2015). However, when ROS reach high concentrations, the balance is lost, for different reasons including low concentrations of antioxidants, causing oxidative stress. This cellular state is defined as a lack of balance between "oxidants and antioxidants in favor of the oxidants, leading to a disruption of redox signaling and control and/or molecular damage" (Lugrin et al., 2014). Oxidative stress is present in several pathologies, such as, diabetes, cancer, and neurodegenerative diseases (Gupta et al., 2014) and causes a modification in lipids, DNA and proteins (Kalyanaraman, 2013). ROS oxidates guanine in the DNA and forms 8-hydroguanine (8-OHG), which can pair with adenine bases during the replication process, transforming GC pairs into TA, leading to several mutations, causing genomic instability (Gill et al., 2016; Klaunig, 2019). The formation of 8-OHG is highly correlated with carcinogenesis. This genetic alteration can cause damage in oncogenes and tumor suppressors leading to mutations known to induce cancer (Gill et al., 2016; Jelic et al., 2021; Kudryavtseva et al., 2016). The reaction of ROS with lipids is known as lipid peroxidation and usually results in the loss of membrane property and consequent modification of cellular and organelle membrane function and structure (Jelic et al., 2021; Klaunig, 2019). Additionally, lipid peroxidation can originate the mutagenic aldehydes malondialdehyde (MDA) and 4-hydroxynonenal (4-HNE), well-known as biomarkers of oxidative stress. Since these biomolecules are uncharged, they can easily migrate through membranes and cytosol and mutate genomic DNA (Kudryavtseva et al., 2016). All these effects on the DNA, lipids and proteins lead to changes in gene expression, cell proliferation and apoptosis. Increased levels of ROS can activated oncogenic signaling pathways, mutagenesis and genomic instability in cancer cells, that promotes cancer progression (Ebrahimi et al., 2020). One of the most important findings regarding oxidative stress and cancer was the difference of ROS levels between malignant and healthy cells. Several studies have demonstrated that cancer cells have often higher ROS levels than healthy cells and can inhibit antioxidant activity in an uncontrolled manner (Avolio et al., 2020; Ebrahimi et al., 2020; Gill et al., 2016; Pisoschi & Pop, 2015). Treatments such as chemotherapy and radiotherapy may indeed produce high concentrations of ROS (Jelic et al., 2021), albeit this is not necessarily a side effect, since it can actually be used as a therapeutic advantage. As stated before, cancer cells, in general, have elevated concentrations of ROS, especially H_2O_2. However, they still need to achieve a balance in these conditions, which requires an antioxidant capacity to ensure cancer cells survival. If the concentration of H_2O_2 is too high it will not be beneficial for cancer cells, causing their death (Egea et al., 2017; Gorrini et al., 2013) (**Figure 3**).

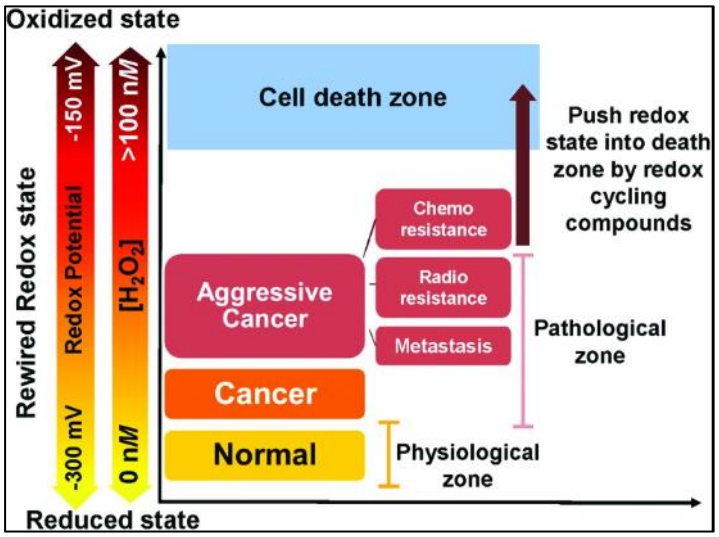

Figure 3. Potential therapeutic effect of increased ROS levels. Healthy cells proliferate in low to moderate ROS levels (yellow zone). However, cancer cells are able to survive in high ROS levels, under oxidative stress (pink zone). This persistant status of oxidative stress can promote metastasis and resistance. Nonetheless, if the ROS levels are pushed to the extreme, this will lead cancer cells to the death zone (blue), where ROS are too toxic for cancer cells. Reproduced from Chaiswing et al., 2018.

1.3.2. Superoxide Dismutase (SOD)

SODs are part of the endogenous antioxidant enzymes, as well as catalase (Cat) and glutathione peroxidase (GPx) (Bresciani et al., 2015), among others. SOD is a metalloprotein responsible for the dismutation of $O_2^{\bullet-}$ to H_2O_2 and oxygen by reducing its metal center followed by a reoxidation by $O_2^{\bullet-}$ (Fukai & Ushio-Fukai, 2011; Larosa & Remacle, 2018), being therefore considered the prime defender against ROS (Wang et al., 2018). SOD is present in all species. In mammals there are three isoforms of this enzyme, that vary depending on the metal present in its active site and where they are formed: the copper/zinc enzyme present in the cytosol (Cu/ZnSOD or SOD1), the manganese SOD (MnSOD or SOD2), present in the mitochondrial matrix and the extracellular SOD (ecSOD or SOD3), as the name stated, can be found in the extracellular matrix (Costa et al., 2021; Huang & Pan, 2020). The fact that all these isoforms exist in different places emphasize the high level of control that exists in mammalian cells to ensure ROS balance (Wang et al., 2018). Although all isoforms are crucial for ROS regulation, MnSOD is considered the most studied in the cancer field, playing a dual role in cancer development.

MnSOD has been shown to be cytoprotective regarding ionizing radiation (Becuwe et al., 2014) and its absence leads to dilated cardiomyopathy and neurodegeneration in mice (Fukai & Ushio-Fukai, 2011). The role that MnSOD has in cancer progression and whether it is a therapeutic target is still controversial. Some studies demonstrated that the presence of MnSOD and its polymorphisms may be a risk factor for breast cancer and can be involved in angiogenesis and metastatic spreading, contributing to a more aggressive tumor (Dhar & St. Clair, 2012; Robbins & Zhao, 2014).

On the other hand, it has also been shown that its overexpression prevents invasiveness, proliferation and promotes apoptosis and poor differentiation (Bonetta, 2018; Robbins & Zhao, 2014). Despite these controversies, it is clear that MnSOD protects cells from radiation, due to its modulating redox balance between radiosensitization and radioresistance, contributing for cell survival (Gupta et al., 2010; Huang & Pan, 2020). However, the clinical use of native SOD has its own disadvantages, such as elevated manufacturing costs, low permeability, high immunogenicity and short half-life (Bonetta, 2018). Moreover, the use of SOD in free form has a low accumulation in inflamed areas and a rapid renal excretion (Younus, 2018).

1.3.3. Other antioxidant enzymes

In order to limit ROS production and maintain the redox balance, cells possess endogenous antioxidant enzymes, *i.e.*, enzymes or cofactors that are involved in the elimination of ROS (Harris & DeNicola, 2020; Jelic et al., 2021). Besides the abovementioned SOD, Cat, GPx and peroxiredoxins (Prdx) are also enzymatic antioxidants responsible for converting the H_2O_2 into H_2O and/or O_2 (**Figure 4**). Although the nuclear factor-erythroid 2-related factor (NRF2) is not an antioxidant enzyme by itself, it is of utmost importance in redox biology, being responsible for the regulation and expression of more than 200 genes that are involved in the antioxidant response (Avolio et al., 2020). Besides controlling the expression of SOD, GPx, glutathione reductase (GR) and thioredoxin reductase (TR), NRF2 is also involved in the protection of cells from chemical carcinogens (Gill et al., 2016).

Catalase is an antioxidant enzyme responsible for transforming H_2O_2 into water and oxygen via a two-stage reaction. The first reaction is based on the oxidation of the heme protein by one H_2O_2 molecule, forming an oxoferryl porphyrin cation radical and water. The oxoferryl porphyrin radical rapidly reacts with the second molecule of H_2O_2 forming H_2O and O_2 and reducing the hypervalent iron intermediate to its resting state, being this the second reaction (Glorieux & Calderon, 2017). There are three types of catalases: typical catalases, catalase-peroxidases and manganese catalases. Typical catalase exists in all domains of life, and it is the only type of Cat present in humans (Galasso et al., 2021). Most of Cat is located in peroxisomes due to its sequence signal that is recognized by peroxisome receptors (Cecerska-Heryć et al., 2021). Besides its prime function, Cat can also be considered a scavenger of peroxynitrite, since it prevents its formation by oxidizing nitric oxide into nitrite in the presence of H_2O_2 (Galasso et al., 2021). In the last years, there has been a consensus concerning the high levels of ROS in cancer cells. However, regarding its antioxidant status, there are still some contradicting results. In LC, like in other types of cancer, there has been mixed results regarding the different antioxidant status of cancer cells and healthy cells. Despite this, most studies found lower catalase levels in cancer cells than in healthy cells (reviewed in Cecerska-Heryć et al., 2021).

The selenoprotein family GPxs enzyme is also responsible for removing H_2O_2 and maintaining the redox status inside the cell. GPx uses H_2O_2 to transform reduced glutathione (GSH) into oxidized glutathione (GSSG). In turn, GR regenerates GSSG into GSH with the help of NADPH. GR can be found in the mitochondria and cytosol. Besides being responsible for the conversion of GSSG into GSH, it is also involved in reactions responsible for oxygen detoxification, such as, the reduction of lipid or nonlipid hydroperoxides (Cecerska-Heryć et al., 2021; Jelic et al., 2021). GSH is the most abundant endogenous small molecule antioxidant and its originally synthesized in the cytosol and then distributed to several organelles (Bansal & Simon, 2018; Harris & DeNicola, 2020). GPx1 is the most abundant enzyme of the GPx family. It can be found in the cytosol and mitochondria, being also present in the peroxisomes (Lubos et al., 2011). GPx1 has also been shown to have a significant impact in cancer cells. An overexpression of this enzyme can protect cancer cells from apoptosis, and consequently, supporting cancer cell survival (Brigelius-Flohé & Flohé, 2020). Recent studies have shown that overexpression of GPx1 can possibly be a novel molecular target for cisplatin-based chemoresistance in NSCLC, since GPx1 can block cisplatin-induced ROS intracellular accumulation and activates PI3K-AKT signaling pathway that can lead to cisplatin resistance (Chen et al., 2019). When inhibited, GPx1 can suppress lung metastases of triple-negative breast cancer cells *in vivo* (Lee et al., 2020).

The Prdxs family is constituted by 6 peroxiredoxins localized in the cytosol, nucleus, mitochondria and/or peroxisomes. Besides catalyzing the reduction of H_2O_2 to water, Prdxs can also reduce alkyl hydroperoxides and peroxynitrite to alcohol and nitrite, respectively (Nicolussi et al., 2017). Prdxs are thiol-specific enzymes that use cysteine-containing active site to reduce peroxide substrates (Park et al., 2016). Prdxs 1-5 have two redox-active cysteine residues. While Prdxs oxidize the substrate, the 2-cys residues are oxidized, so thioredoxins (Trxs) donates an eletron to reduce the Prdxs 1-5. In the case of Prx6, since it only has one cysteine residue, glutathione is called to reduce Prx6 (Forshaw et al., 2019; Park et al., 2016). Since H_2O_2 is a second messenger involved in several signaling pathways, Prdxs can affect many cellular physiological functions like differentiation, apoptosis, lipid metabolism, cell proliferation. Prdxs appear to have a significant impact on cancer cells. Increased or decreased levels of Prdxs have been seen in several types of cancer, inhibiting cancer development or promoting its growth (Nicolussi et al., 2017). Their role in cancer is highly dependent on the type of tumor, stage and the specific Prdx involved. Prdx1, the Prdxs with the highest abundance in tissues and largest cellular distribution, appears to display a dual role regarding carcinogenesis. Some authors have summarized the different effects that Prx1 and its family members can have on different types of cancer. Briefly, *PRDX1* is overexpressed in several types of cancers, including LC, which appears to be involved in the promotion of cancer progression and chemo-/radio-resistance (Nicolussi et al., 2017; Park et al., 2016). Other studies have shown that the knockdown of *PRDX1* in LC significantly inhibits cell migration (Ha et al., 2012). Similarly to Prdx1, Prdx2 also tends to exhibit tumor-suppressive or tumor-promoting function, depending on the cancer and staging

(Nicolussi et al., 2017). In cancer cells, Prdx2 is usually associated to chemo- and radio-resistance (Nicolussi et al., 2017).

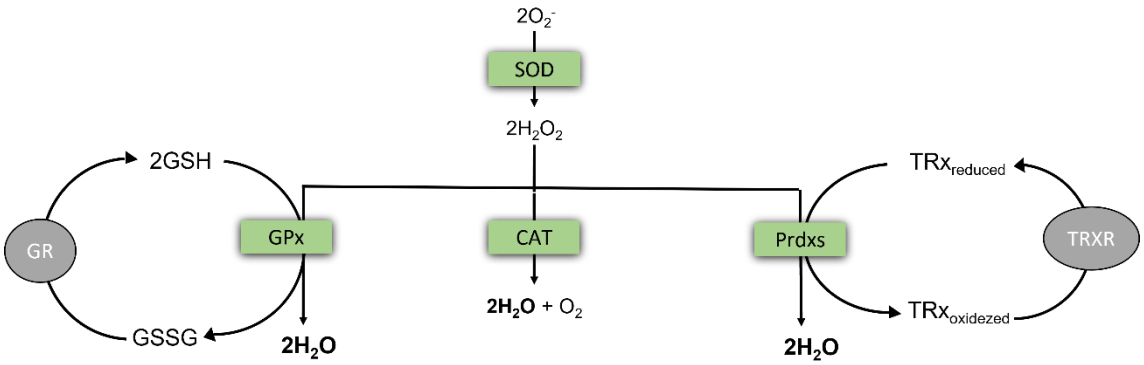

Figure 4. The main antioxidant enzymes responsible for detoxifying $O_2^{\bullet-}$ and H_2O_2. After the superoxide dismutase (SOD) transforms superoxide anion ($O_2^{\bullet-}$) into hydrogen peroxide (H_2O_2) glutathione peroxidase (GPx), catalase (Cat) and peroxiredoxins (Prdxs) can detoxify it into water (H_2O).

1.4 Superoxide dismutase mimics (SODm)

1.4.1. An overview

The use of native SOD was formerly suggested as a possible therapeutic strategy (Fukai & Ushio-Fukai, 2011; Larosa & Remacle, 2018). The clinical use of native SOD has its own disadvantages, such as elevated manufacturing costs, low permeability, high immunogenicity and short half-life (Bonetta, 2018). To overcome these disadvantages, redox-active compounds, also known as SODm, were initially created. These are synthetic compounds with the ability to simulate the properties of native SOD enzymes (Flórido et al., 2019). SODm have low molecular weight and longer half-lifes than native SOD, which leads to less expensive manufacturing and prevents an immunogenic response (Bonetta, 2018; Younus, 2018). These enzymes are capable of disproportionate $O_2^{\bullet-}$, but also scavenge other reactive species like $ONOO^-$ and NO_2 (Costa et al., 2019; Egea et al., 2017). This capability also implies a participation in the redox signaling pathways, affecting proliferation, differentiation and cell death (Costa et al., 2019). Its mode of action (MoA) leads to an additional amount of H_2O_2 present in the cells, which can push its concentration to the limit of toxicity, reducing proliferation and increasing the efficiency of chemotherapy and radiotherapy, and thus constituting an alternative approach for cancer treatment (**Figure 5**) (Egea et al., 2017; Fernandes et al., 2016; Mapuskar et al., 2019). Apart from these benefits it can also protect healthy cells against the adverse effects of chemo/radiotherapy (Bonetta, 2018). ROS levels have been shown to be highly increased in tumor cells, when compared with healthy cells, due to inflammation and mitochondrial dysfunction (Zalewska-Ziob et al., 2019). This aspect combined with the low activity often observed for first-line antioxidants enzymes, MnSOD, Cat, GPx and Prdx, leads to an accumulation of H_2O_2 and $O_2^{\bullet-}$ (Park et al., 2007;

Zalewska-Ziob et al., 2019). So, theoretically, SODm can be used in a relatively large cohort of cancer patients, since high ROS levels and low antioxidant levels are common factors of this disease. Additionally, SODm can provide protection and detoxify ROS in non-malignant cells. The research in the SODm field has been focused on rich coordination chemistry and metal complexes with a metal redox active site, mainly copper (Cu) and manganese (Mn), since they are the same metals used in the native SOD, and also iron (Fe). In addition, Fe and Mn porphyrins have almost endless possibilities in changing the porphyrin core structure, and porphyrins complexes are indeed highly stable (Batinić-Haberle et al., 2010). However, the compounds using Fe have proven to be toxic in *in vivo* studies (Batinić-Haberle et al., 1999). Even though Cu porphyrins displayed SOD-like activity, the "free" Cu(II) produced •OH radical by Fenton chemistry was identified as a disadvantage for biochemical applications (Batinić-Haberle et al., 2010). Therefore, Mn based SODm are the most suitable and stable ones. Inside this category there are cyclic polyamines, salen, nitroxides and porphyrin as the main types of Mn-based SODm (Bonetta, 2018), being the latter the most studied.

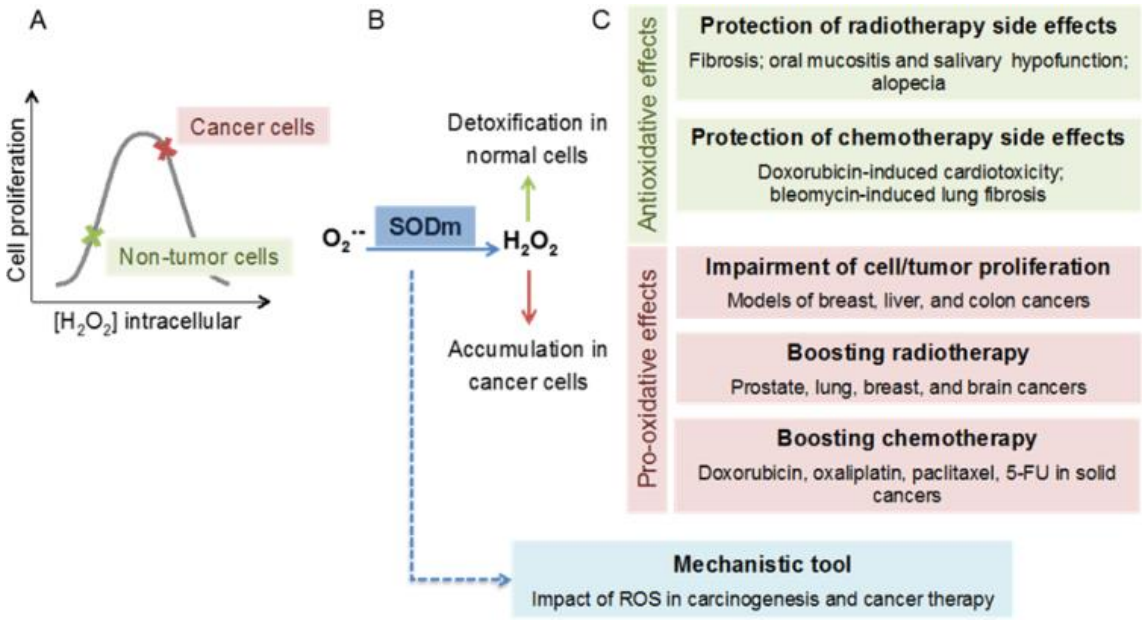

Figure 5. The dual role of SODm and its advantages. (**A**) Proposed model to describe the opposite effects of intracellular H_2O_2 concentration on the proliferation of cancer and normal cells. (**B**) The dual role of SODm in cancer cells and normal cells. (**C**) Potential applications of SODm in cancer treatment (Reproduced from Egea et al., 2017).

1.4.2. Manganese Porphyrins

The activity of manganese porphyrins (MnPs) is based on redox reactions of Mn, which changes the redox state between Mn (III) and Mn(II), similar to native SODs (Fernandes et al., 2010; Mapuskar et al., 2019). Despite MnPs having endless possibilities in changing the porphyrin core structure, there are some rules that must be followed to render them as stable molecules. First, it must have similar thermodynamic and

electrostatic properties to the native enzyme. This consists of having a reduction potential around +300 mV vs Normal Hydrogen Electrode (NHE), since it is in the middle of the potential of reduction (+850 mV vs. NHE) and of oxidation (-160 mV vs. NHE) of $O_2^{\bullet-}$. Chemically, the dismutation of $O_2^{\bullet-}$ by a MnP is a two-step reaction. Firstly, Mn(III) suffers a reduction by $O_2^{\bullet-}$ to generate Mn(II) and O_2 and then $O_2^{\bullet-}$ oxidizes Mn(II) to produce H_2O_2 and reestablish Mn(III) porphyrins (Batinić-Haberle et al., 2010; Fernandes et al., 2010). Other crucial aspect of MnPs is the need for a near-planar structure to bind to nucleic acids. For that, electron-withdrawing groups are placed in *ortho* positions, closer to the Mn site, allowing $O_2^{\bullet-}$ to reach the Mn site. The bioavailability of MnPs combined with its thermodynamics and electrostatics properties determine its efficacy in *in vivo* studies (Batinić-Haberle et al., 2010). MnPs have shown a high bioavailability towards several cellular organelles. Their bioavailability and distributions are due to their positive charges that bounds them toward anionic phosphate groups in the plasma membrane, mitochondria and nucleus. Also, their lipophilicity further enhances their bioavailability (Batinic-Haberle et al., 2021). Besides cancer, MnPs have been studied in several other fields, namely in Alzheimer and Parkinson diseases, radiation injury, amyotrophic lateral sclerosis and cerebral palsy (Batinić-Haberle et al., 2010). More recently three main MnPs have been closely studied regarding their bioavailability and pharmacokinetics: Mn (III) meso-tetrakis (N-ethylpyridinium-2-yl) porphyrin (MnTE-2-PyP^{5+}; MnTE-2-PyP, BMX-010), Mn(III) meso-tetrakis(N-n-hexylpyridinium-2yl) porphyrin (MnTnHex-2-PyP^{5+}; MnTnHex) and Mn (III) meso-tetrakis (N-butoxyethyl pyridine-2-yl) porphyrin (MnTnBuOE-2-PyP^{5+}, MnTnBuOE, MnBuOE, BMX-001).

In MnTE-2-PyP^{5+} the cationic pyridyl nitrogens are in the *ortho* position, resulting in all the properties necessary to make it a stable MnPs (Mapuskar et al., 2019). There were multiple *in vitro* and *in vivo* studies where MnTE-2-PyP^{5+} was assessed in lymphoma (Jaramillo et al., 2015), prostate cancer (Makinde et al., 2010; Tong et al., 2016), breast cancer (Rabbani et al., 2009), skin cancer (Zhao et al., 2005) and colon and cervical tumors (Archambeau et al., 2013). It proved to be radioprotective of healthy cells and radiosensitive for cancer cells, being especially effective when combined with anti-cancer treatments. It reduced several processes involved in cancer progression, such as, cell proliferation, mitosis, vascular density and angiogenesis. For example, when administered alone it reduced the multiplicity of tumors in skin cancer, reducing 31 to 17 papillomas (Zhao et al., 2005). Also, it has shown to be highly effective in reducing side effects that occur during chemo and radiotherapy (Archambeau et al., 2013). However, MnTE-2-PyP^{5+} did not displayed an optimal bioavailability and distributions comparing with other MnPs, so further adjustments were necessary. In this context, the SODm MnBuOE and MnTnHex were further developed and widely studied and constitute the object of study of the present dissertation, since their role in NSCLC *in vitro* has not yet been explored. The inherent characteristics and pharmacological interest of these two compounds will be detailed in the following chapters.

Chapter 2

Aim

Hypothesis

Does MnTnHex and MnBuOE have an impact in NSCLC cells by modulating their viability, cell cycle distribution and migration? And if so, does their combination with cisplatin, revealed the usefulness of these compounds as chemosensitizers?

General aim

As mentioned earlier, LC is the leading cause of cancer-related deaths for both sexes combined, with NSCLC being its most common subtype. NSCLC has a low 5-year survival rate mainly due to the fact that is often diagnosed at advanced stages. This type of cancer tends to develop resistance to platinum-based chemotherapy. Cancer cells, including LC cells, usually possess higher ROS levels and lower antioxidant levels than healthy cells. These features supported the development of a novel approach based on the increase of the ROS levels, particularly H_2O_2, in order to surpass the limit of toxicity, and consequently leading cell death. With this in mind, SODm have been studied in cancer models *in vitro*, being useful in the context of breast cancer, renal cancer and glioblastoma. These compounds can increase ROS levels in cancer cells and boost the efficacy of chemo- and radiotherapy, while at the same time they can provide protection of healthy cells from the adverse effects caused by these standard treatments. Nevertheless, in the scope of NSCLC scarce studies have been performed. For this reason, the main goal of this work was to assess the impact of two very successful SODm, MnTnHex and MnBuOE, in NSCLC cells, alone and combined with cisplatin as a novel therapeutic strategy. This work was developed using two representative NSCLC cell lines, the classical A549 cells, and the H1975 cell line derived from a tumour of a non-smoker.

To achieve the abovementioned main goal different objective were pursued:

- Determination of the antioxidant status of both NSCLC cells by analyzing the gene expression of the main H_2O_2 antioxidant detoxifying enzymes;
- Assessment of the MnTnHex and MnBuOE cytotoxicity profile, alone or in combination with cisplatin, in both NSCLC cell lines using CV and MTS reduction assays;
- Evaluation of the impact of both MnPs, either alone or combined with cisplatin, on collective and individual migration and invasion on both NSCLC cells, by performing wound-healing, chemotaxis and chemoinvasion assays;
- Comprehensive analysis of the exometabolome of NSCLC cells when exposed to MnTnHex, either alone or in combination with cisplatin.

Chapter 3

MnTnHex-2-PyP^{5+} Displays Anticancer Properties and Enhances Cisplatin Effects in Non-Small Cell Lung Cancer Cells

This chapter was adapted from:

Soares, R.B.; Manguinhas, R.; Costa, J.G.; Saraiva, N.; Gil, N.; Rosell, R.; Camões, S.P.; Batinic-Haberle, I.; Spasojevic, I.; Castro, M.; Miranda, J.P.; Amaro, F.; Pinto, J.; Fernandes A.S.; Guedes de Pinho, P.; Oliveira, N.G. MnTnHex-2-PyP^{5+} Displays Anticancer Properties and Enhances Cisplatin Effects in Non-Small Cell Lung Cancer Cells. *Antioxidants* **2022**, 11, 2198.

3.1. Introduction

As abovementioned in Chapter 1, MnTnHex is one of the most promising SODm (**Figure 6**). This redox active compound is the most lipophilic MnP, having a high bioavailability and distribution, while at the same time displaying low toxicity in healthy cells and tissues (Batinic-Haberle et al., 2021). This compound has been studied in different types of cancer, *e.g.,* breast, renal cancer and glioblastoma (Costa et al., 2019; Flórido et al., 2019; Shin et al., 2021; Keir et al., 2011)**.** It was also found to reduce the viability and migration of renal cancer cells, bearing metastatic potential (Costa et al., 2019). In addition, when combined with doxorubicin (dox), MnTnHex reduced the migration of breast cancer cells (Flórido et al., 2019). In mice, MnTnHex was able to significantly delay brain tumor growth by 3 to 34 days depending on the xenograft (Keir et al., 2011). In a comparative study regarding the radioprotective effect of several antioxidant manganese compounds in ataxia-telangiectasia lymphoblastoid cells and wildtype (WT) cells derived from healthy individuals, MnTnHex was the most effective in protecting WT cells from radiation-induced apoptosis and DNA damage at nM levels (Pollard et al., 2009). This compound has also been studied in V79 lung fibroblasts and did not exhibit cytotoxicity (Fernandes et al., 2010). Other studies have been conducted to address the radioprotective effect of MnTnHex in the lungs. Cline *et al.* demonstrated that MnTnHex was able to delay radiation-induced lung lesions in non-human primates (Cline et al., 2018). Also, at the concentration of 0.05 mg/kg MnTnHex did not show any evidence of lung cytotoxicity. Regarding LC cells, there is, however, a lack of information considering the cytotoxic effects of MnPs. The present study intends to fill this gap. In this chapter, the impact of MnTnHex, either as a single drug or combined with cisplatin, was assessed for the first in NSCLC cell lines A549 and H1975.

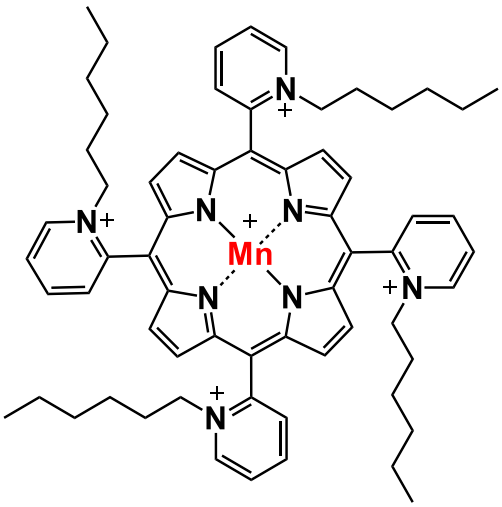

Figure 6. Chemical structure of MnTnHex-2-PyP^{5+} (chemical name: Mn(III)*meso*-tetrakis(*N*-n-hexylpyridinium-2-yl)porphyrin), designated as MnTnHex throughout the text for simplicity**.** Reproduced from Soares et al., 2022 (submitted).

3.2. Materials and Methods

3.2.1. Chemicals

RPMI-1640 with L-glutamine was purchased from Biowest (Nuaillé, France). MnTnHex was synthesized and characterized at Duke University School of Medicine, according to Batinic-Haberle et al. (Batinić-Haberle et al., 2002). Cisplatin, penicillin-streptomycin solution (10,000 units/mL of penicillin; 10 mg/mL of streptomycin), crystal violet (CV), sodium bicarbonate, and O-(2,3,4,5,6-pentafluorobenzyl) hydroxylamine (PFBHA, ≥ 99%) were obtained from Sigma-Aldrich (Madrid, Spain). Ethanol absolute and acetic acid were purchased from Merck (Darmstadt, Germany). Sodium pyruvate was purchased from Lonza (Basel, Switzerland) and trypsin (0.25%), and fetal bovine serum (FBS) from Gibco (Eugene, OR, USA). HEPES and D-Glucose were obtained from AppliChem (Darmstadt, Germany). CellTiter 96® Aqueous MTS (3-(4,5-Dimethylthiazol-2-yl)-5-(3-carboxylmethoxyphenyl)-2-(4-sulfophenyl)-2H-tetrazolium) was acquired from Promega (Madison, WI, USA).

A stock solution of MnTnHex and its dilutions were prepared in Milli-Q water. Cisplatin was dissolved in saline solution (0.9% NaCl) and its aliquoted solutions were stored at -20 ºC. In all cell-based assays, controls were also included, in which cells were exposed to either saline solution or Milli-Q water.

3.2.2. Cell Culture

The human NSCLC cell lines A549 and H1975 (**Figure 7**) were obtained from the American Type Culture Collection (ATCC, Manassas, VA, USA). Both cell lines were cultured in monolayer in RPMI-1640 medium with L-glutamine supplemented with 1 mM HEPES (Applichem Panreac), 200 g/L D-glucose (Applichem Panreac), 100 mM Sodium pyruvate (Lonza), 1.5 g/L sodium bicarbonate (Sigma-Aldrich), 10% FBS, and 1% Pen/Strep. These cells were maintained at 37 °C, under a humidified atmosphere containing 5% CO_2 in air. Henceforward this medium will be designated as complete cell culture medium. The A549 cell line was established in 1972 from an explant tissue culture of lung carcinomatous from a Caucasian male. These cells have a doubling time of approximately 24h (Bible & Kaufmann, 1996) and mutated KRAS (Hanke et al., 2018). Also, they are known for their sensitivity to cisplatin (Huang et al., 2020). The H1975 cell line originated from a non-smoker female with lung adenocarcinoma in 1988, having a duplication time of 30h (Zhao et al., 2015). This cell line has the L858R (exon 21) and T790M (exon 20) double mutation, which causes the cells to be initially sensitive to EGFR-TKIs, due to the L858R mutation, but then acquire resistance to these inhibitors, since they also have an EGFR T790M mutation (Zhao et al., 2015). Therefore, this cell line is known for being resistant to gefitinib.

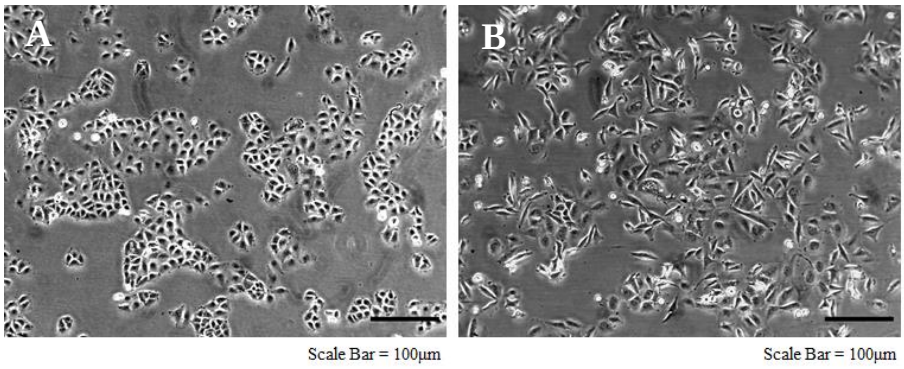

Figure 7. Representative images of A549 and H1975 cell lines. (**A**) A549 cells with low passage number (passage 51) and (**B**) H1975 with low passage number (Passage 15)**.**

3.2.3. Gene expression

The gene expression of the main antioxidant enzymes responsible for detoxifying H_2O_2 (*CAT*, *GPX*, *PRDX*) was assessed using quantitative reverse transcription PCR (RT-qPCR), following a previously described protocol (Cipriano et al., 2020). RNA isolation was performed using TRIzol™ Reagent (Invitrogen, Massachusetts, USA) and quantified for cDNA synthesis. cDNA synthesis was obtained from 0.5 µg of RNA using a commercially available kit (NZYTech, Lisbon, Portugal). The qPCR was performed using PowerUp™ SYBR® Green Master Mix (Applied Biosystems®/ Life Tech-nologies, Austin, TX, USA), according to the manufacturer's instructions. A final reaction volume of 15 µL, with 1 µL of template cDNA and 0.1 µM of forward and reverse primers was used, and the reaction was conducted in the QuantStudio™ 7 Flex Real-Time PCR System (Applied Biosystems™, Massachusetts, EUA). The forward and reverse primers used are present in **Table 1**. The amplification of cDNA comprised of denaturation at 95 °C for 10 min, 40 cycles of denaturation at 95 °C for 15 s, annealing at 60 °C for 1 min and extension at 72 °C for 30 s. As a quality and specificity measurement, a dissociation stage was added to determine the melting temperature in all runs. The relative expression of target genes in each cell line was calculated using the expression $2^{-\Delta Ct}$, where ΔCt = Average Ct (gene of interest) - Average Ct (β-ACTIN) (Takemoto et al., 2019) and normalized to the reference gene β-ACTIN.

Table 1. Primers used for qRT-PCR characterization of NSCLC cells

	Primer sequence	Reference
CAT	F: TGGAGCTGGTAACCCAGTAGG R: CCTTTGCCTTGGAGTATTTGGTA	Singh et al., 2020
GPX1	F: CGCTTCCAGACCATTGACATC R: CGAGGTGGTATTTTCTGTAAGATCA	Romanowska et al., 2007
PRDX1	F: CCACGGAGATCATTGCTTTCA R: AGGTGTATTGACCCATGCTAGAT	Cai et al., 2018
PRDX2	F: CCTTCAAAGAGGTGAAGCTG R: GTTGCTGAACGCGATGAT	Jing et al., 2020

3.2.4. CV Staining Assay

The cytotoxic effects of MnTnHex alone in both NSCLC cell lines were first evaluated by the CV staining assay, following a previously described protocol (Fernandes et al., 2010). Briefly, cells were seeded at $3x10^3$ cells/well in 200 µL of a complete medium in 96-well plates and incubated for 24 h at 37 °C under a 5% CO_2 atmosphere. After the 24 h period, the culture medium was renewed, and the cells were incubated with a range of MnTnHex (0.5-25 µM) concentrations for 72 h. Cells were also incubated with 50 µM of cisplatin as a positive control. After incubation, cells were washed with PBS to remove non-adherent cells (non-viable cells). The adherent cells were fixed with ice-cold 96% ethanol for 15 min and stained with 0.1% CV for 5 min. After washing the microplate with tap water, the stained cells were resuspended in 200 µL of 96% ethanol/1% acetic acid. The absorbance was measured at 595 nm (OD595) using a SPECTROstar OMEGA microplate reader (BMG Labtech, Offen burg, Germany). Absorbance values presented by control cells corresponded to 100% of cell viability. Three independent experiments were performed, and six replicates were used for each condition in each independent experiment. The half-maximal inhibitory concentration (IC_{50}) was calculated based on the concentration-response curve using GraphPad Prism® 7.0 (GraphPad Software, Inc., La Jolla, CA, USA). Image acquisition was performed using a Motic AE2000 Inverted Phase Contrast Microscope and a 40x objective.

3.2.5. MTS Reduction Assay

The MTS reduction assay was performed as a complementary cell viability assay by applying the same conditions as in the CV assay and following a previously described protocol (Guerreiro et al., 2017). This technique determines the cytotoxic effects of compounds based on the ability of cells to convert the soluble tetrazolium salt into a brownish-colored formazan product by a mitochondrial enzyme (NAD-dependent-dehydrogenase). Only viable cells can metabolize this salt. Briefly, after treatment with MnTnHex, cells were washed with PBS, followed by the addition of 100 µL of new complete medium and 20 µL of MTS substrate prepared from the CellTiter 96® Aqueous MTS, according to the manufacturer's instructions. Cells were incubated for 2 h and the results were measured at an absorbance of 490 nm and 690 nm (reference wavelength) using a SPECTROstar OMEGA microplate reader. Absorbance values presented by control cells corresponded to 100% of cell viability. Four independent experiments were performed, and three replicates were used for each condition in each independent experiment. The IC_{50} was also calculated based on the concentration-response curve using GraphPad Prism® 7.0 (GraphPad Software, Inc., La Jolla, CA, USA).

3.2.6. Combinatory Assays with MnTnHex and Cisplatin

The cytotoxic profile of MnTnHex combined with cisplatin in A549 and H1975 cells was evaluated by the CV staining assay, following a similar protocol as previously described. After the initial 24 h incubation period, the culture medium was changed, and

cells were exposed to both compounds simultaneously for 72 h. Two concentrations of MnTnHex were used for both cell lines (0.5 and 1 µM). Cisplatin concentrations used were 1 and 2 µM for A549 cells and 1 and 5 µM for H1975 cells. Four independent experiments were performed, and six replicates were used for each condition in each independent experiment.

3.2.7. Cell Cycle Analysis

To assess the effect of the compounds on cell cycle distribution, cell DNA content was assessed by flow cytometry, following a previously described protocol (Manguinhas et al., 2020). Briefly, A549 and H1975 cells were seeded in 6-well plates at approximately $5x10^4$ and $6x10^4$ cells/well, respectively, and incubated for 24 h. After this period, the culture medium was changed and cells were exposed to MnTnHex (0.5 and 1 µM) and cisplatin (1 µM), both alone or in combination, for 72 h. The medium was collected, and the cells were detached using a 5 mM EDTA solution in PBS at 37 °C. Next, they were washed with cold PBS and fixed with ice-cold 80% ethanol. Cells were stained with propidium iodide (PI) (10 µg/mL) and treated simultaneously with RNase A (20 µg/L) for 15 min and were then analyzed using a Cytek Aurora flow cytometer (Cytek Biosciences, Fremont, CA, USA). Data acquisition was performed using Cytek SpectroFlo software (Cytek Biosciences, Fremont, CA, USA) and was analyzed with FlowJo® (Tree Star Inc., San Carlos, CA, USA). Three to four independent experiments were performed.

3.2.8. Selection of MnTnHex and Cisplatin Concentrations for the Migration Assay

In migration assays, it is crucial to guarantee two conditions. The first one is to only use non-toxic concentrations of compounds, since it is necessary to ensure an effect due to the process alone and not due to a consequence of cytotoxicity. Secondly, the use of the lowest amount of FBS possible is recommended, to guarantee that the observed results are a consequence of the migration processes and not a result of proliferation.

To select the suitable non-toxic concentrations for the migration assay, the MTS reduction assay was performed in A549 and H1975 cell lines, as previously described (Guerreiro et al., 2017). Approximately $8x10^3$ cells/well were seeded in 96-well plates in complete culture medium for 24 h. After this period, the complete medium was replaced by a new cell culture medium containing 2% FBS. Cells were incubated with a range of low concentrations of MnTnHex (0.25-5 µM) or cisplatin (0.25-1 µM) for 32 h in both cell lines. The MTS assays were performed, and non-toxic concentrations of both compounds were selected. Three independent experiments were performed, and three replicates were used for each condition in each independent experiment.

3.2.9. In Vitro Wound-Healing Assay

The *in vitro* wound-healing assay was performed to determine the collective cell migration ability in both NSCLC cells. This assay was performed according to a previously described protocol (Manguinhas et al., 2020). Briefly, A549 and H1975 cells were seeded in 24-well plates at approximately $8x10^4$ and $6.5x10^4$ cells/well, respectively, and incubated for 24 h in complete cell culture medium. After this period, the culture medium was removed, and the injury in the cell monolayer was performed using a 200 µL sterile pipette tip, resulting in a scratch of approximately 0.6-0.8 mm wide. Cells were then washed with PBS to eliminate any cellular debris and incubated with culture medium containing 2% FBS and the desired compounds. A549 cells migrated in the presence of MnTnHex (5 µM) and/or cisplatin (0.5 µM). H1975 cells migrated in the presence of MnTnHex (0.5 µM) and/or cisplatin (1 µM). Both cell lines migrated for 32 h. Image acquisition was performed using a Motic AE2000 Inverted Phase Contrast Microscope and using a 40x objective. Scratch width was measured using Motic Images plus v2.0 software (Motic, Barcelona, Spain) at 0, 8, 24, and 32 h for A549 cells and at 0, 20, 24, and 32 h for H1975 cells, after the injury. The initial time-point was considered as 0% of wound closure and the percentage of cell migration was calculated based on the initial distance. At each time point, two pictures of each scratch were taken for each condition. Three different measures were made for each picture. Three to four independent experiments were performed.

3.2.10. Metabolomics

3.2.10.1. Cell culture and collection of extracellular medium

To assess the exometabolome (extracellular metabolites present in culture medium) of cells when exposed to MnTnHex and/or cisplatin, sample collection and preparation for analysis were performed according to a previously described protocol (Amaro et al., 2020). Briefly, A549 and H975 cells were seeded in 6-well plates at a density of approximately $8x10^4$ and $9x10^4$ cells/well, respectively, and incubated for 24 h in complete cell culture medium. After this incubation period, the medium was renewed and cells were exposed to the compounds for 72 h, using the same concentrations as in the cell cycle assay. Six to seven independent experiments were performed. The extracellular media from each condition and blanks (medium without cells) were collected and centrifuged (1200 x *g*, 5 min, 4 °C). Then, the supernatant was collected and immediately stored at -80 °C until analysis. A pool of the extracellular media of all samples and blanks was also prepared to be used as quality control (QCs) to check the analytical reproducibility of the experiment.

3.2.10.2. GC-MS analysis: sample preparation and equipment

The GC-MS analysis was focused on the profile of volatile carbonyl compounds (VCCs), which include several aldehydes and ketones that may be produced as a result of oxidative stress. The preparation of all samples and VCCs extraction was performed

according to previously described protocols based on headspace solid-phase microextraction (HS-SPME) (Amaro et al., 2020; Lima et al., 2019). Briefly, frozen samples were thawed slowly at room temperature. The analysis of VCCs was performed by placing 1.5 mL of culture medium in a 10 mL glass vial together with 35 µL of the derivatizing agent (PFBHA, 40 g/L). The samples were incubated for 6 min at 62 °C, following by an extraction step of VCCs from sample headspace using a polydimethylsiloxane/divinylbenzene (PDMS/DVB) fiber at the same temperature for 51 min, under continuous stirring (250 rpm). To ensure and evaluate the reproducibility of the analyses, all samples were randomly injected, and the QCs were injected under the same conditions, on every 7 samples. The VCCs adsorbed to the fiber were then analyzed in a 436-GC system (Bruker Daltonics, Fremont, CA) coupled with an EVOQ Triple Quadrupole (TQ) mass detector using a Bruker MS workstation software (version 8.2, Bruker Daltonics, Bremen, Germany). A fused silica capillary column Rxi-5Sil MS (30 m x 0.25 mm x 0.25 µm; RESTEK Corporation, U.S., Bellefonte, Pennsylvania) was used and helium C-60 (Gasin, Portugal) was chosen as the carrier gas (flow rate 1 mL/min). The oven temperature was settled at 40 °C for 1 min, rising to 250 °C (rate 5 °C/min), held for 5 min, followed by increasing to 300 °C (rate 20 °C/min). The MS detector was operated in the electron imf1epact mode (70 eV) at 270 °C. The temperature of transfer line was 260 °C and the manifold was 40 °C. Data acquisition was performed in full scan mode within a *m/z* mass range between 35-600 *m/z* with a scan time of 250 ms.

3.2.10.3. Compound identification and GC-MS data pre-processing

To identify the VCCs detected in the GC-MS chromatogram, a comparison between the MS fragmentation and the mass spectra present in the National Institute of Standards and Technology (NIST 14) database was performed, as well as a comparison with the experimental Kovats retention index (RI) and the ones present in the literature. When possible, the identification of the VCCs was confirmed by comparing the retention time (RT) and MS spectra of the samples with the commercially available standard compounds analyzed under the same conditions. All VCCs identified in culture media are indicated in **Table A1**, as well as a representative chromatogram (**Figure A1**). The GC-MS chromatograms were converted to netCDF and pre-processed in MZmine-2.53 (Pluskal et al., 2010). The pre-processing steps included crop filtering (*m/z* range 50-500, RT range 14.50-49.00 min), peak detection (noise level 5×10^4), chromatogram builder (minimum 5 scans, in-tensity threshold 1×10^5, minimum highest intensity 5×10^4), deconvolution (minimum peak height 1×10^5, baseline level 5×10^4, peak duration 0.02-0.5 min, minimum data points 5), and alignment (*m/z* tolerance 0.1, RT tolerance 0.2). The pre-processed matrix was filtered by excluding all *m/z*-RT pairs with a relative standard deviation (RSD) higher than 30% considering the QCs (n=12), followed by normalization of the area of each *m/z*-RT pair by the total area of all *m/z*-RT pairs with RSD < 30%.

3.2.10.4. Statistical analyses of the GC-MS data

Principal component analysis (PCA) and partial least squares discriminant analysis (PLS-DA) were used to provide visual representations of the similarity and variability among the pre-processed GC-MS data for QCs and each condition under study. The identification of VCCs differing between the classes under study was performed using Volcano plots which represented the *p*-values from a non-parametric test (Mann-Whitney test) and the fold-change (FC) values between two groups under study (cells exposed to MnTnHex or its combination with cisplatin vs. non-exposed cells) for all *m/z*-RT pairs. The PCA, PLS-DA and Volcano plots were performed in the MetaboAnalyst 5.0 (Pang et al., 2021). Finally, the levels of the VCCs selected in the Volcano plots were compared among the groups under study by Kruskal-Wallis ANOVA and represented in boxplots using GraphPad Prism (version 9, San Diego, CA, USA). Statistical significance was considered for p-value < 0.05 (95% confidence interval).

3.2.13. Statistical analysis

The results presented correspond to mean values and respective standard deviations (SD). Prism 7.04 software (GraphPad, La Jolla, CA, USA) was employed for data comparison and the development of artwork. After assessing normality and homogeneity of the variances, the differences in mean values of the results were evaluated by Student´s t-test. Comparison of multiple mean values was performed by one-way ANOVA with post-hoc Tukey and one-way ANOVA with post-hoc Ducan. All analyses were performed with the SPSS statistical package (version 25; SPSS Inc. Chicago, IL, USA) and the level of significance considered was $p < 0.05$ (represented as: *$p < 0.05$, **$p < 0.01$, ***$p < 0.001$ and ****$p<0.0001$).

3.3. Results and Discussion

3.3.1. A549 and H1975 cell lines express low catalase levels

To determine the expression of the main antioxidant enzymes responsible for detoxifying H_2O_2, a qRT-PCR was conducted (**Figure 8**). According to this analysis, the gene expression levels for *CAT* were quite low in both cell lines. CAT is a pivotal cytosolic antioxidant enzyme responsible for dismuting H_2O_2 into H_2O and O_2. Regarding GPX1 (another cytosolic enzyme and major intracellular antioxidant enzyme), low levels were present, particularly in A549 cells. PRDX isoforms 1 and 2 are mainly localized in cytosol. Amongst the PRDXfamily, the isoform 1 possesses the widest cellular distribution and also display the highest abundance in various tissues. It is also the isoform most resistant to peroxidation damage within wide range of H_2O_2 (Neumann et al., 2009).

Importantly, we found that *PRDX1* has high mRNA expression levels in both cell lines. The expression of this gene was more than 2-fold higher in A549 cells than in H1975 cells, albeit this different was not significant. PRDX2 (an isoform more sensitive to peroxidation than PRDX1 (Sharapov et al., 2020)) was present in H1975 cells at low levels, these levels being even lower in A549 cells under our experimental conditions. The A549 cell line also has lower level of GPX1 than H1975 cell, this difference being significant ($p<0.001$).

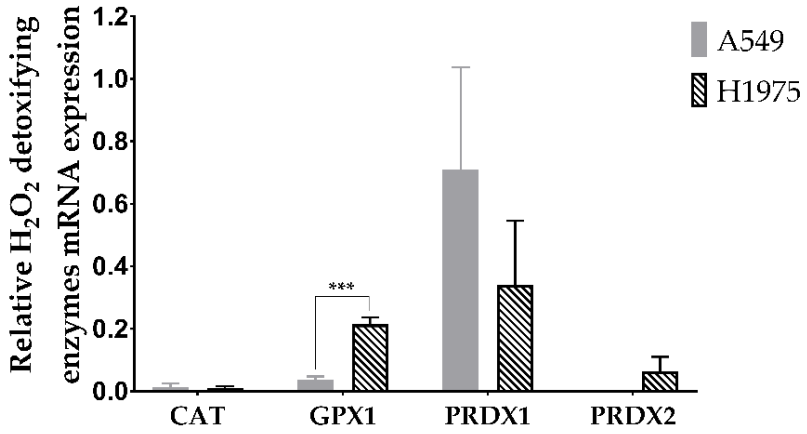

Figure 8. Gene expression analyses of the main H_2O_2 detoxifying enzymes. Values represent mean ± SD (n=3) and are normalized to the reference gene β-ACTIN. ***$p<0.001$ (Student's t-test).

To better characterize both cell lines in terms of basal antioxidant gene expression, the relative expression of the genes that code for the main H_2O_2 processing enzymes was carried out through RT-qPCR.

Our results showed that both NSCLC cell lines exhibited very low levels of CAT, and relatively low levels of GPX1 and PRDX2. PRDX1 was highly expressed and is the predominant peroxiredoxin isoform of cells. According to the Human Protein Atlas (www.proteinatlas.org), comparing A549 cells with several other cell lines show that

these cells rank along those with lower catalase levels. In addition, the levels of PRDX2 were undetected in A549 cells when compared with other cell lines. Similar results in terms of gene expression were observed in studies with lung cancer. Some authors compared the antioxidant levels between tumor and tumor-free lung tissue. The lung tumor tissue showed lower levels of catalase expression than healthy tissue, while similar levels of GPX1 were detected in both cancerous and non-cancerous tissue. In addition, by performing the immunohistochemical localization of catalase, the results revealed lower or no expression of this enzyme in tumor cells (Chung-man Ho et al., 2001). Jiang *et al*. analysed the expression of several PRDXs in multiple cell lines, and the absence of expression of PRDX2 was also found in A549 cells (Jiang et al., 2014). Overall, our analysis, along with the information reported elsewhere, pointed out to the low gene expression level of these key enzymes, particularly catalase, in NSCLC cell lines, suggesting their propensity to changes in redox balance, thus anticipating the usefulness of the MnPs-based redox modulators, in the context of this type of cancer. Cancer cells use high levels of ROS to their own advantage for proliferation. Yet, the balance is delicate, and depending upon their levels of endogenous antioxidants, a tiny amount of external ROS may drive cancer cells into death.

3.3.2. MnTnHex displays a marked cytotoxic effect in NSCLC cells

To establish the cytotoxic profile of MnTnHex in A549 and H1975 cell lines, two different methodologies were used, the CV staining assay and the MTS reduction assay. In both assays and for both NSCLC cell lines, MnTnHex exhibited a concentration-dependent decrease in cell viability (0.5-25 μM) (**Figure 9**). The IC_{50} values for the CV assay were 0.9 μM and 0.7 μM for A549 and H1975 cells, respectively. Moreover, the IC_{50} values for the MTS assay were 2.1 μM in A549 cells and 1.0 μM for H1975 cells. From these results, it is clear that MnTnHex exhibited marked cytotoxic effects in both NSCLC cells. However, in H1975 cells, this compound displayed IC_{50} values lower than the IC_{50} of A549 cells, thus being more cytotoxic. The morphology of cells was also analyzed, suggesting that A549 cells roughly maintain their morphology upon the increase of MnTnHex concentrations (**Figure 9C**). However, in the case of H1975 cells, the morphology appears to be altered for higher MnTnHex concentrations. Indeed, the cells appear to be more elongated than control cells (**Figure 9D**). Finally, considering these results, MnTnHex concentrations of 0.5 and 1 μM were selected for combinatory assays, in both cell lines since these concentrations induced distinct levels of cytotoxicity.

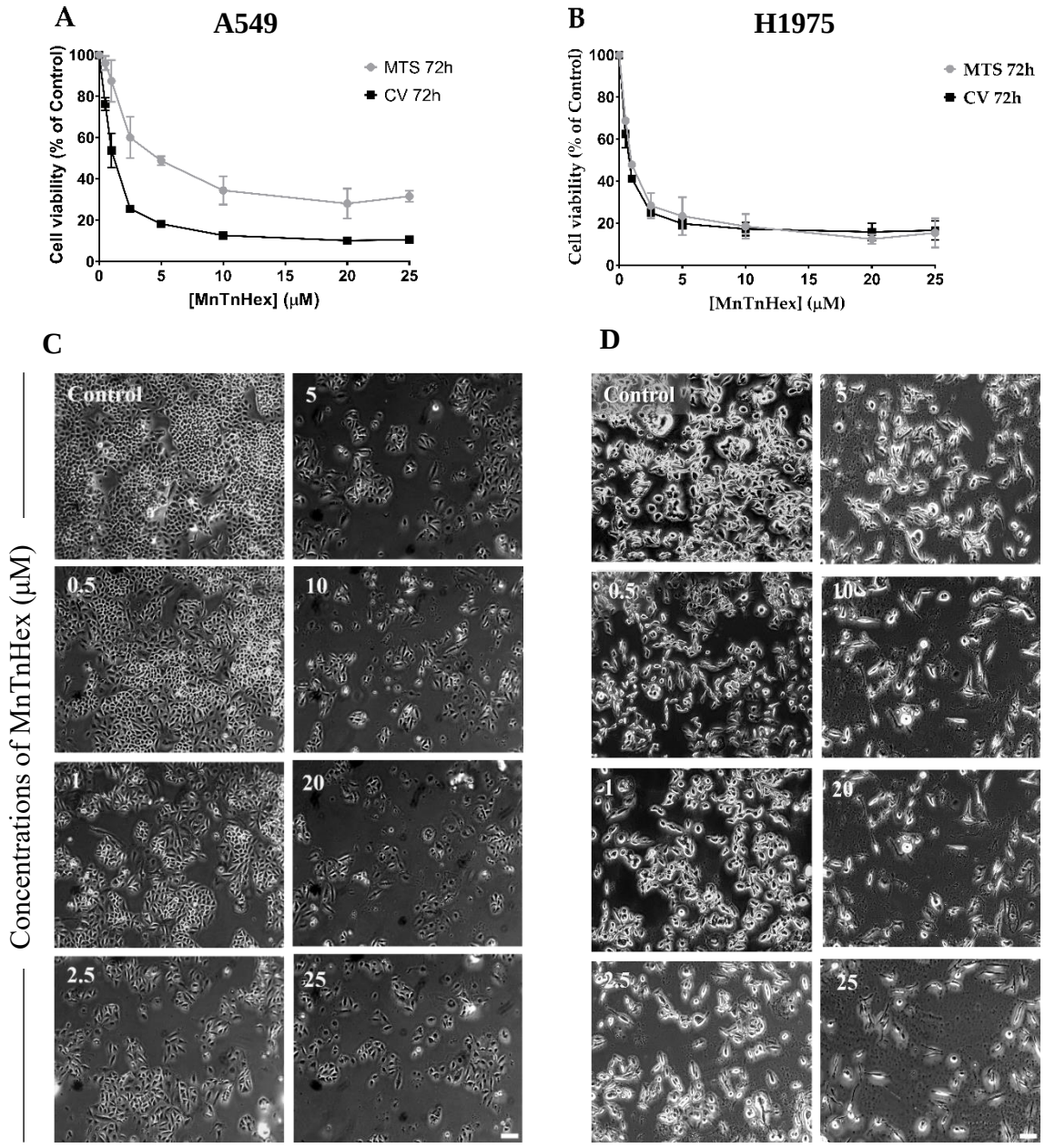

Figure 9. Cytotoxic effects of MnTnHex (0.5 – 25 μM) in A549 cells and H1975 cells. The decrease in cell viability upon exposure to MnTnHex, for 72 h, was assessed by CV and MTS assay in (**A**) A549 cells and (**B**) H1975 cells. Values represent mean ± SD (n = 3-4) and are expressed as percentages of the control cells. (**C**) A549 cell morphology upon treatment with MnTnHex. (**D**) H1975 cell morphology upon treatment with MnTnHex. Scale bar = 100 μm.

We evaluated the cytotoxic impact of MnTnHex in both NSCLC cell lines using complementary methodologies. MnTnHex, as a single drug, exhibited a concentration-dependent decrease in terms of cell viability, revealing quite low IC_{50} values, in some cases reaching sub-micromolar range. This fact, we believe, is of high relevance since it demonstrates the ability of this compound to act as a promising stand-alone drug in

NSCLC. It should be emphasized that our previously published results with MnTnHex using cells of non-tumor origin clearly revealed opposite results. Indeed, this compound had already been assessed in V79 lung fibroblasts (MTT reduction assay, 24-hour incubation) (Fernandes et al., 2010b) as well as in renal cells (Vero cells) (CV assay, 48 h-incubation) (Costa et al., 2016). In both cases, MnTnHex at concentrations up to 25 μM did not show any evidence of cytotoxicity. Conversely, in our previous studies, MnTnHex already exhibited high cytotoxic effects in renal cancer cells (786-O) (Costa et al., 2019), which is in line with the herein observed results with NSCLC cells and demonstrates this important feature in other invasive cancer cells. While there are some experimental differences in the protocols used, it is clear that MnTnHex has differential effects in malignant vs. non-tumor cells.

3.3.3. MnTnHex enhances the cytotoxicity of cisplatin

To assess the effect of MnTnHex combined with cisplatin, NSCLC cells were exposed to both compounds simultaneously, and the effects were evaluated using CV assay. For all combinations tested, a significant decrease in cell viability when compared to the cisplatin-treated cells was observed (**Figure 10**). In A549 cells, the cytotoxicity of cisplatin alone was slight to moderate at 1 and 2 μM, respectively, which was increased when combined with MnTnHex. In absolute percentage values, the decrease in cell viability observed for 1 μM cisplatin, when combined with 0.5 and 1 μM MnTnHex, was 18.8 % ($p<0.01$) and 39.2% ($p<0.001$), respectively, and for 2 μM cisplatin, when combined with the same MnTnHex concentrations, 17.0% ($p<0.05$) and 31.2% ($p<0.001$) (**Figure 10A**).

In H1975 cells, the lowest cisplatin concentration used (1 μM) did not show any cytotoxicity, while the higher concentration (5 μM) displayed clear cytotoxic effects. The concomitant treatment of cisplatin with MnTnHex significantly decreased cell viability when compared with cisplatin alone. In absolute percentages, the combination of 1 μM of cisplatin with 0.5 and 1 μM MnTnHex reduced cell viability by 46.4% ($p<0.001$) and 62.1% ($p<0.001$), respectively. Combining 5 μM cisplatin with the same MnP concentrations led to a reduction in cell viability of 29.7% ($p<0.05$) and 37.8% ($p<0.01$), respectively (**Figure 10B**). The morphology of A549 and H1975 cells upon treatment with MnTnHex and cisplatin are depicted in **Figures 10C** and **10D**, respectively. Overall, by combining MnTnHex with cisplatin, the cytotoxicity of this chemotherapeutic drug was significantly enhanced in NSCLC *in vitro*, this combination being more efficient in H1975 cells.

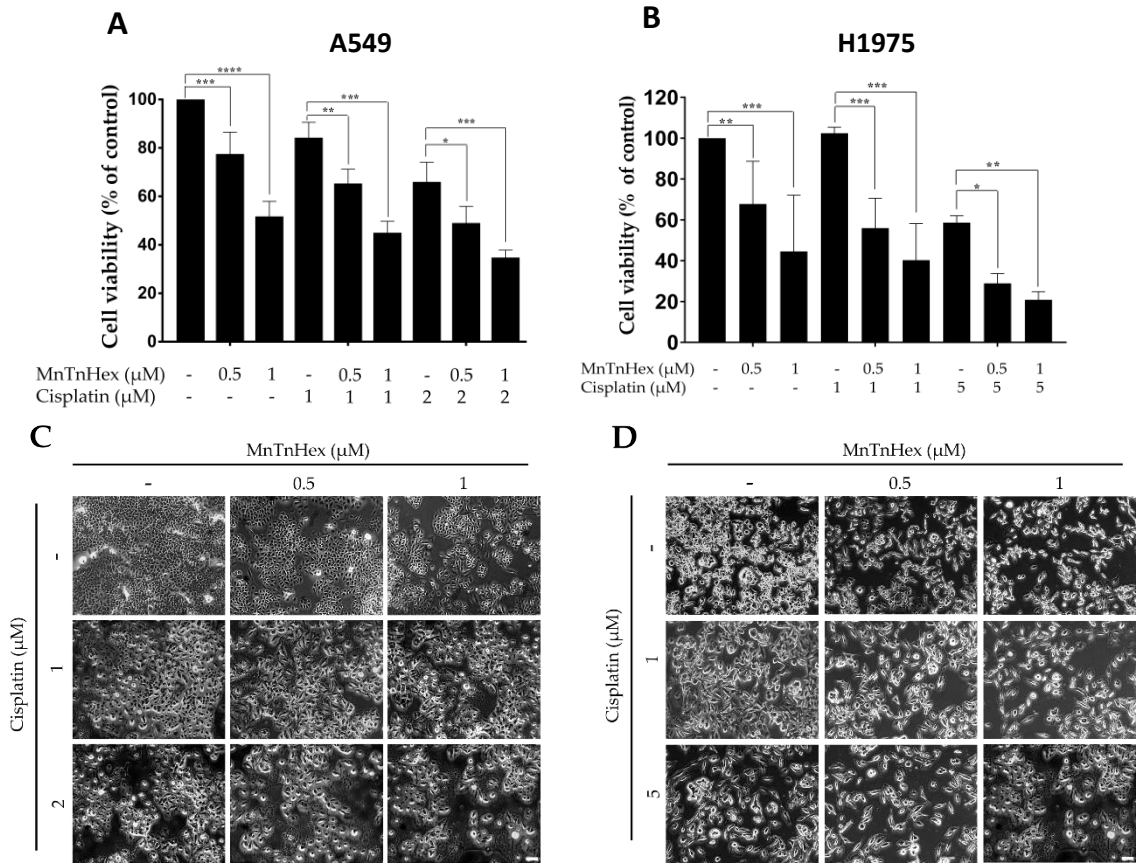

Figure 10. Cytotoxic effect of MnTnHex combined with cisplatin in A549 and H1975 cells. (**A**) Cells were simultaneously treated with MnTnHex (0.5 and 1 μM) and cisplatin (1 and 2 μM) in A549 cells and with MnTnHex (0.5 and 1 μM) and cisplatin (1 and 5 μM) in (**B**) H1975 cells for 72 h. (**C**) A549 cell morphology upon treatment with MnTnHex and/or cisplatin. (**D**) H1975 cell morphology upon treatment with MnTnHex and/or cisplatin. This effect was evaluated using a CV assay. Values represent mean ± SD (n = 4) and are expressed as percentages relative to vehicle-treated control cells. *p < 0.05, **p < 0.01 and ***p < 0.001 (one-way ANOVA with Tukey´s multiple comparisons test) when compared with control and cisplatin-treated cells.

By combining MnTnHex with cisplatin, we further aimed to study a different aspect of the potential usefulness of this compound in NSCLC. That is its ability to increase the efficacy of chemotherapy treatment. Our group has been studying the sensitivity of cisplatin in different cell lines. Regarding A549 cells, these cells are more sensitive to cisplatin than H1975 cells, having IC_{50} values up to 2.8 μM. In the case of H1975 cells, the IC_{50} values for the CV and MTS assay were approximately 10 and 16 μM, respectively, as described in Manguinhas *et al.* (Manguinhas et al., 2020). The IC_{50} values of A549 cells appear to be similar to those found in the literature for the same 72h-incubation period ([IC_{50}] = 3.1 μM) (Davou et al., 2019); ([IC_{50}] = 1.52 μM) (Wu et al., 2015) and ([IC_{50}] = 4.1 μM) (Wang et al., 2021b). Regarding the IC_{50} for the H1975 cells, these values were also similar to the ones found in the literature, using the MTT assay and the same incubation period: [IC_{50}] = 7.62 μM (Huang et al., 2016) and [IC_{50}] = 6.71

μM (Chen et al., 2018). Importantly, it should be mentioned that the IC_{50} values for MnTnHex in the present study are consistently lower than those observed for cisplatin, which is a fact worthwhile to be emphasized. Regarding its role as a chemosensitizer, in the present study, when combined with cisplatin, MnTnHex was able to enhance the cytotoxic impact of this pivotal chemotherapeutic drug. Indeed, in both cell lines, MnTnHex increased the cytotoxicity of cisplatin, being much more effective in H1975 cells. This could be perceived as another beneficial aspect given the resistant pattern of these cells. Regarding the differences observed in our study between the two NSCLC cell lines, several factors might be involved in their sensitivity to a given anticancer drug, including MnTnHex or cisplatin. The expression levels of the genes that code for H_2O_2-detoxifying enzymes may, at least partially, justify these differences observed between cell lines. Other reasons may involve differences between cell lines in terms of other enzymes involved in redox pathways, apoptosis, DNA repair, drug transport, drug detoxification, among others.

3.3.4. MnTnHex enhances cisplatin-induced cell death

The induction of cell death and the cell cycle progression were analyzed by flow cytometry (**Figure 11**). The cellular DNA content assessment showed that MnTnHex *per se* increased the percentage of sub-G1 population in both cell lines at 1 μM. This was also observed at 0.5 μM but only for H1975 cells. Importantly, a strong increase in the percentage of the sub-G1 population was found when cisplatin was added in combination with MnTnHex (**Figure 11D, G**) in both cell lines. In terms of magnitude, the combination reached higher percentage values of sub-G1 cells in the H1975 cell line (~22%) when compared with A549 cells (~16%). Nevertheless, this effect was evident for both concentrations of MnTnHex in A549 cells (0.5 and 1 μM; **Figure 11D**) while for H1975 cells, significant results were only achieved with 1 μM (**Figure 11G**).

For A549 cells, a mild G2/M arrest accompanied by a reduction in G0/G1 was observed when cisplatin and MnTnHex were added in combination, while the individual treatment with each of these compounds did not have a significant effect (**Figure 11E and F**). Overall, these results suggest that the observed reduction in cell viability present in the combinatory study mentioned in Section 3.3.3 and depicted in Figure 10 could be ascribed to the induction of cell death.

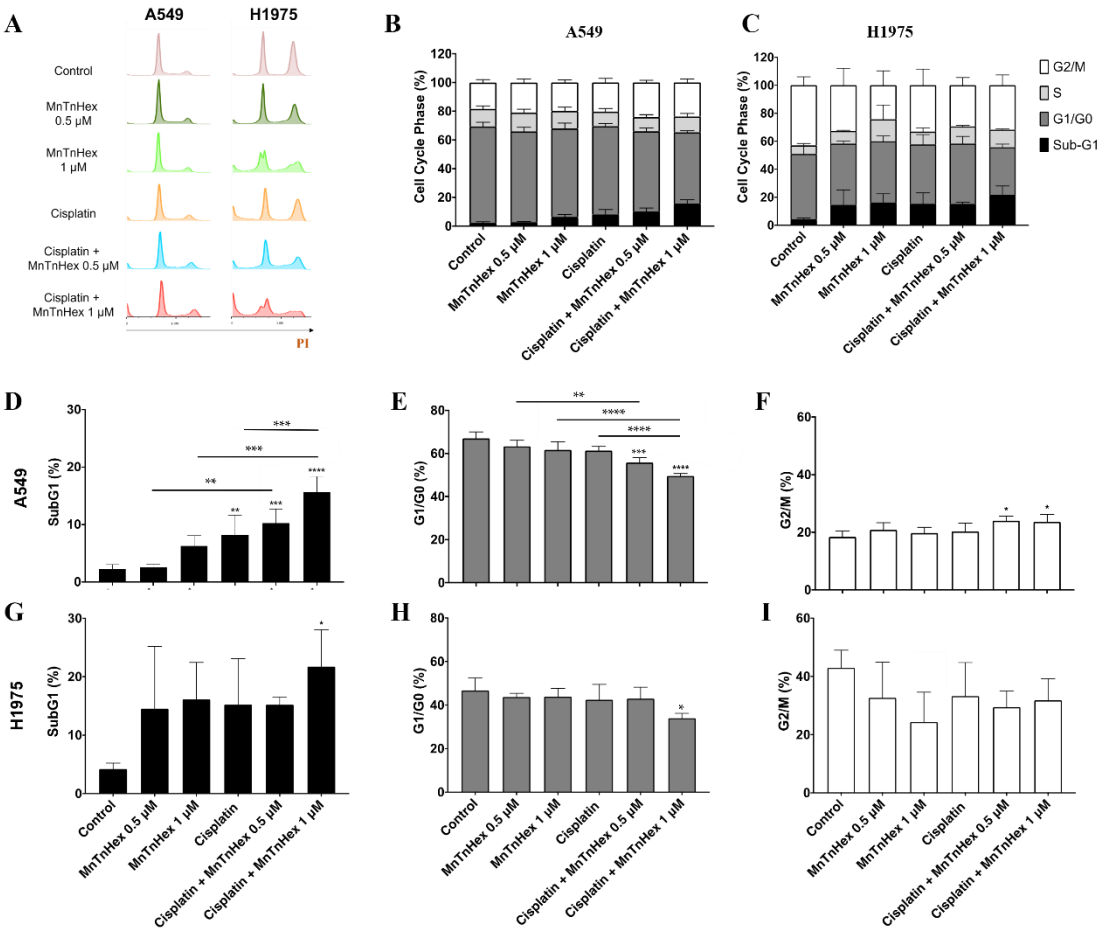

Figure 11. Effect of MnTnHex combined with cisplatin in A549 and H1975 cell cycle. Cells were treated with the indicated concentrations of MnTnHex and cisplatin for 72 h and DNA content was assessed on fixed cells by flow cytometry. (**A**) Representative flow cytometry histograms of PI-stained cells. Summary data of cell cycle populations for (**B**) A549 and (**C**) H1975 cells. Individual populations for (**D-F**) A549 cells and (**G-I**) H1975 cells. Values represent mean ± SD (n = 3-4) and are expressed as percentages of total cells. *p < 0.05, **p < 0.01, ***p < 0.001 and ****p < 0.0001 (one-way ANOVA with Tukey's multiple comparisons test) when compared with control cells, or between any two conditions as indicated in the figure by connecting lines.

Another aspect of this work was the characterization of the cell-cycle distribution of both cell lines treated with MnTnHex combined with cisplatin. For this, we selected a concentration of cisplatin that comprises a low cytotoxicity (1 µM) and concentrations of MnTnHex that, albeit being cytotoxic, did not markedly decreased cell viability (**Figure 10**). This selection of concentrations was chosen with the purpose of better understanding the effective impact of two-drug combination. The sub-G1 data revealed the cytotoxic potential of MnTnHex at 1 µM and recapitulate the impact of this MnP to boost the cytotoxicity of cisplatin in both cell lines. Regarding the cell cycle-checkpoints, it is known that cisplatin can interfere at the G1/S and G2/M checkpoints (Wang et al., 2004). The second checkpoint is generally more affected since cells trapped in G2/M can enter cell cycle arrest. At the concentration levels tested, we did not find these alterations. Nevertheless, when cisplatin was combined with MnTnHex, a mild but

significant increase in the G2/M phase occurred, which may indicate that this combination promotes G2/M cell cycle arrest. However, this effect was only observed in A549 cells. A possible cause may be related to the long incubation period with the compounds. The G2/M arrest may happen early, and arrested cells will either be efficient at repairing damage or induce cell death; thus at 72 h these cells might have either died or progressed to G1/G0.

3.3.5. Selection of MnTnHex and cisplatin non-toxic concentrations for the migration assay

To guarantee that the findings obtained with the wound-healing assay were due to an impairment in cell migration and not a consequence of reduced cell viability, it was necessary to first determine which non-toxic concentrations of MnTnHex and cisplatin should be used. For that, A549 cells were treated with two low concentrations of MnTnHex (1 and 5 µM) and cisplatin (0.25 and 0.5 µM) (**Figure 12A**), and H1975 cells were treated with MnTnHex (0.25 and 0.5 µM) and cisplatin (0.5 and 1 µM) (**Figure 12B**). All experiments were performed using a culture medium with 2% FBS, and cytotoxic effects were assessed using the MTS reduction assay.

In A549 cells, both cisplatin concentrations displayed 100% cell viability. For MnTnHex, both concentrations tested caused only a minor decrease in cell viability. Therefore, we selected the representative non-toxic concentrations of 0.5 µM for cisplatin and 5 µM for MnTnHex. In H1975 cells, none of the two concentrations of cisplatin tested showed cytotoxic effects. For MnTnHex, the concentrations of 0.25 µM and 0.5 µM had a decrease in cell viability of less than 10%. Hence, we chose the non-toxic concentrations of 1 µM for cisplatin and 0.5 µM for MnTnHex.

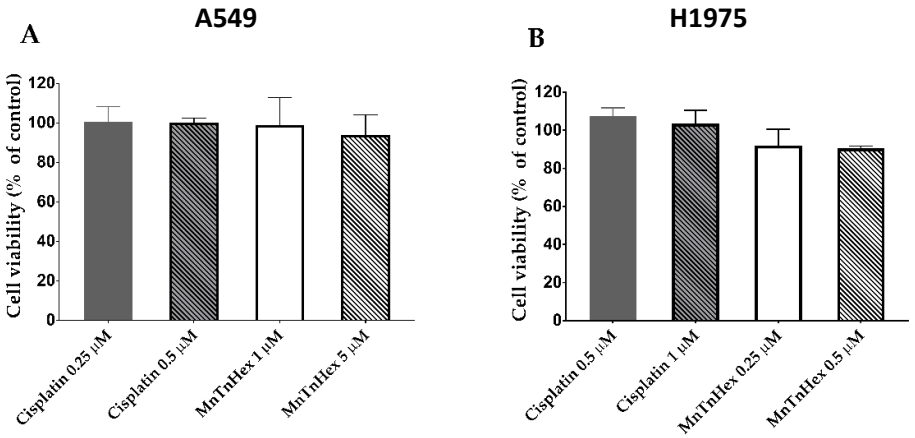

Figure 12. Viability of NSCLC cells when exposed to low concentrations of cisplatin or MnTnHex in culture medium with 2% FBS and assessed by MTS assay. (**A**) Effect of cisplatin (0.25 and 0.5 µM) and MnTnHex (1 and 5 µM) on cell viability in A549 cells, in the presence of 2% FBS. (**B**) Effect of cisplatin (0.5 and 1 µM) and MnTnHex (0.25 and 0.5 µM) on cell viability in H1975, in the presence of 2% FBS. Values represent mean ± SD (n=3) and are expressed as percentages relative to control cells (100% cell viability).

3.3.6. MnTnHex reduces collective migration

Metastases can be considered a systemic disease, being responsible for more the 90% of cancer death (Ganesh & Massagué, 2021). The development of metastases involves several biological complex mechanisms, including the supplying of pro-migratory factors and acceleration of tumor motility (Quail & Joyce, 2013). In LC, metastases are responsible for drastically reducing the survival rate. As mentioned earlier, most NSCLC cases are detected in advanced stages, when metastasis have already developed, which decreases the survival rate to less than 5% (Duma et al., 2019; Luo et al., 2016; Siegel et al., 2020). Therefore, it is crucial to analyze the impact of novel compounds on migration, especially in NSCLC.

After selecting the non-cytotoxic concentrations of both compounds, the migration capability of A549 and H1975 cells was assessed using the wound-healing assay (**Figure 13**) which evaluates the collective cell migration through a horizontal surface. In A549 cells, MnTnHex alone significantly reduced wound closure by approximately 30% ($p<0.01$) at 24 h and 32 h (**Figure 13A, B**). When combined with cisplatin, this compound also tends to reduce cell migration. In H1975 cells, a significant reduction occurred at 24 h, either using MnTnHex alone or combined with cisplatin, of approximately 19% ($p<0.05$) and 15% ($p<0.05$), respectively (**Figure 13D, E**). A similar % of reduction was also observed at 32 h, although without statistical significance.

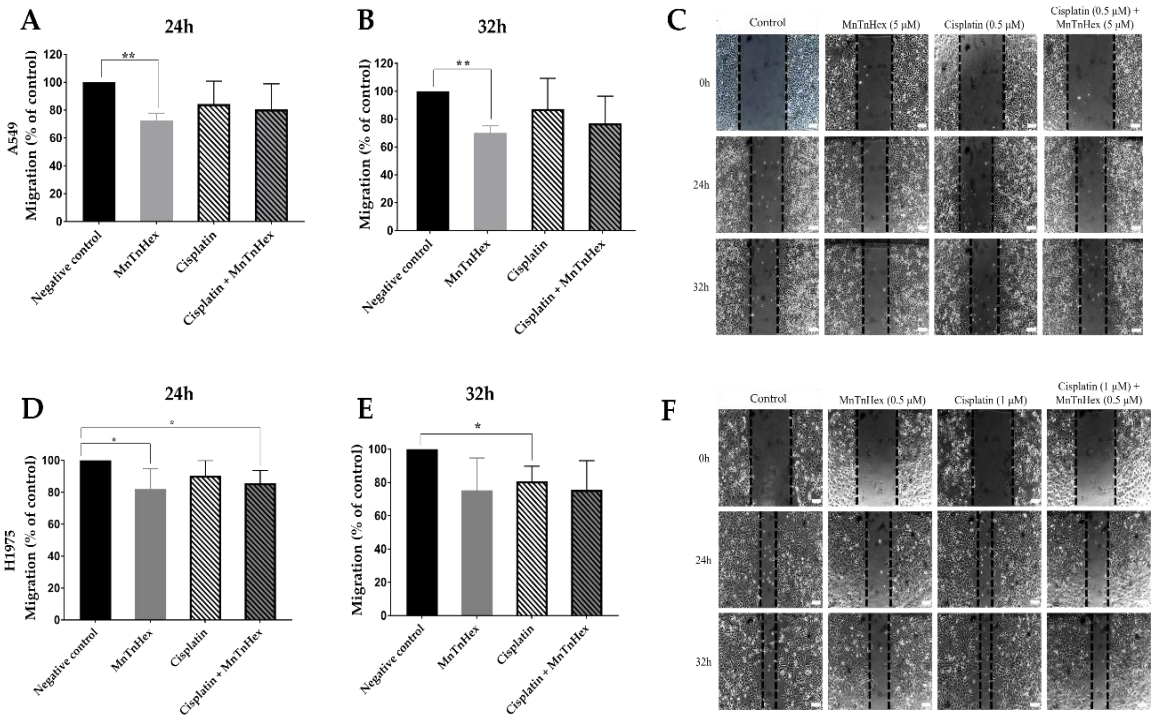

Figure 13. The effect of MnTnHex alone or combined with cisplatin on the collective migration of NSCLC cells. Cell migration was evaluated by wound-healing assay using MnTnHex (5 μM) and/or cisplatin (0.5 μM) in A549 cells at (**A**) 24 h and (**B**) 32 h. (**C**) Representative microscopy images of the wound-healing assay of A549 cells. Cell migration was also evaluated in H1975 cells at (**D**) 24 h and (**E**) 32 h using MnTnHex (0.5 μM) and/or cisplatin (1 μM). (**F**) Representative microscopy images of the wound-

healing assay of H1975 cells. Values for the wound-healing assay represent mean ± SD (n=3 - 4) and are expressed as percentages relative to control cells for each time point. The statistical analysis was performed for each time point, comparing each condition with the control cells; *p < 0.05, **p < 0.01 (Student's t-test). Scale bar = 100 μm.

MnTnHex induced a significant reduction of collective cell migration on both cell lines. Interestingly, there was a more significant reduction of migration in cells exposed to MnTnHex *per se* rather than when combined with cisplatin. Nonetheless, MnTnHex, either alone or combined, appears to induce a slightly higher reduction of migration when com-pared to cisplatin alone.

The impact of MnTnHex on migration has already been studied in other types of cancer in combination with chemotherapy and radiotherapy. While in this study, MnTnHex was effective *per se* in reducing collective cell migration, the same was not observed in renal and breast cancer. In renal cancer, MnTnHex did not affect collective cell migration, although it significantly decreased chemotactic migration (Costa et al., 2019). Flórido *et al.* thoroughly analysed the effect of MnTnHex alone and combined it with dox in breast cancer cell lines (MCF7 and MDA-MB-231). This MnP per se did not alter the collective cell migration and chemotaxis. However, combined with dox, it significantly reduced cell motility and chemotactic migration on both cell lines (Flórido et al., 2019). When MnTnHex was combined with radiotherapy, it significantly reduced the migration and invasion of mouse mammary carcinoma 4T1 cells when compared to control and radiation therapy alone. Similar to the results obtained in this work, MnTnHex as a single drug was the best in reducing migration (Shin et al., 2021).

3.3.7. MnTnHex alone and/or combined with cisplatin induced alterations in the NSCLC cells' metabolic response

First, the analytical reproducibility of the metabolomics experiment was confirmed by unsupervised analysis (PCA) of GC-MS data (**Figure A2**), including all samples under study and QCs, which revealed a well-defined QCs cluster. From a multivariate discriminant analysis (PLS-DA) perspective, no clear separation was found between the extracellular media of A549 or H1975 cells exposed to MnTnHex (0.5 and 1 μM) and cisplatin (1 μM) alone or in combination. Hence, altered levels of VCCs were investigated from an univariate analysis perspective using Volcano plots (**Figure 14**).

Among the 21 VCCs detected in extracellular media of both cell lines by our experimental approach (**Table A1**), statistically significant VCCs were only found in the extracellular medium of H1975 cells exposed to 1 μM of MnTnHex (**Figure 14A**) and 1 μM of MnTnHex combined with 1 μM cisplatin (**Figure 14B**) when compared with the control group. Cisplatin alone did not significantly increase levels of VCCs, possibly being possibly an inferior external source of H_2O_2 relative to MnTnHex. Interestingly, significant alterations were observed for the same VCCs in both exposed groups (**Figure 14C**), namely isobutanal, 3-methylpentanal and benzaldehyde. The relative comparison with blanks (*i.e*. culture medium without cells), also represented in **Figure 14C**, allowed the interpretation of VCCs alterations in terms of release or uptake by cells. Thus, our

findings unveiled that H1975 cells exposed to both conditions released significantly higher levels of isobutanal and 3-methylpentanal and uptook lower levels of benzaldehyde than control cells. Although no statistically significant alterations were found for extracellular media of exposed A549 cells, the same trend was observed for isobutanal and benzaldehyde levels, showing a similar behavior for higher release of isobutanal and lower uptook of benzaldehyde after exposure to MnTnHex alone and combined with cisplatin (**Figure A3**).

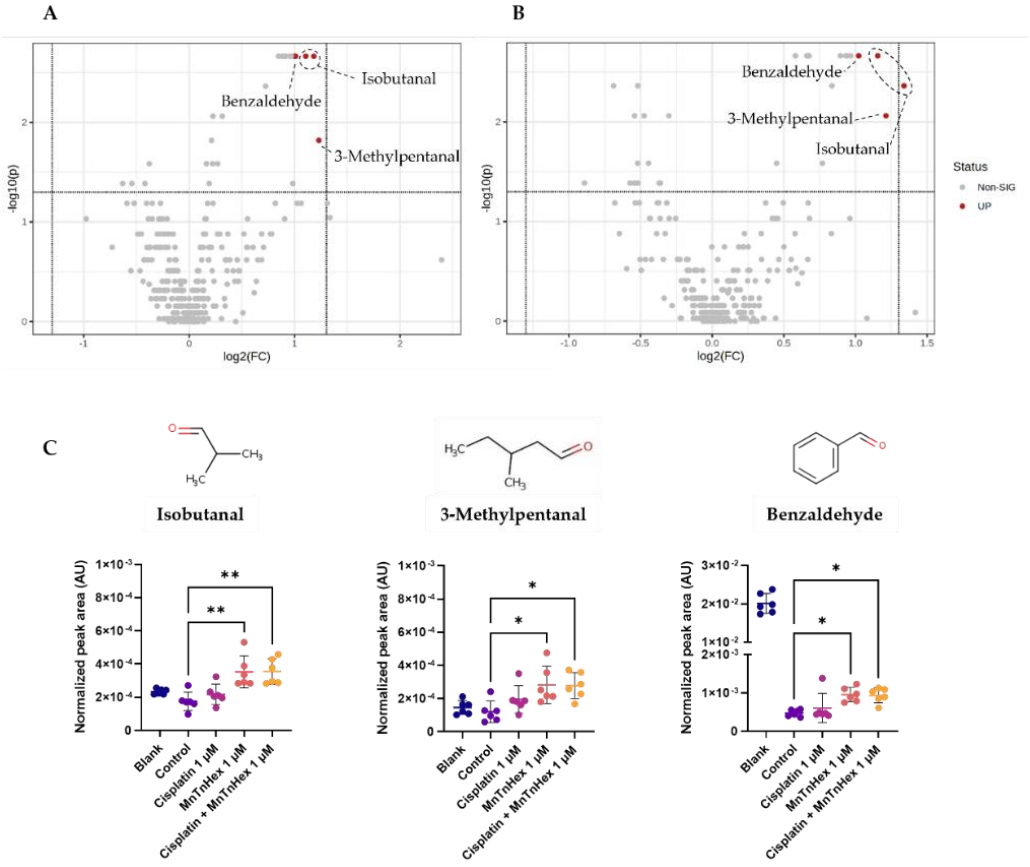

Figure 14. GC-MS-based metabolomics analysis of the extracellular media of H1975 cells exposed to MnTnHex and cisplatin, alone and combined. (**A**) Volcano plot of the GC-MS data of H1975 cells exposed to MnTnHex (1 µM) 72 h compared with controls. (**B**) Volcano plot of GC-MS data of H1975 cells co-exposed to cisplatin (1 µM) and MnTnHex (1 µM) compared with controls, indicating the statistical significance (p-value) vs. the magnitude of change (fold change). Statistical significance was assessed using the Mann-Whitney test and p-values<0.05 were considered significant. The grey dots indicate non-significant m/z-RT pairs, while the red dots indicate statistically significant m/z-RT pairs corresponding to isobutanal, 3-methylpentanal and benzaldehyde as marked. (**C**) Boxplots representing the normalized peak areas of the three significant VCCs. Statistical significance was assessed using the Kruskal-Wallis ANOVA test (* $p < 0.05$, ** $p < 0.01$).

Metabolomics is an emerging research field that has been used in recent years to gain further mechanistic data supporting the MoA of drugs and other xenobiotics. In the area of SODm and other redox-active drugs, scarce information on this topic is

available. Regarding the release/uptake of VCCs to/from culture medium by NSCLC cells, we found the higher levels of isobutanal and 3-methylpentanal. The increase in aldehyde levels is likely related to the MnTnHex/H_2O_2-driven catalysis of lipid peroxidation and/or oxidation of corresponding alcohols (Janfaza et al., 2019). However, the results were only significant for H1975 cells. Of note, a similar trend in A549 cells was also observed. The treatment with higher concentrations of MnTnHex might result in more pronounced effects in both cell lines. Nevertheless, we aimed to evaluate this aspect of the metabolome at MnTnHex concentrations that were not markedly toxic, avoiding other potential interferences. Performing studies at lower levels of Mn porphyrin is also clinically more relevant; the Mn(III) *meso*-tetrakis(*N*-n-butoxyethylpyridinium-2yl) (MnBuOE-2-PyP^{5+}, MnBuOE) analog is used in clinic at ~0.2 mg/kg (www.clinicaltrials.gov).

Regarding the uptake of lower levels of benzaldehyde, other authors showed that this metabolite is uptaken by mammalian cells (Mochalski et al., 2014) and may be oxidized by aldehyde dehydrogenases (ALDHs) to the corresponding carboxylic acid (Klyosov, 1996). These alterations appear to be a consequence of the mechanism of action of MnTnHex (**Figure 14C**) since a similar behavior was observed for H1975 cells exposed to MnTnHex alone and combined with cisplatin, whereas no significant changes were observed for cisplatin alone. Finally, it should be mentioned that the analysis of other metabolome alterations, for instance, in the endometabolome, may be important to better characterize the impact of MnTnHex in the context of NSCLC.

Overall, the present study reveals that MnTnHex affects NSCLC cells *in vitro* at different levels. This redox-active drug, *per se*, markedly reduces the viability of NSCLC cells, according to the endpoints explored, displaying very low IC_{50} values. It alters the cell cycle distribution and induces cell death. It further increases the cytotoxicity of cisplatin and most so in H1975 cells, suggesting its usefulness for a combination therapy. Moreover, MnTnHex *per se* or combined with cisplatin reduces collective cell migration pointing out to be also effective in this important metastatic feature of malignancy. Finally, concerning the metabolomics, few VCCs associated with oxidative stress, likely resulting from MnTnHex/H_2O_2-induced catalysis of peroxidation, were identified in the culture medium of MnTnHex treated cells. Overall, this work suggests that MnTnHex should be considered as a promising drug candidate for NSCLC.

Chapter 4

MnTnBuOE-2-PyP^{5+} impairs migration and invasion of NSCLC cells alone or combined with cisplatin

4.1. Introduction

MnBuOE is a derivative of MnTnHex, differing in terms of chemical structure by the introduction of an oxygen atom in each of the four alkyl chains (**Figure 15**). This modification allowed a reduction of toxicity due to a disruption in the surfactant properties, maintaining the characteristic lipophilicity of MnTnHex (Batinic-Haberle et al., 2014). Therefore, MnBuOE aims to present the ideal balance between toxicity, lipophilicity and bioavailability. The PK profile of MnBuOE has demonstrated that it does not possess any genotoxic risk to humans (Batinic-Haberle et al., 2021). Similar to MnTnHex, MnBuOE can cross the BBB, which allows it to be used in several studies regarding brain function (Weitzel et al., 2015, 2016), in which it has been shown to improve memory and maintain dendritic length in mice exposed to chemotherapy (McElroy et al., 2020), as well as, promoting hippocampal neurogenesis after radiation (Leu et al., 2017). MnBuOE has also been studied in different types of cancer. Ashcraft *et al.* (2015) proved that MnBuOE broadened the therapeutic window of radiotherapy, in head and neck cancer, by decreasing the dose of radiation necessary to control the tumor and increased the resistance of normal tissues to any injury caused by radiation. Also, this compound has been shown to enhance the chemotherapy treatment in rectal and anal cancer (Kosmacek et al., 2016). However, a recent study tried to show the impact of MnPs on distant metastasis of mammary carcinoma, using MnBuOE alone or combined with radiation, was not successful (Boss et al., 2021). Nonetheless, MnBuOE has proven to be very promising alone or combined with chemotherapy and radiation in clinical trials, since it is currently in clinical trials as a radioprotector. Several clinical trials are now in Phase II, such as, a study in high grade glioma (NCT02655601), brain metastasis (NCT03608020) and head and neck cancer (NCT04607642). MnBuOE is also in Phase I clinical trials as radioprotector of normal cells in patients with anal cancer (NCT03386500).

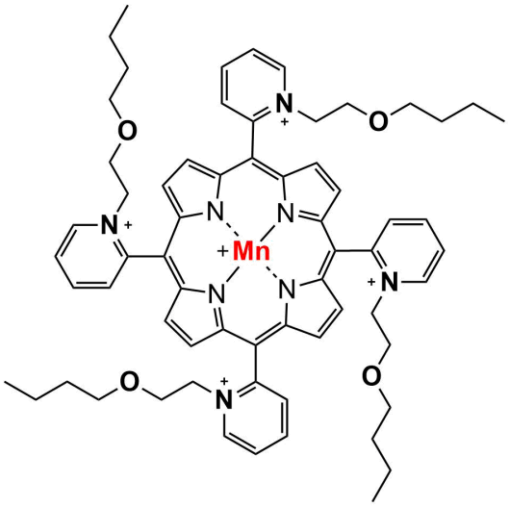

Figure 15. Chemical structure of MnBuOE-2-PyP^{5+}. (Chemical name: Mn(III) meso-tetrakis (N-n-butoxyethylpyridinium-2yl) designated as MnBuOE throughout the text for simplicity.

4.2. Materials and Methods

4.2.1. Chemicals

RPMI-1640 with L-glutamine was acquired from Biowest (Nuaillé, France). MnBuOE was synthesized and characterized at Duke University School of Medicine, according to Batinic-Haberle et al. (Batinić-Haberle et al., 2002). Cisplatin, penicillin-streptomycin solution (10,000 units/mL of penicillin; 10 mg/mL of streptomycin), CV, and sodium bicarbonate were purchased from Sigma-Aldrich (Madrid, Spain). Ethanol absolute and acetic acid were obtained from Merck (Darmstadt, Germany). Sodium pyruvate was purchased from Lonza (Basel, Switzerland), trypsin (0.25%) and FBS from Gibco (Eugene, OR, USA). HEPES and D-Glucose were obtained from AppliChem (Darmstadt, Germany). CellTiter 96® Aqueous MTS was acquired from Promega (Madison, WI, USA).

A stock solution of MnBuOE and its diluted solution were prepared in Milli-Q water. Cisplatin was dissolved in saline solution (0.9% NaCl) and solutions were aliquoted and stored at -20 ºC. In all cell-based assays, vehicle-treated controls were also included, in which cells were exposed to either saline solution or Milli-Q water.

4.2.2. Cell Culture

The human NSCLC cell lines A549 and H1975 were obtained from the American Type Culture Collection (ATCC, Manassas, VA, USA). Both cell lines were cultured and maintained as described in Chapter 3.

4.2.3. CV Staining Assay

The cytotoxicity effects of MnBuOE alone, in both NSCLC cells, were evaluated by CV staining assay, according to the previously described protocol mentioned in 3.2.4 (Fernandes et al., 2010). Briefly, ~$3x10^3$ cells were seeded in 200 µL of complete medium in 96-well plates and incubated for 24 h at 37 °C under 5% CO_2 atmosphere. After incubation, the culture medium was renewed, and the cells were incubated with a range of MnBuOE (0.5-200 µM) concentrations for 72 h, to determine a concentration-response profile and calculate its IC_{50} values. Cisplatin (50 µM) was used as a positive control for both cell lines. After the incubation, the CV assay was carried out as previously mentioned. Absorbance values presented by control cells (untreated cells) corresponded to 100% cell viability. Five independent experiments were executed, and six replicates were used for each condition in each independent experiment. The IC_{50} was calculated based on the concentration-response curve using GraphPad Prism® 7.0 (GraphPad Software, Inc., La Jolla, CA, USA). Image acquisition was performed using a Motic AE2000 Inverted Phase Contrast Microscope and using a 40x objective.

4.2.4. MTS Reduction Assay

The MTS assay was performed as a confirmatory assay for cell viability, applying the same conditions as in the CV assay and following the previously described

protocol mentioned in 3.2.5 (Guerreiro et al., 2017). Briefly, after seeding the cells at approximately $3x10^3$ cells/well and incubating them for 24 h, they were treated with a range of MnBuOE concentrations (0.5 – 100 µM) for 72 h. The MTS assay was performed as mentioned early. In short, after treatment, the medium was removed, and the wells were washed with PBS. Cells were incubated with 100 µL of complete medium and 20 µL of MTS substrate for 2 h, according to the manufacturer's instructions. Cisplatin (50 µM) was used as a positive control. Absorbance values presented by control cells corresponded to 100% of cell viability. Four independent experiments were performed, and three replicates were used for each condition in each independent experiment. The IC_{50} was also calculated based on the concentration-response curve using GraphPad Prism® 7.0 (GraphPad Software, Inc., La Jolla, CA, USA).

4.2.5. Combinatory Assays with MnBuOE and Cisplatin

The cytotoxic effects of MnBuOE combined with cisplatin, in NSCLC cells, were evaluated by CV staining assay, following a similar protocol as abovementioned. After the initial 24 h incubation period, the culture medium was changed and cells were exposed to both compounds simultaneously for 72 h. The MnBuOE concentrations remained the same in both cell lines (10 and 20 µM). Cisplatin concentrations used were 1 and 2 µM for A549 cells and 1 and 5 µM for H1975 cells. Four independent experiments were performed, and six replicates were used for each condition in each independent experiment.

4.2.6. Selection of MnBuOE and Cisplatin Concentrations for Migration/Invasion Assays

To establish the suitable non-cytotoxic concentrations for the migration assays, a MTS reduction assay was performed in A549 and H1975 cell lines, as previously described. Approximately $8x10^3$ cells/well were seeded in 96-well plates in complete culture medium for 24 h. After incubation, the complete medium was replaced by a new cell culture medium containing 2% FBS, and cells were incubated with a range of low concentrations of MnBuOE (5-20 µM) or cisplatin (0.25-1 µM) for 32 h in both cell lines. Three to four independent experiments were performed, and three replicates were used for each condition in each independent experiment.

4.2.7. In Vitro Wound-Healing assay

To determine the migratory collective capacity of both NSCLC cells, an *in vitro* wound-healing assay was performed as described in 3.2.9, according to a previously described protocol (Manguinhas et al., 2020). Briefly, A549 and H975 cells were seeded in 24-well plates at approximately $8x10^4$ and $6.5x10^4$ cells/well, respectively, and incubated for 24 h in complete cell culture medium. After 24 h, the medium was removed and an injury was inflicted in the cell monolayer of each well, using a 200 µL sterile pipette tip, resulting in a scratch of approximately 0.6-0.8 mm wide. Cells were then rinsed with warm PBS, to remove any cellular debris and detached cells. Cells were

incubated with warm culture medium containing 2% FBS and MnBuOE and/or cisplatin. A549 cells migrated in the presence of MnBuOE (5 and 10 µM) and/or cisplatin (0.5 µM). H1975 cells migrated in the presence of MnBuOE (5 µM) and/or cisplatin (1 µM). Both cell lines migrated up to 32 h. Image acquisition was performed using a Motic AE2000 Inverted Phase Contrast Microscope and using a 40x objective. The evaluation of wound closure and its measures were performed as previously described, following the same timepoints. Three different measures were made for each picture. Five to seven independent experiments were performed.

4.2.8. Chemotaxis migration assay

A chemotactic migration assay was conducted to evaluate the single-cell migration capacity of NSCLC cells when exposed to compounds, following a similar protocol already described (Flórido et al., 2019; Manguinhas et al., 2020). This assay was performed in 24-well plates with transwell inserts with transparent polyethylene terephthalate (PET) membranes containing 8 µm pores (BD Falcon, Bedford, MA, USA). A549 and H975 cells were seeded in 24-well plates at approximately $2x10^4$ and $5x10^4$cells/well in 2% FBS medium on top of the transwell insert and complete culture medium was placed in the lower chamber, functioning as a chemoattractant. After seeding, H1975 cells were exposed to MnBuOE (5 µM) and/or cisplatin (1 µM) and A549 cells were subjected to MnBuOE (5 and 10 µM) and/or cisplatin (0.5 µM). The compounds were added to both compartments and H1975 and A549 cells were incubated for 20 h and 24 h, respectively. After the cells migrated during this period, non-migrating cells were gently removed from the upper chamber with a cotton swab. Migrating cells, present at the bottom of the membrane, were fixed with 600 µL cold 96% ethanol for 10 min and stained with an equal volume of 0.1% CV in 10% ethanol, for 15 min. The inserts were carefully rinsed with tap water and dried for at least 24 h. Five representative fields were selected and photographed for each condition, using a Motic S6 (Motic, Barcelona, Spain) placed on a Motic AE2000 Inverted Phase Contrast Microscope with amplification of 100x. In each picture, stained cells were manually counted using the software Motic Images plus v3.0 (Motic, Barcelona, Spain). The counted cells were expressed as percentages of control cells and three independent experiments were performed.

4.2.9. Chemoinvasion

The invasive capacity of H1975 cells was analyzed through a chemoinvasion assay, following a similar protocol already described (Manguinhas et al., 2020). This procedure is very similar to the one previously detailed in the chemotaxis assay. The main difference is the addition of 50 µL of ECM gel (1:25 dilution in serum-free medium). The use of a serum-free medium prevents cell entrapment in the gel due to the chemoattraction effect caused by the complete medium that is placed in the lower chamber. The addition of this coating step mimics the structure of the extracellular matrix, allowing the observation of an invasion-like process, similar to *in vivo* conditions. The seeding density was approximately $2x10^4$ cells/well. The concentrations used and the analysis of results was conducted similarly to the abovementioned chemotactic migration assay. Three independent experiments were performed.

4.2.10. Statistical Analysis

The results presented correspond to mean values and SD. Prism 7.04 software (GraphPad, La Jolla, CA, USA) was employed for data comparison and the development of artwork. After assessing normality and homogeneity of the variances, the differences in mean values of the results were evaluated by Student´s t-test. Comparison of multiple mean values was performed by one-way ANOVA with post-hoc Tukey and one-way ANOVA with post-hoc Ducan. All analyses were performed with the SPSS statistical package (version 25; SPSS Inc. Chicago, IL, USA) and the level of significance considered was $p < 0.05$ (represented as: *$p < 0.05$, **$p < 0.01$, ***$p < 0.001$ and ****$p < 0.0001$).

4.3. Results and Discussion

4.3.1. Effect of MnBuOE on cell viability in NSCLC cells

The effect of MnBuOE was assessed in two NSCLC cell lines resorting to two complementary methodologies, CV staining and MTS reduction assay. Both assays showed that it was required high concentrations of MnBuOE to observe cytotoxic effects in both cell lines. In the case of A549 cells, no cytotoxic effects were observed up to the maximum tested concentration of 100 µM. However, in the CV staining assay, there is a modest decrease in cell viability, with the highest concentration tested (200 µM) caused a decrease in cell viability of approximately 30% (Figure **16A**). In the case of H1975 cells, both methodologies pointed in the same direction, with a stronger reduction in cell viability. Nevertheless, in the MTS assay, the maximum concentration tested (100 µM) induced cytotoxicity of approximately 45%, whereas with the CV staining assay it was necessary to reach the concentration of 200 µM to induce a cytotoxic effect of approximately 49% (**Figure 16B**). Although it was not possible to calculate the estimate IC_{50} in both cell lines, the decrease in cell viability in H1975 cells was close to 50%, thus we can anticipate that the IC_{50} for the MTS and CV assays is roughly 100 and 200 µM, respectively. In either case it is much higher than the IC_{50} values found in Chapter 3 for MnTnHex. Moreover, considering these results, H1975 cells revealed a higher sensitivity to MnBuOE than A549 cells. Regarding cell morphology, A549 cells appear to maintain their features throughout the increase of MnBuOE concentrations (**Figure 16C**), while H1975 cells seem to exhibit a narrower morphology in the highest concentration tested (**Figure 16D**). According to these results, the MnBuOE concentrations of 10 and 20 µM were chosen for the combinatory assays.

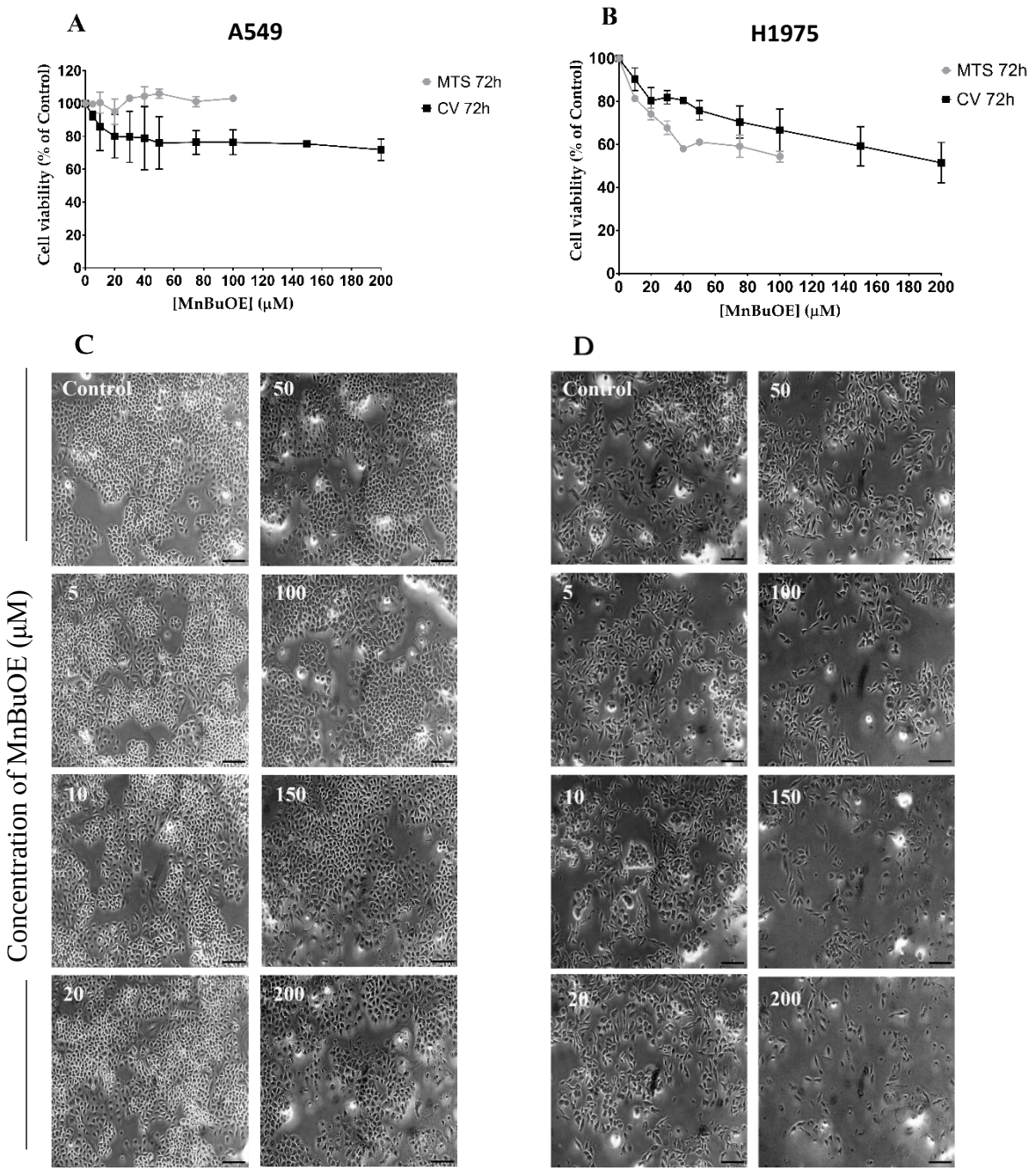

Figure 16. Cytotoxic effects of MnBuOE (0.5 – 200 µM) in A549 cells and H1975 cells. The decrease in cell viability when exposed to MnBuOE, for 72 h, was assessed by CV and MTS assay in (**A**) A549 cells and (**B**) H1975 cells. Values represent mean ± SD (n = 3-5) and are expressed as percentages of the vehicle-treated control cells. (**C**) A549 cell morphology upon treatment with MnBuOE. (**D**) H1975 cell morphology upon treatment with MnBuOE. Scale bar = 150 µm (**C** and **D**).

Regarding the discrepancy in the results obtained using two different methodologies, this may reflect the distinct sensitivities that these two mechanistically different endpoints possess. In order to have more information in terms of the characterization of the concentration-response profile, a third methodology should be

used, specifically the clonogenic assay. Regarding the effect of MnBuOE in other types of cancer, Yulyana *et al.* demonstrated the impact of this MnP in glioblastoma multiforme. A human glioma cell line (ΔGli36) and an immortalized normal human astrocytes cell line (iNHA) were exposed to high concentrations of MnBuOE (until 500 μM). The ΔGli36 cells suffered a decrease in cell viability of approximately 30% similar to the cytotoxic profile observed in A549 cells (Yulyana et al., 2016). There are a few studies where it was possible to observe significant effects of MnBuOE with low concentrations. In colorectal cancer cells (HT-29 cells) there was a reduction in the number of colonies when cells were exposed to 0.5 μM of MnBuOE (Kosmacek et al., 2016). In thyroid cancer, the cell lines BCPAP and KTC-1 were exposed to low concentrations of MnBuOE, 0.5 μM and 0.25 μM, respectively. In this study, MnBuOE also reduced the number of colonies in both cell lines (Patel et al., 2020).

4.3.2. Impact of MnBuOE combined with cisplatin on cell viability in NSCLC cells

To evaluate if MnBuOE could potentiate the cytotoxicity of cisplatin in A549 and H1975 cells, these two compounds were simultaneously incubated in these cells and the effects were evaluated using the CV staining assay. In A549 cells, the co-incubation of MnBuOE with cisplatin did not arouse any significant effect comparing with the MnP alone, being only observed marginal decreases in terms of cell viability in co-treated cells (**Figure 17A**). In contrast, in the case of H1975 cells, the combination of MnBuOE with cisplatin suggested a possible chemosensitizing effect in all the combinations tested ($p<0.0001$) (**Figure 17B**). The lowest cisplatin concentration used (1 μM) did not display any cytotoxicity, whereas the higher concentration used (5 μM) induced a cytotoxic effect of approximately 40%. Nevertheless, when cisplatin was combined with MnBuOE, its cytotoxicity was significantly enhanced. In absolute percentages, the combination of cisplatin 1 μM with MnBuOE 10 μM impaired cell viability by 39.6% ($p<0.0001$). When combined with 20 μM, cells suffered a reduction in cell viability of 45.2% ($p<0.0001$). The combination of the same MnP concentrations (10 and 20 μM) with cisplatin 5 μM induced a reduction in cell viability of 34.3% ($p<0.0001$) and 37.9% ($p<0.0001$), respectively. So, even though there was no significant effect on A549 cells, there was an impressive reduction of cell viability in H1975 cells when MnBuOE was combined with cisplatin.

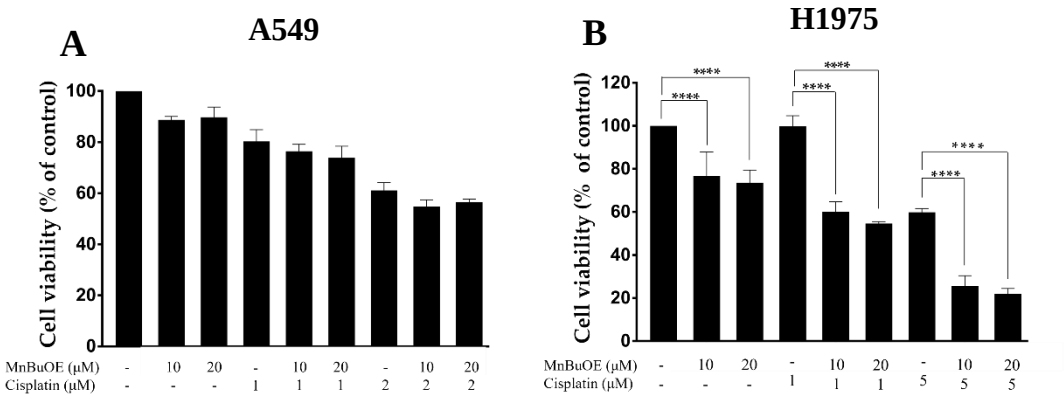

Figure 17. Cytotoxic effect of MnBuOE combined with cisplatin in A549 and H1975 cells. Cells were simultaneously treated with (**A**) MnBuOE (10 and 20 μM) and cisplatin (1 and 2 μM) in A549 cells and with (**B**) MnBuOE (10 and 20 μM) and cisplatin (1 and 5 μM) in H1975 cells, for 72 h and assessed by CV assay. Values represent mean ± SD (n = 2-4) and are expressed as percentages relative to control cells. ****p <0.0001 (one-way ANOVA with Tukey´s multiple comparisons test) when compared with control cells and cisplatin-treated cells.

The inherent sensitivities that both cell lines possess when exposed to cisplatin or to MnBuOE have already been addressed in Chapter 3 and in this section, respectively, which might explain these differences observed upon the combination of both drugs. Briefly, H1975 cells have a higher resistance to cisplatin when compared to A549 cells, therefore it was necessary to also use an even higher concentration of cisplatin in H1975 cells (5 μM). The lack of significant effect observed in A549 cells can thus be possibly due to the lower sensibility that A549 cells had already shown when were exposed to MnBuOE alone.

The enhanced effect that MnBuOE combined with cisplatin caused in H1975 cells sustains the possibility that this compound can be used as chemosensitizer. In addition, other studies have shown that MnBuOE can be radio- and chemoprotective. In colorectal cancer, fibroblasts were able to maintain their cell morphology and inhibit cellular senescence when treated with MnBuOE and radiation. Despite protecting healthy cells, MnBuOE did not protect HT-29 colorectal cancer cells. In fact, when MnBuOE was combined with radiation and chemoradiation it decreased tumor clonogenicity and improved the chemotherapeutic compounds' ability to reduce cancer cell growth (Kosmacek et al., 2016). Two human thyroid cancer cell lines (BCPAP and KTC-1) co-exposed to MnBuOE and radiation showed a decreased thyroid cancer growth when compared to cells exposed only to radiation (Patel et al., 2020).

4.3.3. Selection of MnBuOE and cisplatin non-toxic concentrations for the migration/invasion assays

As mentioned earlier, it is necessary to use non-cytotoxic concentrations when assessing the effect of cytotoxic compounds in migration and invasion, so that the results obtained are due to an impairment in cell migration and not due to a reduction in cell viability. In addition, this cell viability assay was performed using culture medium with 2% FBS, to ensure that there was no cell proliferation.

A549 cells were treated with two low concentrations of cisplatin (0.25 and 0.5 μM). We also tested the concentration of 1 μM cisplatin, but it was already cytotoxic at 32 h (data not shown). H1975 cells were incubated with cisplatin (0.5 and 1 μM). Both cell lines were treated with the same MnBuOE concentrations (5 and 10 μM). All experiments were performed for 32 h and the cytotoxic effects were assessed through MTS assay. In A549 cells, both cisplatin concentrations displayed cell viability of 100%, so we decided to select the concentration of 0.5 μM as the representative non-toxic

concentration. In the case of MnBuOE, none of the concentrations tested lead to reduction in cell viability, so we selected both concentrations for the migration and invasion assays. This selection allowed us to determine if there was a dose-response effect on these endpoints (**Figure 18A**).

In H1975 cells, both cisplatin concentrations had a percentage of cell viability slightly higher than 100%. For MnBuOE, the concentration of 5 and 10 µM had a decrease in cell viability of approximately 7% and 23%, respectively. Since the concentration of 10 µM MnBuOE was already cytotoxic, we chose the non-cytotoxic concentrations of 1 µM for cisplatin and 5 µM for MnBuOE (**Figure 18B**).

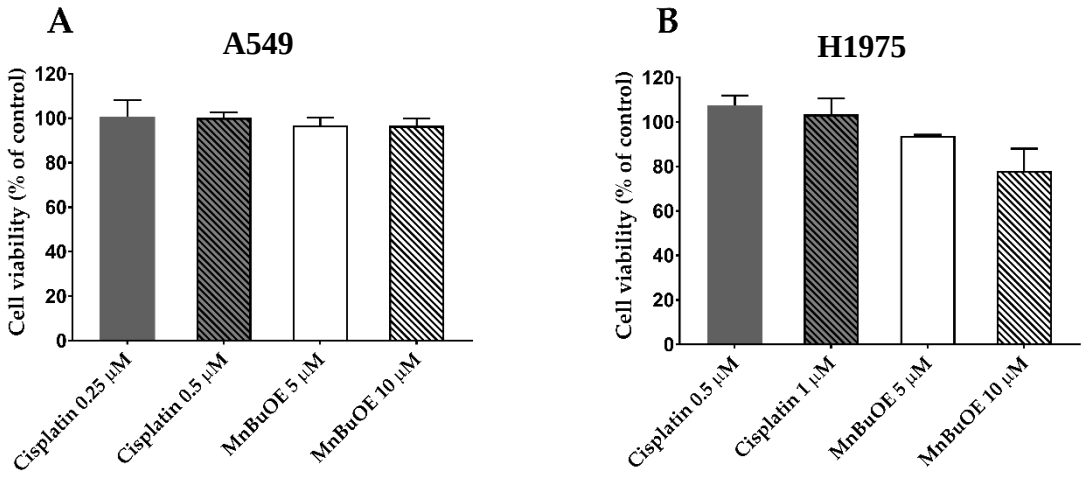

Figure 18. Viability of NSCLC cells when exposed to low concentrations of cisplatin or MnBuOE in culture medium with 2% FBS and assessed by MTS assay. (**A**) Effect of cisplatin (0.25 and 0.5 µM) and MnBuOE (5 and 10 µM) on cell viability in A549 cells, in the presence of 2% FBS. (**B**) Effect of cisplatin (0.5 and 1 µM) and MnBuOE (5 and 10 µM) on cell viability in H1975 cells, in the presence of 2% FBS (**B**). Values represent mean ± SD (n=3) and are expressed as percentages relative to control cells (100% cell viability).

4.3.4. MnBuOE per se and/or combined with cisplatin reduces collective migration in NSCLC cells

The impact of metastases and their importance in NSCLC has already been mentioned throughout this work. Given the lipophilicity of MnBuOE and its ability to cross the BBB, it is crucial to analyze the impact of this novel compound on the impairment of migration. Therefore, the effect of MnBuOE alone and combined with cisplatin was evaluated using the wound-healing assay.

In A549 cells, MnBuOE significantly reduced collective migration both alone and combined with cisplatin at 24 h and 32 h (**Figure 19A,B**). With the highest concentration tested (10 µM), MnBuOE was able to reduce migration by approximately 24% at 24 h ($p<0.05$) and 32 h ($p<0.01$). The lowest concentration tested was able to decrease migration by approximately 20%, albeit this different was not statistically

significant. Nonetheless, when MnBuOE was combined with cisplatin it was possible to observe a higher reduction in cell motility. When cisplatin is combined with 5 and 10 µM MnBuOE, there is a decrease of migration of approximately 30% ($p<0.01$) and 36% ($p<0.01$) at 24 h, respectively, and a reduction of 29% ($p<0.05$) and 41% ($p<0.001$) at 32 h, respectively. The results obtained in this cell line suggests that the effect of MnBuOE may be concentration-dependent.

In H1975 cells, MnBuOE also reduced cell motility both alone and combined with cisplatin. When alone, MnBuOE impaired migration by approximately 13% ($p<0.001$) and 18% ($p<0.01$), at 24 h and 32 h respectively (**Figure 19C,D**). Similarly to A549 cells, the best condition tested was the MnP combined with cisplatin. This combination was able to reduce migration by 30% ($p<0.001$) and 37% ($p<0.001$), at 24 h and 32 h, respectively. Interestingly, this MnBuOE seems to have a slightly higher effect in H1975 cells, which, as abovementioned, possess a more invasive phenotype than A549 cells. Overall, MnBuOE appeared to have a higher effect on migration than on cell viability, so further assays related to cell migration were performed to better understand the important aspect of the MnP.

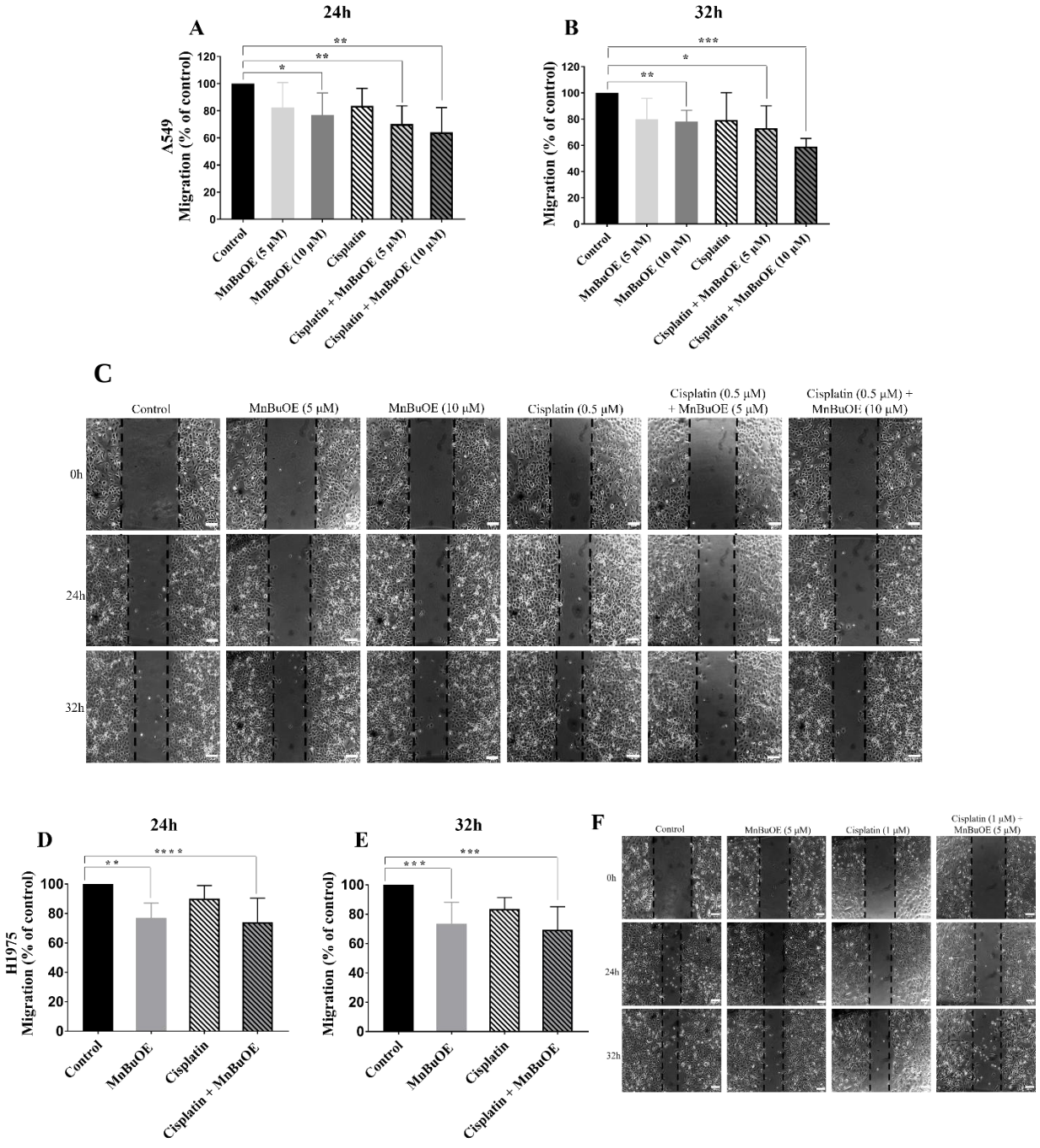

Figure 19. The effect of MnBuOE alone or combined with cisplatin on the collective migration of NSCLC cells. Cell migration was evaluated by wound-healing assay using (**A,B**) MnBuOE (5 and 10 µM) and cisplatin (0.5 µM) in A549 cells and (**D,E**) using MnBuOE (5 µM) and cisplatin (1 µM) in H1975 cells. Representative microscopy images of the wound-healing assay of (**C**) A549 cells and of (**D**) H1975 cells. Values for the wound-healing assay represent mean ± SD (n= 5-6) and are expressed as percentages relative to control cells. The statistical analysis was performed for each time point, comparing each condition with the control cells; *p < 0.05, **p < 0.01, ***p<0.001 and ****p<0.0001 (Student's t-test). Scale bar = 100 µm.

4.3.5. MnBuOE alone and in combination with cisplatin decreases chemotactic cell migration and invasion in NSCLC cells

Cell individual migration and invasion are crucial steps in the movement and development of metastases to peripheral organs. Single-cell migration occurs without cell-cell interaction with neighboring cells, unlike collective migration, and it happens in the early stages of invasion in the metastatic process (Pijuan et al., 2019). Considering these processes and the effect of MnBuOE in collective cell migration, the influence of MnBuOE alone or combined with cisplatin on chemotactic cell migration and invasion was further evaluated by a transwell migration assay and a transwell chemoinvasion assay, respectively.

Regarding the chemotactic individual cell migration, MnBuOE was able to significantly reduced cell migration, either alone or combined with cisplatin, in both NSCLC cell lines. The concentrations used were the same as in the collective cell migration so that the results could be compared. In A549 cells, MnBuOE *per se* was able to significantly reduce this type of migration in a concentration-dependent manner (**Figure 20A**). Cells exposed to the lowest MnBuOE concentration (5 µM) reduced 28% ($p<0.0001$) of migrating cells, while at 10 µM it reduced migration by 35% ($p<0.0001$). Although cisplatin alone significantly decreased individual migration ($p<0.0001$), MnBuOE combined with cisplatin was the condition that most reduced chemotactic cell migration. These conditions also appeared to occur in a concentration-dependent manner, since cisplatin combined with MnBuOE 5 µM and 10 µM impaired cell migration by 39% ($p<0.0001$) and 51% ($p<0.0001$), respectively. Similarly to A549 cells, MnBuOE could reduce individual migration in H1975 cells (**Figure 20B**). When used alone, MnBuOE significantly decreased migration by approximately 30% ($p<0.01$). Once again cisplatin alone could significantly reduce migration ($p<0.01$). Nonetheless, MnBuOE combined with cisplatin caused the most reduction in individual cell migration, leading to a decrease of approximately 45% ($p<0.0001$). This decrease was also statistically significant when comparing the combination of the two compounds with cisplatin-treated cells ($p<0.001$). Representative images of the chemotaxis migration assay are represented in **Figure 20C** and **D**.

Invasive cells need to cross basement membranes to form new blood vessels and reach peripheral organs (Albini & Benelli, 2007). Therefore, the transwell chemoinvasion assay was performed similarly to the transwell chemotactic assay but with the addition of an ECM gel to better mimic the crossing of these basement membranes. This procedure was only performed in H1975 cells, being the evaluation of the effect of MnBuOE in A549 cells planned to be executed in the near future. The selection of H1975 cell as a prioritary cell line to be studied in this assay was due to its more aggressive characteristics, already addressed, which may be relevant in the scope of this endpoint. Unlike the results observed in terms of collective and individual cell migration, in the cell invasion assay MnBuOE alone was the condition that most reduced cell invasion, decreasing this feature in approximately 34% ($p<0.001$) (**Figure 20E**). Nonetheless, when MnBuOE was combined with cisplatin it also reduced invasion by approximately 18% ($p<0.05$).

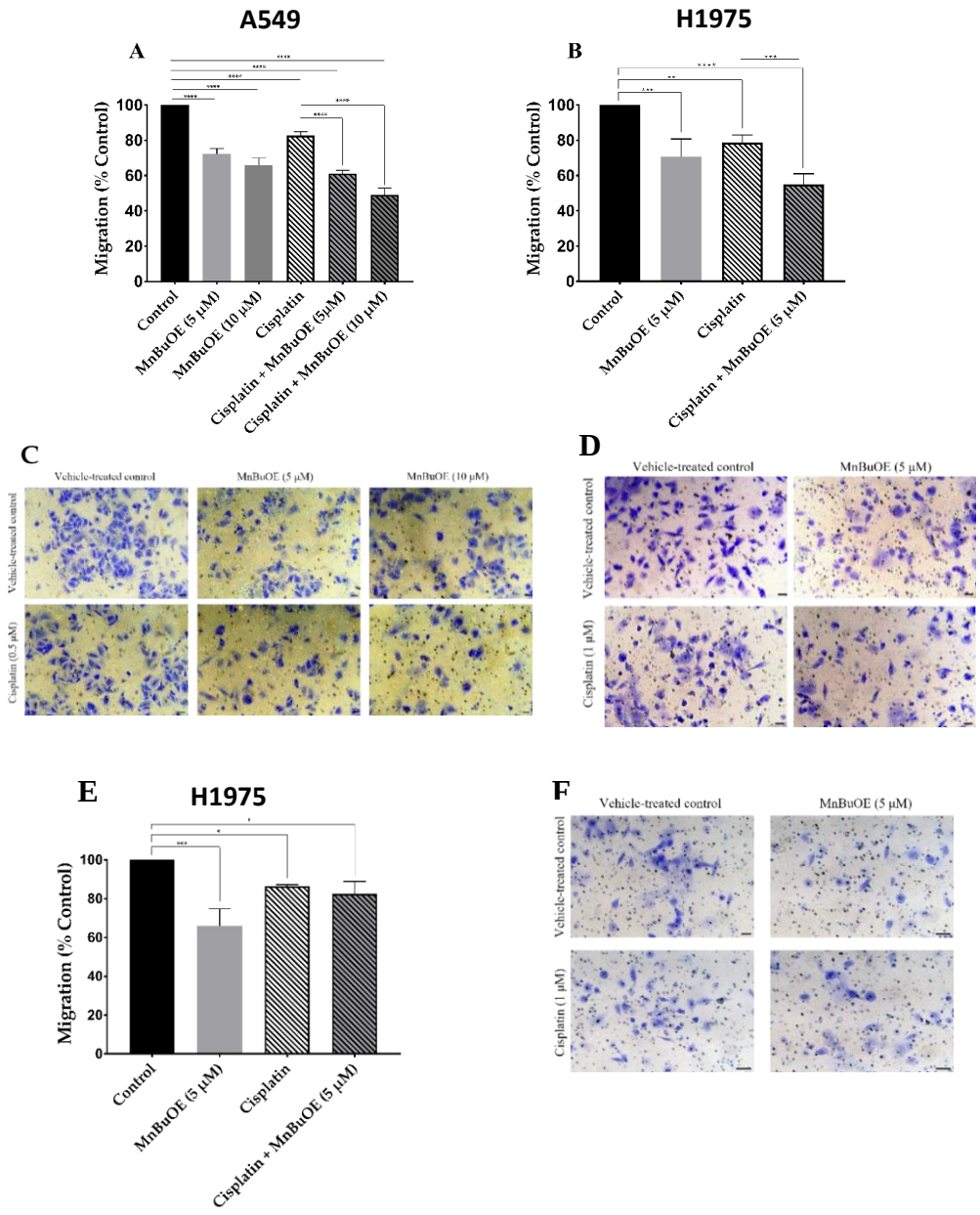

Figure 20. Effect of MnBuOE on chemotactic migration and chemoinvasion in NSCLC cells exposed to cisplatin. Chemotactic cell migration was measured using a transwell migration assay in (**A**) A549 cells and (**B**) H1975 cells. Representative microscopy images of the transwell migration assay, where migrated (**C**) A549 cells and (**D**) H1975 cells are stained with crystal violet (scale bar = 150 µm). Values represent the mean ± SD (n = 3) and are expressed as percentages relative to vehicle-treated control cells: ***p<0.001 and ****p<0.0001 (one-way ANOVA with Tukey´s multiple comparisons test). (**E**) Transwell chemoinvasion was evaluated for a 20 h period on H1975 cells. (**F**) Representative microscopy images of invading cells stained with crystal violet. Scale bar = 150 µm. Values represent the mean ± SD (n = 3) and are expressed as percentages relative to vehicle-treated control cells: *p<0.05 and ***p<0.001 (one-way ANOVA with Tukey´s multiple comparisons test).

Overall, the analyzes of these endpoints suggests that MnBuOE affects NSCLC cells at different levels, especially in assays related with migration and invasion. Despite displaying moderate results regarding cell viability, MnBuOE alone or combined with cisplatin was able to significantly reduce collective and individual migration, where the best condition tested was this MnP combined with cisplatin. In the case of invasion, MnBuOE alone lead to the highest impairment. Nonetheless, MnBuOE combined with cisplatin also significantly reduced invasion. It should be emphasized that, similarly to what was observed in Chapter 3, H1975 cells displayed a higher sensitivity to MnBuOE than A549. Overall, this work suggests that MnBuOE should be considered as a promising drug candidate for NSCLC.

Chapter 5

Concluding Remarks and future directions

NSCLC is a very complex oncological disease for which novel pharmacological approaches are clearly need, particularly with the development of novel drugs to be used alone or through the proposal of the combination of these new drugs with standard chemo- and radiotherapy regimens.

The results obtained during this project with NSCLC cells allowed us to evaluate the beneficial effects of MnTnHex (Chapter 3) and MnBuOE (Chapter 4), both leading compounds of the Mn-based class of SODm (Batinic-Haberle et al., 2021; Bonetta, 2018). The data generated in this work would be important to support the usefulness of these compounds to be considered as a novel therapeutic strategy in the treatment of NSCLC.

Firstly, the characterization of the antioxidant status concerning the expression of the key enzymes responsible for the detoxification of H_2O_2 was carried out (Chapter 3). This was an important experimental achievement of this thesis, confirming that the NSCLC cell lines used have particularly low levels of catalase, but also of GPX1 and PRDX2, in line with some indications present in the literature and in databases (*i.e.*, Human Protein Atlas). Furthermore, we have also analyzed the effect that these MnPs could show in chemotherapy by combining them with cisplatin (Chapters 3 and 4). Multiple endpoints were assessed, including cell viability, cell cycle distribution, migration, invasion and evaluation of the exometabolome. The first experimental chapter (Chapter 3), focused on MnTnHex, gathered a higher number of endpoints, providing additional information in terms of cell cycle distribution and exometabolome analysis while Chapter 4 was more focused in the impairment of the motility of both cell lines, incorporating an invasion assay that was not studied in the previous Chapter. The selection of the endpoints evaluated was determined by the initial assessment of the comparison of cytotoxic effects of both MnPs and afterwards for their behavior in the collective migration assay.

MnTnHex displayed high cytotoxicity in both NSCLC cell lines, with some IC_{50} at submicromolar range, varying between 0.7 and 2.1 µM. In turn, MnBuOE exhibited a much lower cytotoxic effect when compared to MnTnHex, given that it was necessary to expose the cells to 200 µM to achieve a cytotoxicity burden near the IC_{50}. Despite these differences, H1975 cells demonstrated to be more sensitive to both compounds than A549 cells. The differential cytotoxic effects between these compounds can be partially explained by the inherent differences in terms of the distribution of both compounds. MnTnHex is known for its large bioavailability, tissue penetration and retention distribution. MnBuOE comparing with MnTnHex has a lower bioavailability. Moreover, the addition of the oxygen atoms in the alkyl pyridyl chains of MnTnHex, originated a less toxic compound, MnBuOE (Batinic-Haberle et al., 2014, 2021; Rajic et al., 2012), therefore it is possible that higher concentrations of this MnP are necessary to achieve the same cytotoxic effects observed with the MnTnHex. Nevertheless, it should be reinforced that MnTnHex at the same concentration range revealed to be non-toxic in two different cell types of non-tumour origin as mentioned in Chapter 3.

When MnTnHex was combined with cisplatin, it was able to enhance cisplatin cytotoxicity in both cell lines, whereas MnBuOE only displayed an effect on H1975 cells. Nevertheless, this effect appeared to be synergistic. Importantly, both compounds, either alone or combined with cisplatin, were more cytotoxic in H1975 cells. It is worth emphasizing that H1975 cells are more resistance to cisplatin than A549 cells. A possible explanation for the different sensitivities that these cells possess when exposed to MnPs may rely on their antioxidant status as well as in other factors already mentioned in the discussion of Chapter 3. Nonetheless, more studies regarding the enzymatic activity of these enzymes and the gene expression of other antioxidant enzymes should be performed. In addition, it should also be studied if these compounds can help overcome the resistance that malignant cells tend to develop to cisplatin, given that the higher effect was observed in the more resistance cells.

Regarding the migration processes, MnTnHex reduced collective migration by 30% in A549 cells, and when combined with cisplatin it also tends to reduce collective migration. In the case of H1975 cells, at the 24 h it was able to observe a significant reduction both in MnTnHex *per se* and when combined with cisplatin. When cells were exposed to MnBuOE, it was possible to observe a robust effect on cell motility. In A549 cells we observed a concentration-dependent effect, and when MnBuOE was combined with cisplatin it reduced up to 41% of collective migration. Similar results were observed in H1975 cells, where MnBuOE combined with cisplatin reduced collective migration by 37%. Given these overall results, MnTnHex appears to display a more cytotoxic profile, whereas MnBuOE appears to have a higher effect on the migration processes. Therefore, as abovementioned, different endpoints were conducted according to the SODm in evaluation. In the case of MnTnHex we also analyzed the metabolome of cells when exposed to MnTnHex alone or combined with cisplatin to get further cytotoxicity mechanistic insights and found that cells had higher levels of isobutanal and 3-methylpentanal, which is likely to the MnTnHex/H_2O_2-driven catalysis of lipid peroxidation and/or oxidation of corresponding alcohols. Also, lower uptake levels of benzaldehyde were found. Albeit these metabolites were only significant for H1975 cells, a similar trend was found in A549 cells.

Additional endpoints involving migration, such as, chemotactic migration and invasion were performed for MnBuOE. This SODm was able to significantly reduce individual migration by itself on both cell lines, but when combined with cisplatin an impressive reduction of 51% and 45%, was observed for A549 and H1975 cells respectively. Interestingly, in invasion, MnBuOE alone appears to possess higher effect than when combined with cisplatin.

Overall, this work constitutes the first approach to increase our knowledge on the usefulness of MnPs in the context of NSCLC. Nevertheless, additional studies should be performed to elucidate the underlying mechanisms involved and to gather additional data to support this application. Again, the prioritization of the future assays to be performed will differ according to each MnP.

In the case of MnTnHex, an apoptosis assay should be executed as complementary endpoint of the cell cycle distribution since we observed that the cytotoxic effects of MnTnHex were indeed caused by the induction of cell death. This assay could be conducted by flow cytometry, using a double staining of live cells apoptosis kit with Alexa® Fluor 488 Annexin V and PI. Additionally, a caspase activation-based assay should be performed to obtain more mechanistically information regarding the signaling pathways that are activated when cells are exposed to MnTnHex. Since this compound is highly cytotoxic and in view of increase in H_2O_2 described for SODm, genotoxicity assays, particularly the cytokinesis-block micronucleus assay or the comet assay, could also be performed. In fact, the cytotoxicity observed could be a consequence of the excess of DNA lesions that might trigger apoptosis.

Currently, the analysis of other alterations of the metabolome in MnTnHex-treated cells, *i.e.*, the evaluation of the endometabolome, are also being performed. These studied are important to better characterize the impact of MnTnHex in the context of NSCLC. These studies are being carried out resorting to a complementary methodology, specifically nuclear magnetic resonance (NMR) spectroscopy, which may shed some light on this topic.

For MnBuOE it would be interesting to understand the anti-migratory effect that this compound possesses in a mechanistically perspective. Since MnBuOE had such an impressive effect on migration, the analysis of some of the genes involved in migration could be addressed, particularly the collagenases MMP-2 and MMP-9 (zymographic assays).

The effect of SODm with cisplatin also needs further elucidation, in this case for both compounds since in both cases clear beneficial results were found. To assess if the effect of these compounds as chemosensitizers might be due to an accumulation of ROS caused by SODm and cisplatin, an assessment of these ROS levels should be conducted. Through fluorescent microscopy and resorting to fluorescent probes, cells would be exposed to SODm alone, cisplatin alone and then combine and observe the ROS accumulation. Also, to determine if this possible increase of mitochondrial ROS leads to an additional damage in the mitochondrial membrane potential and triggers apoptosis, a mitochondrial membrane potential assay could be conducted as well.

Finally, given the protective role that SODm may display in healthy cells and tissues, further studies should be conducted using normal human lung cells. In this sense the healthy bronchial epithelial cell line BEAS-2B cells has been acquired and the first set of studies will be soon performed. With these assays we pretend to better understand the possible effects that these compounds might have *per se* or in minimizing the adverse effects caused by chemotherapy, such as nephrotoxicity.

Overall, the results obtained in this study highlight the potential of MnTnHex and MnBuOE for LC therapy, which might be valuable in combination with cisplatin, allowing the use of lower doses of this drug toward an improved efficacy.

References

Abu-Surrah, A., & Kettunen, M. (2006). Platinum Group Antitumor Chemistry: Design and development of New Anticancer Drugs Complementary to Cisplatin. *Current Medicinal Chemistry*, *13*(11), 1337–1357. https://doi.org/10.2174/092986706776872970

Albini, A., & Benelli, R. (2007). The chemoinvasion assay: A method to assess tumor and endothelial cell invasion and its modulation. *Nature Protocols*, *2*(3), 504–511. https://doi.org/10.1038/nprot.2006.466

Amaro, F., Pinto, J., Rocha, S., Margarida, A., Miranda-gonçalves, V., Jer, C., Henrique, R., Bastos, M. D. L., Carvalho, M., & Pinho, P. G. De. (2020). *Volatilomics Reveals Potential Biomarkers for Identification of Renal Cell Carcinoma : An In Vitro Approach*.

Antonia, S. J., Villegas, A., Daniel, D., Vicente, D., Murakami, S., Hui, R., Kurata, T., Chiappori, A., Lee, K. H., de Wit, M., Cho, B. C., Bourhaba, M., Quantin, X., Tokito, T., Mekhail, T., Planchard, D., Kim, Y.-C., Karapetis, C. S., Hiret, S., … Özgüroğlu, M. (2018). Overall Survival with Durvalumab after Chemoradiotherapy in Stage III NSCLC. *New England Journal of Medicine*, *379*(24), 2342–2350. https://doi.org/10.1056/nejmoa1809697

Archambeau, J. O., Tovmasyan, A., Pearlstein, R. D., Crapo, J. D., & Batinic-Haberle, I. (2013). Superoxide dismutase mimic, MnTE-2-PyP5+ ameliorates acute and chronic proctitis following focal proton irradiation of the rat rectum. *Redox Biology*, *1*(1), 599–607. https://doi.org/10.1016/j.redox.2013.10.002

Armstrong, D. K., Bundy, B., Wenzel, L., Huang, H. Q., Baergen, R., Lele, S., Copeland, L. J., Walker, J. L., & Burger, R. A. (2006). Intraperitoneal Cisplatin and Paclitaxel in Ovarian Cancer. *New England Journal of Medicine*, *354*(1), 34–43. https://doi.org/10.1056/nejmoa052985

Avolio, R., Matassa, D. S., Criscuolo, D., Landriscina, M., & Esposito, F. (2020). Modulation of mitochondrial metabolic reprogramming and oxidative stress to overcome Chemoresistance in Cancer. *Biomolecules*, *10*(1), 1–23. https://doi.org/10.3390/biom10010135

Bansal, A., & Celeste Simon, M. (2018). Glutathione metabolism in cancer progression and treatment resistance. *Journal of Cell Biology*, *217*(7), 2291–2298. https://doi.org/10.1083/jcb.201804161

Barta, J. A., Powell, C. A., & Wisnivesky, J. P. (2019). Global epidemiology of lung cancer. *Annals of Global Health*, *85*(1), 1–16. https://doi.org/10.5334/aogh.2419

Batinić-Haberle, I., Rebouças, J. S., & Spasojević, I. (2010). Superoxide dismutase mimics: Chemistry, pharmacology, and therapeutic potential. *Antioxidants and Redox Signaling*, *13*(6), 877–918. https://doi.org/10.1089/ars.2009.2876

Batinić-Haberle, I., Spasojević, I., Hambright, P., Benov, L., Cmmbliss, A. L., & Fridovich, I. (1999). Relationship among redox potentials, proton dissociation constants of pyrrolic nitrogens, and in vivo and in vitro superoxide dismutating activities of manganese(III) and iron(III) water-soluble porphyrins. *Inorganic Chemistry*, *38*(18), 4011–4022. https://doi.org/10.1021/ic990118k

Batinić-Haberle, I., Spasojević, I., Stevens, R. D., Hambright, P., & Fridovich, I. (2002). Manganese(III) meso-tetrakis(ortho-N-alkylpyridyl)porphyrins. Synthesis, characterization, and catalysis of O2/·- dismutation. *Journal of the Chemical Society, Dalton Transactions*, *13*, 2689–2696. https://doi.org/10.1039/b201057g

Batinic-Haberle, I., Tovmasyan, A., Huang, Z., Duan, W., Du, L., Siamakpour-Reihani, S., Cao, Z., Sheng, H., Spasojevic, I., & Alvarez Secord, A. (2021). H2O2-Driven Anticancer Activity of Mn Porphyrins and the Underlying Molecular Pathways. *Oxidative Medicine and Cellular Longevity*, *2021*. https://doi.org/10.1155/2021/6653790

Batinic-Haberle, I., Tovmasyan, A., Roberts, E. R. H., Vujaskovic, Z., Leong, K. W., & Spasojevic, I. (2014). SOD therapeutics: latest insights into their structure-activity relationships and impact on the cellular redox-based signaling pathways. *Antioxidants & Redox Signaling*, *20*(15), 2372–2415. https://doi.org/10.1089/ars.2012.5147

Becuwe, P., Ennen, M., Klotz, R., Barbieux, C., & Grandemange, S. (2014). Manganese superoxide dismutase in breast cancer: From molecular mechanisms of gene regulation to biological and clinical significance. *Free Radical Biology and Medicine*, *77*, 139–151. https://doi.org/10.1016/j.freeradbiomed.2014.08.026

Berkel, C., & Cacan, E. (2021). Estrogen- and estrogen receptor (ER)-mediated cisplatin chemoresistance in cancer. *Life Sciences*, *286*(July), 120029. https://doi.org/10.1016/j.lfs.2021.120029

Bonetta, R. (2018). Potential Therapeutic Applications of MnSODs and SOD-Mimetics. *Chemistry - A European Journal*, *24*(20), 5032–5041. https://doi.org/10.1002/chem.201704561

Boss, M. K., Oberley-Deegan, R. E., Batinic-Haberle, I., Talmon, G. A., Somarelli, J. A., Xu, S., Kosmacek, E. A., Griess, B., Mir, S., Shrishrimal, S., Teoh-Fitzgerald, M., Spasojevic, I., & Dewhirst, M. W. (2021). Manganese porphyrin and radiotherapy improves local tumor response and overall survival in orthotopic murine mammary carcinoma models. *Radiation Research*, *195*(2), 128–139. https://doi.org/10.1667/RADE-20-00109.1

Bouhifd, M., Beger, R., Flynn, T., Guo, L., Harris, G., Hogberg, H., Kaddurah-Daouk, R., Kamp, H., Kleensang, A., Maertens, A., Odwin-Dacosta, S., Pamies, D., Robertson, D., Smirnova, L., Sun, J., Zhao, L., & Hartung, T. (2015). t 4 Workshop Report * : Quality Assurance of Metabolomics HHS Public Access. *Altex*, *32*(4), 319–326.

Bresciani, G., da Cruz, I. B. M., & González-Gallego, J. (2015). Manganese superoxide dismutase and oxidative stress modulation. *Advances in Clinical Chemistry*, *68*, 87–130. https://doi.org/10.1016/bs.acc.2014.11.001

Brigelius-Flohé, R., & Flohé, L. (2020). Regulatory Phenomena in the Glutathione Peroxidase Superfamily. *Antioxidants and Redox Signaling*, *33*(7), 498–516. https://doi.org/10.1089/ars.2019.7905

Broderick, S. R. (2020). Adjuvant and Neoadjuvant Immunotherapy in Non-small Cell Lung Cancer. *Thoracic Surgery Clinics*, *30*(2), 215–220. https://doi.org/10.1016/j.thorsurg.2020.01.001

Brown, S., Banfill, K., Aznar, M. C., Whitehurst, P., & Finn, C. F. (2019). The evolving role of radiotherapy in non-small cell lung cancer. *British Journal of Radiology*, *92*(1104). https://doi.org/10.1259/bjr.20190524

Browning, R. J., Reardon, P. J. T., Parhizkar, M., Pedley, R. B., Edirisinghe, M., Knowles, J. C., & Stride, E. (2017). Drug Delivery Strategies for Platinum-Based Chemotherapy. *ACS Nano*, *11*(9), 8560–8578. https://doi.org/10.1021/acsnano.7b04092

Buonerba, C., Federico, P., D'Aniello, C., Rescigno, P., Cavaliere, C., Puglia, L., Ferro, M., Altieri, V., Perdonà, S., De Placido, S., & Lorenzo, G. Di. (2011). Phase II trial of cisplatin plus prednisone in docetaxel-refractory castration-resistant prostate cancer patients. *Cancer Chemotherapy and Pharmacology*, *67*(6), 1455–1461. https://doi.org/10.1007/s00280-011-1594-z

Cai, A. L., Zeng, W., Cai, W. L., Liu, J. L., Zheng, X. W., Liu, Y., Yang, X. C., Long, Y., & Li, J. (2018). Peroxiredoxin-1 promotes cell proliferation and metastasis through enhancing Akt/mTOR in human osteosarcoma cells. *Oncotarget*, *9*(9), 8290–8302. https://doi.org/10.18632/oncotarget.23662

Cecerska-Heryć, E., Surowska, O., Heryć, R., Serwin, N., Napiontek-Balińska, S., & Dołęgowska, B. (2021). Are antioxidant enzymes essential markers in the diagnosis and monitoring of cancer patients – A review. *Clinical Biochemistry*, *93*(March), 1–8. https://doi.org/10.1016/j.clinbiochem.2021.03.008

Cetintas, V. B., Kucukaslan, A. S., Kosova, B., Tetik, A., Selvi, N., Cok, G., Gunduz, C., & Eroglu, Z. (2012). Cisplatin resistance induced by decreased apoptotic activity in non-small-cell lung cancer cell lines. *Cell Biology International*, *36*(3), 261–265. https://doi.org/10.1042/cbi20110329

Chaiswing, L., Clair, W. H. S., & Clair, D. K. S. (2018). Redox Paradox: A Novel Approach to Therapeutics-Resistant Cancer. *Antioxidants and Redox Signaling*, *29*(13), 1237–1272. https://doi.org/10.1089/ars.2017.7485

Chen, B., Shen, Z., Wu, D., Xie, X., Xu, X., Lv, L., Dai, H., Chen, J., & Gan, X. (2019). Glutathione peroxidase 1 promotes NSCLC resistance to cisplatin via ROS-induced activation of PI3K/AKT pathway. *BioMed Research International*, *2019*. https://doi.org/10.1155/2019/7640547

Chen, P., Li, J., Chen, Y. C., Qian, H., Chen, Y. J., Su, J. Y., Wu, M., & Lan, T. (2016). The functional status of DNA repair pathways determines the sensitization effect to cisplatin in non-small cell lung cancer cells. *Cellular Oncology*, *39*(6), 511–522. https://doi.org/10.1007/s13402-016-0291-7

Chen, X., Yang, Y., & Katz, S. I. (2018). Dexamethasone pretreatment impairs the thymidylate synthase inhibition mediated flare in thymidine salvage pathway activity in non-small cell lung cancer. *PLoS ONE*, *13*(8), 1–9. https://doi.org/10.1371/journal.pone.0202384

Chung-man Ho, J., Zheng, S., A Comhair, S. A., Farver, C., & Erzurum, S. C. (2001). Differential Expression of Manganese Superoxide Dismutase and Catalase in Lung Cancer 1. In *CANCER RESEARCH* (Vol. 61).

Cipriano, M., Pinheiro, P. F., Sequeira, C. O., Rodrigues, J. S., Oliveira, N. G., Antunes, A. M. M., Castro, M., Marques, M. M., Pereira, S. A., & Miranda, J. P. (2020). Nevirapine biotransformation insights: An integrated in vitro approach unveils the biocompetence and glutathiolomic profile of a human hepatocyte-like cell 3d model. *International Journal of Molecular Sciences*, *21*(11), 1–18. https://doi.org/10.3390/ijms21113998

Cline, J. M., Dugan, G., Bourland, J. D., Perry, D. L., Stitzel, J. D., Weaver, A. A., Jiang, C., Tovmasyan, A., Owzar, K., Spasojevic, I., Batinic-Haberle, I., & Vujaskovic, Z. (2018). Post-irradiation treatment with a superoxide dismutase mimic, MnTnHex-2-PyP5+, mitigates radiation injury in the lungs of non-human primates after whole-thorax exposure to ionizing radiation. *Antioxidants*, *7*(3), 1–17. https://doi.org/10.3390/ANTIOX7030040

Clish, C. B. (2015). Metabolomics: an emerging but powerful tool for precision medicine. *Molecular Case Studies*, *1*(1), a000588. https://doi.org/10.1101/mcs.a000588

Collins, L. G., Haines, C., Perkel, R., & Enck, R. E. (2007). Lung cancer: Diagnosis and management. *American Family Physician*, *75*(1), 56–63.

Costa, J. G., Saraiva, N., Batinic-Haberle, I., Castro, M., Oliveira, N. G., & Fernandes, A. S. (2019). The SOD mimic MnTnHex-2-pyp5+ reduces the viability and migration of 786-O human renal cancer cells. *Antioxidants*, *8*(10), 1–14. https://doi.org/10.3390/antiox8100490

Costa, J. G., Saraiva, N., Guerreiro, P. S., Louro, H., Silva, M. J., Miranda, J. P., Castro, M., Batinic-Haberle, I., Fernandes, A. S., & Oliveira, N. G. (2016). Ochratoxin A-induced cytotoxicity, genotoxicity and reactive oxygen species in kidney cells: An integrative approach of complementary endpoints. *Food and Chemical Toxicology*, *87*, 65–76. https://doi.org/10.1016/j.fct.2015.11.018

Costa, T. J., Barros, P. R., Arce, C., Santos, J. D., da Silva-Neto, J., Egea, G., Dantas, A. P., Tostes, R. C., & Jiménez-Altayó, F. (2021). The homeostatic role of hydrogen peroxide, superoxide anion and nitric oxide in the vasculature. *Free Radical Biology and Medicine*, *162*(October 2020), 615–635. https://doi.org/10.1016/j.freeradbiomed.2020.11.021

Crona, D. J., Faso, A., Nishijima, T. F., McGraw, K. A., Galsky, M. D., & Milowsky, M. I. (2017). A Systematic Review of Strategies to Prevent Cisplatin-Induced Nephrotoxicity. *The Oncologist*, *22*(5), 609–619. https://doi.org/10.1634/theoncologist.2016-0319

Dasari, S., & Bernard Tchounwou, P. (2014). Cisplatin in cancer therapy: Molecular mechanisms of action. In *European Journal of Pharmacology* (Vol. 740, pp. 364–378). Elsevier. https://doi.org/10.1016/j.ejphar.2014.07.025

Davou, G., Chuwang, N., Essien, U., Choji, T., Echeonwu, B., & Lugos, M. (2019). Cytotoxicity analysis of etoposide and cisplatin on cell lines from human lung cancer and normal human lung. *International Research Journal of Medicine and Medical Sciences*, *7*(2), 40–47. https://doi.org/10.30918/irjmms.72.19.022

Desilets, A., Adam, J. P., & Res, D. S. (2020). Management of cisplatin-associated toxicities in bladder cancer patients. *Current Opinion in Supportive and Palliative Care*, *14*(3), 286–292. https://doi.org/10.1097/SPC.0000000000000505

Dhar, S. K., & St. Clair, D. K. (2012). Manganese superoxide dismutase regulation and cancer. *Free Radical Biology and Medicine*, *52*(11–12), 2209–2222. https://doi.org/10.1016/j.freeradbiomed.2012.03.009

Duffy, E. A., Fitzgerald, W., Boyle, K., & Rohatgi, R. (2018). Nephrotoxicity: Evidence in patients receiving cisplatin therapy. *Clinical Journal of Oncology Nursing*, *22*(2), 175–183. https://doi.org/10.1188/18.CJON.175-183

Duma, N., Santana-Davila, R., & Molina, J. R. (2019). Non–Small Cell Lung Cancer: Epidemiology, Screening, Diagnosis, and Treatment. *Mayo Clinic Proceedings*, *94*(8), 1623–1640. https://doi.org/10.1016/j.mayocp.2019.01.013

Ebrahimi, S. O., Reiisi, S., & Shareef, S. (2020). miRNAs, oxidative stress, and cancer: A comprehensive and updated review. *Journal of Cellular Physiology*, *235*(11), 8812–8825. https://doi.org/10.1002/jcp.29724

Egea, J., Fabregat, I., Frapart, Y. M., Ghezzi, P., Görlach, A., Kietzmann, T., Kubaichuk, K., Knaus, U. G., Lopez, M. G., Olaso-Gonzalez, G., Petry, A., Schulz, R., Vina, J., Winyard, P., Abbas, K., Ademowo, O. S., Afonso, C. B., Andreadou, I., Antelmann, H., … Daiber, A. (2017). European contribution to the study of ROS: A summary of the findings and prospects for the future from the COST action BM1203 (EU-ROS). *Redox Biology*, *13*(May), 94–162. https://doi.org/10.1016/j.redox.2017.05.007

Fernandes, A. S., Gaspar, J., Cabral, M. F., Rueff, J., Castro, M., Batinic-Haberle, I., Costa, J., & Oliveira, N. G. (2010). Protective role of ortho-substituted Mn(III) N-alkylpyridylporphyrins against the oxidative injury induced by tert-butylhydroperoxide. *Free Radical Research*, *44*(4), 430–440. https://doi.org/10.3109/10715760903555844

Fernandes, A. S., Saraiva, N., & Oliveira, N. G. (2016). *Redox Therapeutics in Breast Cancer: Role of SOD Mimics*. 451–467. https://doi.org/10.1007/978-3-319-30705-3_18

Fernandes, A. S., Serejo, J., Gaspar, J., Cabral, F., Bettencourt, A. F., Rueff, J., Castro, M.,

Costa, J., & Oliveira, N. G. (2010). Oxidative injury in V79 Chinese hamster cells: Protective role of the superoxide dismutase mimetic MnTM-4-PyP. *Cell Biology and Toxicology*, *26*(2), 91–101. https://doi.org/10.1007/s10565-009-9120-3

Flórido, A., Saraiva, N., Cerqueira, S., Almeida, N., Parsons, M., Batinic-Haberle, I., Miranda, J. P., Costa, J. G., Carrara, G., Castro, M., Oliveira, N. G., & Fernandes, A. S. (2019). The manganese(III) porphyrin MnTnHex-2-PyP 5+ modulates intracellular ROS and breast cancer cell migration: Impact on doxorubicin-treated cells. *Redox Biology*, *20*(September 2018), 367–378. https://doi.org/10.1016/j.redox.2018.10.016

Forshaw, T. E., Holmila, R., Nelson, K. J., Lewis, J. E., Kemp, M. L., Tsang, A. W., Poole, L. B., Lowther, W. T., & Furdui, C. M. (2019). Peroxiredoxins in cancer and response to radiation therapies. *Antioxidants*, *8*(1), 1–24. https://doi.org/10.3390/antiox8010011

Fukai, T., & Ushio-Fukai, M. (2011). Superoxide dismutases: Role in redox signaling, vascular function, and diseases. *Antioxidants and Redox Signaling*, *15*(6), 1583–1606. https://doi.org/10.1089/ars.2011.3999

Galasso, M., Gambino, S., Romanelli, M. G., Donadelli, M., & Scupoli, M. T. (2021). Browsing the oldest antioxidant enzyme: catalase and its multiple regulation in cancer. *Free Radical Biology and Medicine*, *172*(May), 264–272. https://doi.org/10.1016/j.freeradbiomed.2021.06.010

Ganesh, K., & Massagué, J. (2021). Targeting metastatic cancer. In *Nature Medicine* (Vol. 27, Issue 1, pp. 34–44). Nature Research. https://doi.org/10.1038/s41591-020-01195-4

Ghosh, S. (2019). Cisplatin: The first metal based anticancer drug. *Bioorganic Chemistry*, *88*(October 2018), 102925. https://doi.org/10.1016/j.bioorg.2019.102925

Gill, J. G., Piskounova, E., & Morrison, S. J. (2016). Cancer, oxidative stress, and metastasis. *Cold Spring Harbor Symposia on Quantitative Biology*, *81*(1), 163–175. https://doi.org/10.1101/sqb.2016.81.030791

Glorieux, C., & Calderon, P. B. (2017). Catalase, a remarkable enzyme: Targeting the oldest antioxidant enzyme to find a new cancer treatment approach. *Biological Chemistry*, *398*(10), 1095–1108. https://doi.org/10.1515/hsz-2017-0131

Gorrini, C., Harris, I. S., & Mak, T. W. (2013). Modulation of oxidative stress as an anticancer strategy. *Nature Reviews Drug Discovery*, *12*(12), 931–947. https://doi.org/10.1038/nrd4002

Guerreiro, P. S., Corvacho, E., Costa, J. G., Saraiva, N., Fernandes, A. S., Castro, M., Miranda, J. P., & Oliveira, N. G. (2017). The APE1 redox inhibitor E3330 reduces collective cell migration of human breast cancer cells and decreases chemoinvasion and colony formation when combined with docetaxel. *Chemical Biology and Drug Design*, *90*(4), 561–571. https://doi.org/10.1111/cbdd.12979

Gupta, A., Srivastava, S., Prasad, R., Natu, S. M., Mittal, B., Negi, M. P. S., & Srivastava, A. N. (2010). Oxidative stress in non-small cell lung cancer patients after chemotherapy: Association with treatment response. *Respirology*, *15*(2), 349–356. https://doi.org/10.1111/j.1440-1843.2009.01703.x

Gupta, R. K., Patel, A. K., Shah, N., Chaudhary, A. K., Jha, U. K., Yadav, U. C., Gupta, P. K., & Pakuwal, U. (2014). Oxidative stress and antioxidants in disease and cancer: A review. *Asian Pacific Journal of Cancer Prevention*, *15*(11), 4405–4409. https://doi.org/10.7314/APJCP.2014.15.11.4405

Ha, B., Kim, E. K., Kim, J. H., Lee, H. N., Lee, K. O., Lee, S. Y., & Jang, H. H. (2012). Human peroxiredoxin 1 modulates TGF-β1-induced epithelial-mesenchymal transition through its peroxidase activity. *Biochemical and Biophysical Research Communications*, *421*(1), 33–

37. https://doi.org/10.1016/j.bbrc.2012.03.103

Hanke, N. T., Imler, E., Marron, M. T., Seligmann, B. E., Garland, L. L., & Baker, A. F. (2018). Characterization of carfilzomib-resistant non-small cell lung cancer cell lines. *Journal of Cancer Research and Clinical Oncology*, *144*(7), 1317–1327. https://doi.org/10.1007/s00432-018-2662-0

Harris, I. S., & DeNicola, G. M. (2020). The Complex Interplay between Antioxidants and ROS in Cancer. *Trends in Cell Biology*, *30*(6), 440–451. https://doi.org/10.1016/j.tcb.2020.03.002

Haynes, B., Saadat, N., Myung, B., & Shekhar, M. P. V. (2015). Crosstalk between translesion synthesis, Fanconi anemia network, and homologous recombination repair pathways in interstrand DNA crosslink repair and development of chemoresistance. In *Mutation Research - Reviews in Mutation Research* (Vol. 763, pp. 258–266). Elsevier. https://doi.org/10.1016/j.mrrev.2014.11.005

Herbst, R. S., Morgensztern, D., & Boshoff, C. (2018). The biology and management of non-small cell lung cancer. *Nature*, *553*(7689), 446–454. https://doi.org/10.1038/nature25183

Hoy, H., Lynch, T., & Beck, M. (2019). Surgical Treatment of Lung Cancer. *Critical Care Nursing Clinics of North America*, *31*(3), 303–313. https://doi.org/10.1016/j.cnc.2019.05.002

Huang, G., & Pan, S. T. (2020). ROS-Mediated Therapeutic Strategy in Chemo-/Radiotherapy of Head and Neck Cancer. *Oxidative Medicine and Cellular Longevity*, *2020*. https://doi.org/10.1155/2020/5047987

Huang, J. Q., Liang, H. L., Zhang, X. C., Xie, Z., & Jin, T. E. (2016). Synergistic antitumor activity of pro-apoptotic agent PAC-1 with cisplatinum by the activation of CASP3 in pulmonary adenocarcinoma cell line H1299. *Asia-Pacific Journal of Clinical Oncology*, *12*(1), 41–51. https://doi.org/10.1111/ajco.12419

Huang, Y., Lei, L., & Liu, Y. (2020). Propofol improves sensitivity of lung cancer cells to cisplatin and its mechanism. *Medical Science Monitor*, *26*, 1–9. https://doi.org/10.12659/MSM.919786

Janfaza, S., Khorsand, B., Nikkhah, M., & Zahiri, J. (2019). Digging deeper into volatile organic compounds associated with cancer. *Biology Methods and Protocols*, *4*(1), 1–11. https://doi.org/10.1093/biomethods/bpz014

Jaramillo, M. C., Briehl, M. M., Batinic-Haberle, I., & Tome, M. E. (2015). Manganese (III) meso-tetrakis N-ethylpyridinium-2-yl porphyrin acts as a pro-oxidant to inhibit electron transport chain proteins, modulate bioenergetics, and enhance the response to chemotherapy in lymphoma cells. *Free Radical Biology and Medicine*, *83*, 89–100. https://doi.org/10.1016/j.freeradbiomed.2015.01.031

Jelic, M. D., Mandic, A. D., Maricic, S. M., & Srdjenovic, B. U. (2021). Oxidative stress and its role in cancer. In *Journal of Cancer Research and Therapeutics* (Vol. 17, Issue 1, pp. 22–28). Wolters Kluwer Medknow Publications. https://doi.org/10.4103/jcrt.JCRT_862_16

Jiang, D. M., Gupta, S., Kitchlu, A., Meraz-Munoz, A., North, S. A., Alimohamed, N. S., Blais, N., & Sridhar, S. S. (2021). Defining cisplatin eligibility in patients with muscle-invasive bladder cancer. *Nature Reviews Urology*, *18*(2), 104–114. https://doi.org/10.1038/s41585-020-00404-6

Jiang, H., Wu, L., Mishra, M., Chawsheen, H. A., & Wei, Q. (2014). Expression of peroxiredoxin 1 and 4 promotes human lung cancer malignancy. *American Journal of Cancer Research*, *4*(5), 445–460.

Jing, X., Du, L., Niu, A., Wang, Y., Wang, Y., & Wang, C. (2020). Silencing of PRDX2 Inhibits the Proliferation and Invasion of Non-Small Cell Lung Cancer Cells. *BioMed Research International*, *2020*. https://doi.org/10.1155/2020/1276328

Kalyanaraman, B. (2013). Teaching the basics of redox biology to medical and graduate students: Oxidants, antioxidants and disease mechanisms. *Redox Biology*, *1*(1), 244–257. https://doi.org/10.1016/j.redox.2013.01.014

Kelland, L. (2007). The resurgence of platinum-based cancer chemotherapy. *Nature Reviews Cancer*, *7*(8), 573–584. https://doi.org/10.1038/nrc2167

Kennedy, A. D., Wittmann, B. M., Evans, A. M., Miller, L. A. D., Toal, D. R., Lonergan, S., Elsea, S. H., & Pappan, K. L. (2018). Metabolomics in the clinic: A review of the shared and unique features of untargeted metabolomics for clinical research and clinical testing. *Journal of Mass Spectrometry*, *53*(11), 1143–1154. https://doi.org/10.1002/jms.4292

Kitagawa, R., Katsumata, N., Shibata, T., Kamura, T., Kasamatsu, T., Nakanishi, T., Nishimura, S., Ushijima, K., Takano, M., Satoh, T., & Yoshikawa, H. (2015). Paclitaxel plus carboplatin versus paclitaxel plus cisplatin in metastatic or recurrent cervical cancer: The open-label randomized phase III trial JCOG0505. *Journal of Clinical Oncology*, *33*(19), 2129–2135. https://doi.org/10.1200/JCO.2014.58.4391

Klaunig, J. E. (2019). Oxidative Stress and Cancer. *Current Pharmaceutical Design*, *24*(40), 4771–4778. https://doi.org/10.2174/1381612825666190215121712

Klaunig, J. E., & Wang, Z. (2018). Oxidative stress in carcinogenesis. *Current Opinion in Toxicology*, *7*, 116–121. https://doi.org/10.1016/j.cotox.2017.11.014

Klyosov, A. A. (1996). Kinetics and specificity of human liver aldehyde dehydrogenases toward aliphatic, aromatic, and fused polycyclic aldehydes. *Biochemistry*, *35*(14), 4457–4467. https://doi.org/10.1021/bi9521102

Kosmacek, E. A., Chatterjee, A., Tong, Q., Lin, C., & Oberley-Deegan, R. E. (2016). MnTnBuOE-2-PyP protects normal colorectal fibroblasts from radiation damage and simultaneously enhances radio/chemotherapeutic killing of colorectal cancer cells. *Oncotarget*, *7*(23), 34532–34545. https://doi.org/10.18632/oncotarget.8923

Kryczka, J., Kryczka, J., Czarnecka-Chrebelska, K. H., & Brzeziańska-Lasota, E. (2021). Molecular mechanisms of chemoresistance induced by cisplatin in NSCLC cancer therapy. *International Journal of Molecular Sciences*, *22*(16). https://doi.org/10.3390/ijms22168885

Kudryavtseva, A. V., Krasnov, G. S., Dmitriev, A. A., Alekseev, B. Y., Kardymon, O. L., Sadritdinova, A. F., Fedorova, M. S., Pokrovsky, A. V., Melnikova, N. V., Kaprin, A. D., Moskalev, A. A., & Snezhkina, A. V. (2016). Mitochondrial dysfunction and oxidative stress in aging and cancer. *Oncotarget*, *7*(29), 44879–44905. https://doi.org/10.18632/oncotarget.9821

Kumar, N., Shahjaman, M., Mollah, M. N. H., Islam, S. M. S., & Hoque, M. A. (2017). Serum and Plasma Metabolomic Biomarkers for Lung Cancer. *Bioinformation*, *13*(06), 202–208. https://doi.org/10.6026/97320630013202

Landmesser, M. E., Raup-Konsavage, W. M., Lehman, H. L., & Stairs, D. B. (2020). Loss of p120ctn causes EGFR-targeted therapy resistance and failure. *PLoS ONE*, *15*(10 October), 1–14. https://doi.org/10.1371/journal.pone.0241299

Larosa, V., & Remacle, C. (2018). Insights into the respiratory chain and oxidative stress. *Bioscience Reports*, *38*(5), 1–14. https://doi.org/10.1042/BSR20171492

Lee, E., Choi, A., Jun, Y., Kim, N., Yook, J. I., Kim, S. Y., Lee, S., & Kang, S. W. (2020).

Glutathione peroxidase-1 regulates adhesion and metastasis of triple-negative breast cancer cells via FAK signaling. *Redox Biology*, *29*(November 2019), 101391. https://doi.org/10.1016/j.redox.2019.101391

Legin, A. A., Schintlmeister, A., Jakupec, M. A., Galanski, M., Lichtscheidl, I., Wagner, M., & Keppler, B. K. (2014). NanoSIMS combined with fluorescence microscopy as a tool for subcellular imaging of isotopically labeled platinum-based anticancer drugs. *Chemical Science*, *5*(8), 3135–3143. https://doi.org/10.1039/c3sc53426j

Leu, D., Spasojevic, I., Nguyen, H., Deng, B., Tovmasyan, A., Weitner, T., Sampaio, R. S., Batinic-Haberle, I., & Huang, T. T. (2017). CNS bioavailability and radiation protection of normal hippocampal neurogenesis by a lipophilic Mn porphyrin-based superoxide dismutase mimic, MnTnBuOE-2-PyP5+. *Redox Biology*, *12*(January), 864–871. https://doi.org/10.1016/j.redox.2017.04.027

Li, Y. R., & Trush, M. (2016). Defining ROS in Biology and Medicine. *Reactive Oxygen Species*, *1*(1), 9–21. https://doi.org/10.20455/ros.2016.803

Liang, J., Bi, N., Wu, S., Chen, M., Lv, C., Zhao, L., Shi, A., Jiang, W., Xu, Y., Zhou, Z., Wang, W., Chen, D., Hui, Z., Lv, J., Zhang, H., Feng, Q., Xiao, Z., Wang, X., Liu, L., … Wang, L. (2017). Etoposide and cisplatin versus paclitaxel and carboplatin with concurrent thoracic radiotherapy in unresectable stage III non-small cell lung cancer: A multicenter randomized phase III trial. *Annals of Oncology*, *28*(4), 777–783. https://doi.org/10.1093/annonc/mdx009

Lima, A. R., Pinto, J., Azevedo, A. I., Barros-Silva, D., Jerónimo, C., Henrique, R., de Lourdes Bastos, M., Guedes de Pinho, P., & Carvalho, M. (2019). Identification of a biomarker panel for improvement of prostate cancer diagnosis by volatile metabolic profiling of urine. *British Journal of Cancer*, *121*(10), 857–868. https://doi.org/10.1038/s41416-019-0585-4

Liu, L., & Liu, X. (2019). Contributions of drug transporters to blood-brain barriers. In *Advances in Experimental Medicine and Biology* (Vol. 1141). https://doi.org/10.1007/978-981-13-7647-4_9

Lubos, E., Loscalzo, J., & Handy, D. E. (2011). Glutathione peroxidase-1 in health and disease: From molecular mechanisms to therapeutic opportunities. *Antioxidants and Redox Signaling*, *15*(7), 1957–1997. https://doi.org/10.1089/ars.2010.3586

Lugrin, J., Rosenblatt-Velin, N., Parapanov, R., & Liaudet, L. (2014). The role of oxidative stress during inflammatory processes. *Biological Chemistry*, *395*(2), 203–230. https://doi.org/10.1515/hsz-2013-0241

Luo, J., Song, J., Feng, P., Wang, Y., Long, W., Liu, M., & Li, L. (2016). Elevated serum apolipoprotein E is associated with metastasis and poor prognosis of non-small cell lung cancer. *Tumor Biology*, *37*(8), 10715–10721. https://doi.org/10.1007/s13277-016-4975-4

Makinde, A. Y., Rizvi, A., Crapo, J. D., Pearlstein, R. D., Slater, J. M., & Gridley, D. S. (2010). A metalloporphyrin antioxidant alters cytokine responses after irradiation in a prostate tumor model. *Radiation Research*, *173*(4), 441–452. https://doi.org/10.1667/RR1765.1

Makovec, T. (2019). Cisplatin and beyond: Molecular mechanisms of action and drug resistance development in cancer chemotherapy. *Radiology and Oncology*, *53*(2), 148–158. https://doi.org/10.2478/raon-2019-0018

Manguinhas, R., Fernandes, A. S., Costa, J. G., Saraiva, N., Camões, S. P., Gil, N., Rosell, R., Castro, M., Miranda, J. P., & Oliveira, N. G. (2020). Impact of the ape1 redox function inhibitor e3330 in non-small cell lung cancer cells exposed to cisplatin: Increased cytotoxicity and impairment of cell migration and invasion. *Antioxidants*, *9*(6), 1–18.

https://doi.org/10.3390/antiox9060550

Mao, Y., Yang, D., He, J., & Krasna, M. J. (2016). Epidemiology of Lung Cancer. *Surgical Oncology Clinics of North America*, *25*(3), 439–445. https://doi.org/10.1016/j.soc.2016.02.001

Mapuskar, K. A., Anderson, C. M., Spitz, D. R., Batinic-Haberle, I., Allen, B. G., & E. Oberley-Deegan, R. (2019). Utilizing Superoxide Dismutase Mimetics to Enhance Radiation Therapy Response While Protecting Normal Tissues. *Seminars in Radiation Oncology*, *29*(1), 72–80. https://doi.org/10.1016/j.semradonc.2018.10.005

McElroy, T., Brown, T., Kiffer, F., Wang, J., Byrum, S. D., Oberley-Deegan, R. E., & Allen, A. R. (2020). Assessing the effects of redox modifier MnTnBuOE-2-PyP 5+ on cognition and hippocampal physiology following doxorubicin, cyclophosphamide, and paclitaxel treatment. *International Journal of Molecular Sciences*, *21*(5). https://doi.org/10.3390/ijms21051867

Meng, Y., Jin, J., Gong, C., Miao, H., Tao, Z., Li, T., Cao, J., Wang, L., Wang, B., Zhang, J., & Hu, X. (2021). Phase II study of chidamide in combination with cisplatin in patients with metastatic triple-negative breast cancer. *Annals of Palliative Medicine*, *10*(11), 11255–11264. https://doi.org/10.21037/apm-21-1139

Miller, M., & Hanna, N. (2021). Advances in systemic therapy for non-small cell lung cancer. *The BMJ*, *375*, 1–16. https://doi.org/10.1136/bmj.n2363

Mochalski, P., Al-Zoairy, R., Niederwanger, A., Unterkofler, K., & Amann, A. (2014). Quantitative analysis of volatile organic compounds released and consumed by rat L6 skeletal muscle cells in vitro. *Journal of Breath Research*, *8*(4). https://doi.org/10.1088/1752-7155/8/4/046003

Moghbeli, M. (2021). MicroRNAs as the critical regulators of Cisplatin resistance in ovarian cancer cells. *Journal of Ovarian Research*, *14*(1), 1–16. https://doi.org/10.1186/s13048-021-00882-1

Nagasaka, M., & Gadgeel, S. M. (2018). Role of chemotherapy and targeted therapy in early-stage non-small cell lung cancer. *Expert Review of Anticancer Therapy*, *18*(1), 63–70. https://doi.org/10.1080/14737140.2018.1409624

Nasim, F., Sabath, B. F., & Eapen, G. A. (2019). Lung Cancer. *Medical Clinics of North America*, *103*(3), 463–473. https://doi.org/10.1016/j.mcna.2018.12.006

Neumann, C. A., Cao, J., & Manevich, Y. (2009). Peroxiredoxin 1 and its role in cell signaling. In *Cell Cycle* (Vol. 8, Issue 24, pp. 4072–4078). Taylor and Francis Inc. https://doi.org/10.4161/cc.8.24.10242

Nicolussi, A., D'Inzeo, S., Capalbo, C., Giannini, G., & Coppa, A. (2017). The role of peroxiredoxins in cancer. *Molecular and Clinical Oncology*, *6*(2), 139–153. https://doi.org/10.3892/mco.2017.1129

Nooreldeen, R., & Bach, H. (2021). Current and future development in lung cancer diagnosis. *International Journal of Molecular Sciences*, *22*(16). https://doi.org/10.3390/ijms22168661

Ogawa, F., Walters, M. S., Shafquat, A., O'Beirne, S. L., Kaner, R. J., Mezey, J. G., Zhang, H., Leopold, P. L., & Crystal, R. G. (2019). Role of KRAS in regulating normal human airway basal cell differentiation. *Respiratory Research*, *20*(1), 1–16. https://doi.org/10.1186/s12931-019-1129-4

Pang, Z., Chong, J., Zhou, G., De Lima Morais, D. A., Chang, L., Barrette, M., Gauthier, C., Jacques, P. É., Li, S., & Xia, J. (2021). MetaboAnalyst 5.0: Narrowing the gap between

raw spectra and functional insights. *Nucleic Acids Research*, *49*(W1), W388–W396. https://doi.org/10.1093/nar/gkab382

Park, E. M., Ramnath, N., Yang, G. Y., Ahn, J. Y., Park, Y., Lee, T. Y., Shin, H. S., Yu, J., Ip, C., & Park, Y. M. (2007). High superoxide dismutase and low glutathione peroxidase activities in red blood cells predict susceptibility of lung cancer patients to radiation pneumonitis. *Free Radical Biology and Medicine*, *42*(2), 280–287. https://doi.org/10.1016/j.freeradbiomed.2006.10.044

Park, M. H., Jo, M., Kim, Y. R., Lee, C. K., & Hong, J. T. (2016). Roles of peroxiredoxins in cancer, neurodegenerative diseases and inflammatory diseases. In *Pharmacology and Therapeutics* (Vol. 163, pp. 1–23). Elsevier Inc. https://doi.org/10.1016/j.pharmthera.2016.03.018

Patel, A., Kosmacek, E. A., Fisher, K. W., Goldner, W., & Oberley-Deegan, R. E. (2020). MnTnBuOE-2-PyP treatment protects from radioactive iodine (I-131) treatment-related side effects in thyroid cancer. *Radiation and Environmental Biophysics*, *59*(1), 99–109. https://doi.org/10.1007/s00411-019-00820-2

Patil, V. M., Noronha, V., Joshi, A., Agarwal, J., Ghosh-Laskar, S., Budrukkar, A., Murthy, V., Gupta, T., Mahimkar, M., Juvekar, S., Arya, S., Mahajan, A., Agarwal, A., Purandare, N., Rangarajan, V., Balaji, A., Chaudhari, S. V., Banavali, S., Kannan, S., … Prabhash, K. (2019). A randomized phase 3 trial comparing nimotuzumab plus cisplatin chemoradiotherapy versus cisplatin chemoradiotherapy alone in locally advanced head and neck cancer. *Cancer*, *125*(18), 3184–3197. https://doi.org/10.1002/cncr.32179

Pijuan, J., Barceló, C., Moreno, D. F., Maiques, O., Sisó, P., Marti, R. M., Macià, A., & Panosa, A. (2019). In vitro cell migration, invasion, and adhesion assays: From cell imaging to data analysis. *Frontiers in Cell and Developmental Biology*, *7*(JUN), 1–16. https://doi.org/10.3389/fcell.2019.00107

Pisoschi, A. M., & Pop, A. (2015). The role of antioxidants in the chemistry of oxidative stress: A review. *European Journal of Medicinal Chemistry*, *97*, 55–74. https://doi.org/10.1016/j.ejmech.2015.04.040

Pluskal, T., Castillo, S., Villar-Briones, A., & Orešič, M. (2010). MZmine 2: Modular framework for processing, visualizing, and analyzing mass spectrometry-based molecular profile data. *BMC Bioinformatics*, *11*. https://doi.org/10.1186/1471-2105-11-395

Pollard, J. M., Reboucas, J. S., Durazo, A., Kos, I., Fike, F., Panni, M., Gralla, E. B., Valentine, J. S., Batinic-Haberle, I., & Gatti, R. A. (2009). Radioprotective effects of manganese-containing superoxide dismutase mimics on ataxia-telangiectasia cells. *Free Radical Biology and Medicine*, *47*(3), 250–260. https://doi.org/10.1016/j.freeradbiomed.2009.04.018

Poprac, P., Jomova, K., Simunkova, M., Kollar, V., Rhodes, C. J., & Valko, M. (2017). Targeting Free Radicals in Oxidative Stress-Related Human Diseases. *Trends in Pharmacological Sciences*, *38*(7), 592–607. https://doi.org/10.1016/j.tips.2017.04.005

Qi, L., Luo, Q., Zhang, Y., Jia, F., Zhao, Y., & Wang, F. (2019). Advances in Toxicological Research of the Anticancer Drug Cisplatin [Review-article]. *Chemical Research in Toxicology*, *32*(8), 1469–1486. https://doi.org/10.1021/acs.chemrestox.9b00204

Quail, D. F., & Joyce, J. A. (2013). Microenvironmental regulation of tumor progression and metastasis. In *Nature Medicine* (Vol. 19, Issue 11, pp. 1423–1437). Nat Med. https://doi.org/10.1038/nm.3394

Rabbani, Z. N., Spasojevic, I., Zhang, X., Moeller, B. J., Haberle, S., Vasquez-Vivar, J., Dewhirst, M. W., Vujaskovic, Z., & Batinic-Haberle, I. (2009). Antiangiogenic action of

redox-modulating Mn(III) meso-tetrakis(N-ethylpyridinium-2-yl)porphyrin, MnTE-2-PyP5+, via suppression of oxidative stress in a mouse model of breast tumor. *Free Radical Biology and Medicine*, *47*(7), 992–1004. https://doi.org/10.1016/j.freeradbiomed.2009.07.001

Rajic, Z., Tovmasyan, A., Spasojevic, I., Sheng, H., Lu, M., Li, A. M., Gralla, E. B., Warner, D. S., Benov, L., & Batinic-Haberle, I. (2012). A new SOD mimic, Mn(III) ortho N-butoxyethylpyridylporphyrin, combines superb potency and lipophilicity with low toxicity. *Free Radical Biology and Medicine*, *52*(9), 1828–1834. https://doi.org/10.1016/j.freeradbiomed.2012.02.006

Raudenska, M., Balvan, J., Fojtu, M., Gumulec, J., & Masarik, M. (2019). Unexpected therapeutic effects of cisplatin. *Metallomics*, *11*(7), 1182–1199. https://doi.org/10.1039/c9mt00049f

Robbins, D., & Zhao, Y. (2014). Manganese superoxide dismutase in cancer prevention. *Antioxidants and Redox Signaling*, *20*(10), 1628–1645. https://doi.org/10.1089/ars.2013.5297

Rodriguez-Canales, J., Parra-Cuentas, E., & Wistuba, I. I. (2016). Diagnosis and molecular classification of lung cancer. *Cancer Treatment and Research*, *170*, 25–46. https://doi.org/10.1007/978-3-319-40389-2_2

Romanowska, M., Kikawa, K. D., Fields, J. R., Maciag, A., North, S. L., Shiao, Y. H., Kasprzak, K. S., & Anderson, L. M. (2007). Effects of selenium supplementation on expression of glutathione peroxidase isoforms in cultured human lung adenocarcinoma cell lines. *Lung Cancer*, *55*(1), 35–42. https://doi.org/10.1016/j.lungcan.2006.09.007

Romaszko, A. M., & Doboszynska, A. (2018). Multiple primary lung cancer: A literature review. *Advances in Clinical and Experimental Medicine*, *27*(5), 717–722. https://doi.org/10.17219/acem/68631

Rosell, R., Mendez, P., Isla, D., & Taron, M. (2007). Platinum resistance related to a functional NER pathway. *Journal of Thoracic Oncology*, *2*(12), 1063–1066. https://doi.org/10.1097/JTO.0b013e31815ba2a1

Safirstein, R., Miller, P., & Guttenplan, J. B. (1984). Uptake and metabolism of cisplatin by rat kidney. *Kidney International*, *25*(5), 753–758. https://doi.org/10.1038/ki.1984.86

Schabath, M. B., & Cote, M. L. (2019). Cancer progress and priorities: Lung cancer. *Cancer Epidemiology Biomarkers and Prevention*, *28*(10), 1563–1579. https://doi.org/10.1158/1055-9965.EPI-19-0221

Sharapov, M. G., Goncharov, R. G., Filkov, G. I., Trofimenko, A. V., Boyarintsev, V. V., & Novoselov, V. I. (2020). Comparative study of protective action of exogenous 2-cys peroxiredoxins (Prx1 and prx2) under renal ischemia-reperfusion injury. *Antioxidants*, *9*(8), 1–23. https://doi.org/10.3390/antiox9080680

Shin, S. W., Choi, C., Kim, H., Kim, Y., Park, S., Kim, S. Y., Batinic-Haberle, I., & Park, W. (2021). MnTnHex-2-PyP5+, coupled to radiation, suppresses metastasis of 4T1 and MDA-MB-231 breast cancer via AKT/Snail/EMT pathways. *Antioxidants*, *10*(11), 1–18. https://doi.org/10.3390/antiox10111769

Siddik, Z. H. (2003). Cisplatin: Mode of cytotoxic action and molecular basis of resistance. *Oncogene*, *22*(47 REV. ISS. 6), 7265–7279. https://doi.org/10.1038/sj.onc.1206933

Siegel, R. L., Miller, K. D., Fuchs, H. E., & Jemal, A. (2022). Cancer statistics, 2022. *CA: A Cancer Journal for Clinicians*, *72*(1), 7–33. https://doi.org/10.3322/caac.21708

Siegel, R. L., Miller, K. D., & Jemal, A. (2020). Cancer statistics, 2020. *CA: A Cancer Journal*

for Clinicians, *70*(1), 7–30. https://doi.org/10.3322/caac.21590

Singh, A., Prakash, V., Gupta, N., Kumar, A., Kant, R., & Kumar, D. (2022). Serum Metabolic Disturbances in Lung Cancer Investigated through an Elaborative NMR-Based Serum Metabolomics Approach. *ACS Omega*, *7*(6), 5510–5520. https://doi.org/10.1021/acsomega.1c06941

Singh, B., Patwardhan, R. S., Jayakumar, S., Sharma, D., & Sandur, S. K. (2020). Oxidative stress associated metabolic adaptations regulate radioresistance in human lung cancer cells. *Journal of Photochemistry and Photobiology B: Biology*, *213*(October), 112080. https://doi.org/10.1016/j.jphotobiol.2020.112080

Sosa, V., Moliné, T., Somoza, R., Paciucci, R., Kondoh, H., & LLeonart, M. E. (2013). Oxidative stress and cancer: An overview. *Ageing Research Reviews*, *12*(1), 376–390. https://doi.org/10.1016/j.arr.2012.10.004

Sung, H., Ferlay, J., Siegel, R. L., Laversanne, M., Soerjomataram, I., Jemal, A., & Bray, F. (2021). Global Cancer Statistics 2020: GLOBOCAN Estimates of Incidence and Mortality Worldwide for 36 Cancers in 185 Countries. *CA: A Cancer Journal for Clinicians*, *71*(3), 209–249. https://doi.org/10.3322/caac.21660

T. Keir, S., W. Dewhirst, M., P. Kirkpatrick, J., D. Bigner, D., & Batinic-Haberle, I. (2012). Cellular Redox Modulator, ortho Mn(III) meso-tetrakis(N-n-Hexylpyridinium-2-yl)porphyrin, MnTnHex-2-PyP5+ in the Treatment of Brain Tumors. *Anti-Cancer Agents in Medicinal Chemistry*, *11*(2), 202–212. https://doi.org/10.2174/187152011795255957

Takemoto, S., Nakamura, Y., Gyoutoku, H., Senju, H., Ogawara, D., Ikeda, T., Yamaguchi, H., Kitazaki, T., Nakano, H., Nakatomi, K., Tomari, S., Sato, S., Nagashima, S., Fukuda, M., & Mukae, H. (2019). Phase II trial of a non-platinum triplet for patients with advanced non-small cell lung carcinoma (NSCLC) overexpressing ERCC1 messenger RNA. *Thoracic Cancer*, *10*(3), 452–458. https://doi.org/10.1111/1759-7714.12958

Teng, Q., Huang, W., Collette, T. W., Ekman, D. R., & Tan, C. (2009). A direct cell quenching method for cell-culture based metabolomics. *Metabolomics*, *5*(2), 199–208. https://doi.org/10.1007/s11306-008-0137-z

Thakur, S. K., Singh, D. P., & Choudhary, J. (2020). Lung cancer identification: a review on detection and classification. *Cancer and Metastasis Reviews*, *39*(3), 989–998. https://doi.org/10.1007/s10555-020-09901-x

Tong, Q., Zhu, Y., Galaske, J. W., Kosmacek, E. A., Chatterjee, A., Dickinson, B. C., & Oberley-Deegan, R. E. (2016). MnTE-2-PyP modulates thiol oxidation in a hydrogen peroxide-mediated manner in a human prostate cancer cell. *Free Radical Biology and Medicine*, *101*(402), 32–43. https://doi.org/10.1016/j.freeradbiomed.2016.09.019

Travis, W. D., Brambilla, E., Nicholson, A. G., Yatabe, Y., Austin, J. H. M., Beasley, M. B., Chirieac, L. R., Dacic, S., Duhig, E., Flieder, D. B., Geisinger, K., Hirsch, F. R., Ishikawa, Y., Kerr, K. M., Noguchi, M., Pelosi, G., Powell, C. A., Tsao, M. S., & Wistuba, I. (2015). The 2015 World Health Organization Classification of Lung Tumors: Impact of Genetic, Clinical and Radiologic Advances since the 2004 Classification. *Journal of Thoracic Oncology*, *10*(9), 1243–1260. https://doi.org/10.1097/JTO.0000000000000630

Uprety, D., Mandrekar, S. J., Wigle, D., Roden, A. C., & Adjei, A. A. (2020). Neoadjuvant Immunotherapy for NSCLC: Current Concepts and Future Approaches. *Journal of Thoracic Oncology*, *15*(8), 1281–1297. https://doi.org/10.1016/j.jtho.2020.05.020

Wagener-Ryczek, S., Heydt, C., Süptitz, J., Michels, S., Falk, M., Alidousty, C., Fassunke, J., Ihle, M. A., Tiemann, M., Heukamp, L., Wolf, J., Büttner, R., & Merkelbach-Bruse, S. (2020). Mutational spectrum of acquired resistance to reversible versus irreversible EGFR

tyrosine kinase inhibitors. *BMC Cancer*, *20*(1), 1–11. https://doi.org/10.1186/s12885-020-06920-3

Wang, D., Zhao, C., Xu, F., Zhang, A., Jin, M., Zhang, K., Liu, L., Hua, Q., Zhao, J., Liu, J., Yang, H., & Huang, G. (2021). Cisplatin-resistant NSCLC cells induced by hypoxia transmit resistance to sensitive cells through exosomal PKM2. *Theranostics*, *11*(6), 2860–2875. https://doi.org/10.7150/THNO.51797

Wang, G., Reed, E., & Li, Q. Q. (2004). Molecular basis of cellular response to cisplatin chemotherapy in non-small cell lung cancer (Review). *Oncology Reports*, *12*(5), 955–965. https://doi.org/10.3892/or.12.5.955

Wang, Y., Branicky, R., Noë, A., & Hekimi, S. (2018). Superoxide dismutases: Dual roles in controlling ROS damage and regulating ROS signaling. *Journal of Cell Biology*, *217*(6), 1915–1928. https://doi.org/10.1083/jcb.201708007

Weitzel, D. H., Tovmasyan, A., Ashcraft, K. A., Boico, A., Birer, S. R., Roy Choudhury, K., Herndon, J., Rodriguiz, R. M., Wetsel, W. C., Peters, K. B., Spasojevic, I., Batinic-Haberle, I., & Dewhirst, M. W. (2016). Neurobehavioral radiation mitigation to standard brain cancer therapy regimens by Mn(III) n-butoxyethylpyridylporphyrin-based redox modifier. *Environmental and Molecular Mutagenesis*, *57*(5), 372–381. https://doi.org/10.1002/em.22021

Weitzel, D. H., Tovmasyan, A., Ashcraft, K. A., Rajic, Z., Weitner, T., Liu, C., Li, W., Buckley, A. F., Prasad, M. R., Young, K. H., Rodriguiz, R. M., Wetsel, W. C., Peters, K. B., Spasojevic, I., Herndon, J. E., Batinic-Haberle, I., & Dewhirst, M. W. (2015). Radioprotection of the brain white matter by Mn(III) N-butoxyethylpyridylporphyrin-based superoxide dismutase mimic MnTnBuOE-2-PyP5+. *Molecular Cancer Therapeutics*, *14*(1), 70–79. https://doi.org/10.1158/1535-7163.MCT-14-0343

Wu, T., Wang, M. C., Jing, L., Liu, Z. Y., Guo, H., Liu, Y., Bai, Y. Y., Cheng, Y. Z., Nan, K. J., & Liang, X. (2015). Autophagy facilitates lung adenocarcinoma resistance to cisplatin treatment by activation of AMPK/mTOR signaling pathway. *Drug Design, Development and Therapy*, *9*, 6421–6431. https://doi.org/10.2147/DDDT.S95606

Xie, M., Xu, X., & Fan, Y. (2021). KRAS-Mutant Non-Small Cell Lung Cancer: An Emerging Promisingly Treatable Subgroup. *Frontiers in Oncology*, *11*(May), 1–11. https://doi.org/10.3389/fonc.2021.672612

Younus, H. (2018). Therapeutic potentials of superoxide dismutase. *International Journal of Health Sciences*, *12*(3), 88–93.

Yulyana, Y., Tovmasyan, A., Ho, I. A. W., Sia, K. C., Newman, J. P., Ng, W. H., Guo, C. M., Hui, K. M., Batinic-Haberle, I., & Lam, P. Y. P. (2016). Redox-Active Mn Porphyrin-based Potent SOD Mimic, MnTnBuOE-2-PyP5+, Enhances Carbenoxolone-Mediated TRAIL-Induced Apoptosis in Glioblastoma Multiforme. *Stem Cell Reviews and Reports*, *12*(1), 140–155. https://doi.org/10.1007/s12015-015-9628-2

Zalewska-Ziob, M., Adamek, B., Kasperczyk, J., Romuk, E., Hudziec, E., Chwalińska, E., Dobija-Kubica, K., Rogoziński, P., & Bruliński, K. (2019). Activity of Antioxidant Enzymes in the Tumor and Adjacent Noncancerous Tissues of Non-Small-Cell Lung Cancer. *Oxidative Medicine and Cellular Longevity*, *2019*, 1–9. https://doi.org/10.1155/2019/2901840

Zhang, J., Ye, Z. wei, Tew, K. D., & Townsend, D. M. (2021). Cisplatin chemotherapy and renal function. *Advances in Cancer Research*, *152*, 305–327. https://doi.org/10.1016/bs.acr.2021.03.008

Zhao, B. X., Wang, J., Song, B., Wei, H., Lv, W. P., Tian, L. M., Li, M., & Lv, S. (2015).

Establishment and biological characteristics of acquired gefitinib resistance in cell line NCI-H1975/gefinitib-resistant with epidermal growth factor receptor T790M mutation. *Molecular Medicine Reports*, *11*(4), 2767–2774. https://doi.org/10.3892/mmr.2014.3058

Zhao, Y., Chaiswing, L., Oberley, T. D., Batinic-Haberle, I., St. Clair, W., Epstein, C. J., & St. Clair, D. (2005). A mechanism-based antioxidant approach for the reduction of skin carcinogenesis. *Cancer Research*, *65*(4), 1401–1405. https://doi.org/10.1158/0008-5472.CAN-04-3334

Attachments

Table A1. List of volatile carbonyl compounds (VCCs) identified in the extracellular culture medium of H1975 and A549 cells by HS-SPME-GC-MS.

Nº	Compound	RT (min)	*m/z*	Rematch
1	acetaldehyde	14.43 / 14.64	117, 161, 209	928
2	acetone	16.23 / 16.41	161, 206, 253	927
3	propanal	16.84 / 17.04	161, 195, 236	903
4	isobutanal	17.96	195, 250	893
5	2-butenal	18.36 / 18.45	161, 195, 250	885
6	pentanal	19.30	161, 195, 239	860
7	3-methyl-2-butanone	19.61 / 19.75	100, 253, 281	793
8	2-pentanone	20.31 / 20.51	195, 236, 253	872
9	3-methylpentanal	20.39	161, 239	792
10	4-methyl-2-pentanone	21.37 / 21.88	236, 253, 295	794
11	2-hexanone	22.47 / 22.74	195, 253, 236	853
12	heptanal	24.15	239, 252	816
13	cyclopentanone	24.24	232, 279	721
14	cyclohexanone	26.02	195, 276, 293	856
15	octanal	28.68	207, 239	729
16	benzaldehyde	29.40	271, 301	827
17	nonanal	30.84	207, 239	851
18	decanal	32.89	207, 239	817
19	glyoxal	34.59 / 34.69 / 34.75	161, 252, 448	921
20	methylglyoxal	34.83 / 35.06 / 35.36	117, 265, 462	910
21	dimethylglyoxal	35.92	279, 476	792

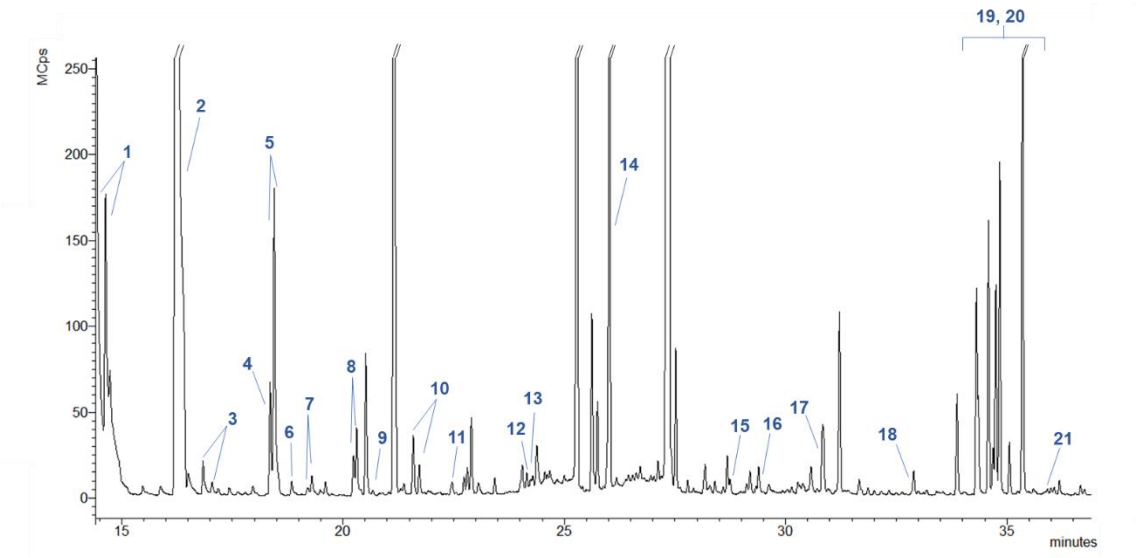

Figure A1. Representative HS-SPME-GC-MS chromatogram of the extracellular culture medium of the H1975 cells with identification of volatile carbonyl compounds (VCCs), as listed in the first column of the Table S1.

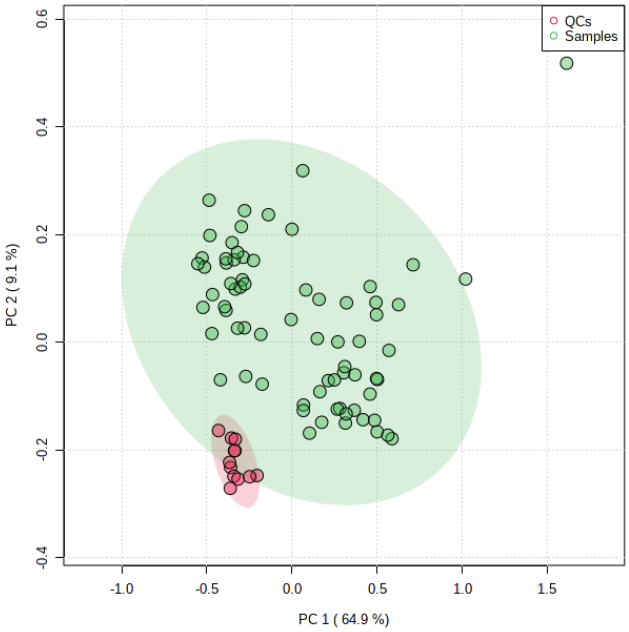

Figure A2. Principal component analysis (PCA) scores plot of the HS-SPME-GC-MS chromatograms of extracellular media of all samples under study (H1975 and A549 cells exposed to MnTnHex alone and/or combined with cisplatin and controls, *n*=71, green circles) and the quality control samples (QCs, *n*=12, red circles).

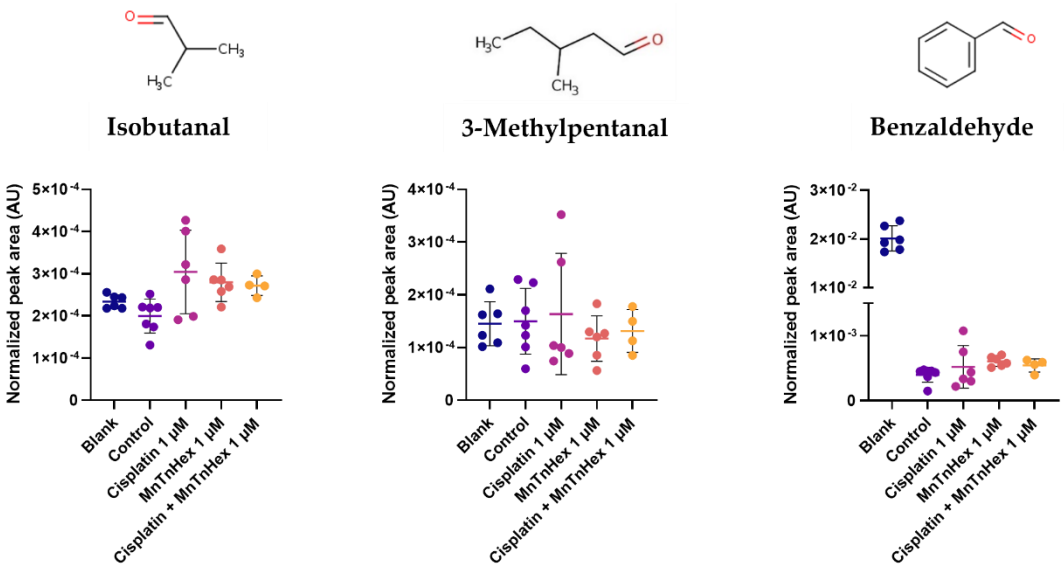

Figure A3. GC-MS-based metabolomics analysis of the extracellular medium of A549 cells exposed to MnTnHex and cisplatin, alone and combined. Boxplots representing the normalized peak areas of the three VCCs (isobutanal, 3-methylpentanal and benzaldehyde).